APPENDIX G: UNDERWATER SOUND MODELLING

Eureka 3D Marine Seismic Survey

Acoustic Modelling for Assessing Marine Fauna Sound Exposures

JASCO Applied Sciences (Australia) Pty Ltd

3 May 2023

Submitted to:

RPS

Authors:

P001728-001
Document 03034
Version 1.0

Suggested citation:

Koessler, M.W., and C.R. McPherson. 2023. Eureka 3D Marine Seismic Survey: Acoustic Modelling for Assessing Marine Fauna Sound Exposures. Document 03034, Version 1.0. Technical report by JASCO Applied Sciences for RPS Australia.

The results presented herein are relevant within the specific context described in this report. They could be misinterpreted if not considered in the light of all the information contained in this report. Accordingly, if information from this report is used in documents released to the public or to regulatory bodies, such documents must clearly cite the original report, which shall be made readily available to the recipients in integral and unedited form.

Contents

Executive Summary 1
1. Introduction 4
1. Modelling Scenarios 5
2. Noise Effect Criteria 7
2.1. Marine Mammals 8
2.2. Fish, Fish Eggs, and Fish Larvae 8
2.3. Sea Turtles 9
2.4. Invertebrates 10
2.4.1. Benthic Invertebrates (Crustaceans and Bivalves) 10
2.4.2. Plankton 11
2.4.3. Squid 11
2.5. Human Health Assessment Threshold 12
3. Methods 14
3.1. Parameter Overview 14
3.2. Acoustic Source Model 14
3.3. Sound Propagation Models 14
3.4. Geometry and Modelled Regions 15
3.5. Accumulated SEL 15
4. Results 17
4.1. Acoustic Source Levels and Directivity 17
4.2. Per-pulse Sound Fields 17
4.2.1. Tabulated Results 18
4.2.2. Sound Field Maps and Graphs 21
4.3. Multiple Source Fields 1
4.3.1. Tabulated Results 1
4.3.2. Sound Level Contour Maps 3
5. Discussion and Summary 4
5.1. Per-Pulse Sound Fields 4
5.2. Multiple Pulse Sound Fields 4
5.3. Summary 5
Glossary 9
Literature Cited 18
Appendix A. Acoustic Metrics A-1
Appendix B. Acoustic Source Model B-1
Appendix C. Sound Propagation Models C-1
Appendix D. Methods and Parameters D-1

Appendix E. Model Validation Information..... E-1

Figures

Figure 1. Overview of key survey features, modelled locations and the two survey scenarios. 6
Figure 2. *Site 1, SPL, 2495 in³ source, tow azimuth 0°*: Sound level contour map of unweighted maximum-over-depth sound field in 10 dB steps, and the isopleths for behavioural response thresholds for marine mammals and turtles. 21
Figure 3. *Site 2, SPL, 2495 in³ source, tow azimuth 0°*: Sound level contour map of unweighted maximum-over-depth sound field in 10 dB steps, and the isopleths for behavioural response thresholds for marine mammals and turtles. 22
Figure 4. *Site 3, SPL, 2495 in³ source, tow azimuth 0°*: Sound level contour map of unweighted maximum-over-depth sound field in 10 dB steps, and the isopleths for behavioural response thresholds for marine mammals and turtles. 22
Figure 5. *Site 4, SPL, 2495 in³ source, tow azimuth 0°*: Sound level contour map of unweighted maximum-over-depth sound field in 10 dB steps, and the isopleths for behavioural response thresholds for marine mammals and turtles. 23
Figure 6. *Site 5, SPL, 2495 in³ source, tow azimuth 0°*: Sound level contour map of unweighted maximum-over-depth sound field in 10 dB steps, and the isopleths for behavioural response thresholds for marine mammals and turtles. 23
Figure 7. *Site 6, SPL, 2495 in³ source, tow azimuth 0°*: Sound level contour map of unweighted maximum-over-depth sound field in 10 dB steps, and the isopleths for behavioural response thresholds for marine mammals and turtles. 24
Figure 8. *Site 1, Scenario 1, tow azimuth 0°, SPL*: Sound level contours (vertical slice), perpendicular to (broadside, top) and along the tow direction (endfire, bottom). For context the behavioural response threshold for marine mammals is highlighted in orange. 25
Figure 9. *Site 3, Scenario 1,tow azimuth 0°, SPL*: Sound level contours (vertical slice), perpendicular to (broadside, top) and along the tow direction (endfire, bottom). For context the behavioural response threshold for marine mammals is highlighted in orange. 26
Figure 10. *Site 4, Scenario 2,tow azimuth 0°, SPL*: Sound level contours (vertical slice), perpendicular to (broadside, top) and along the tow direction (endfire, bottom). For context the behavioural response threshold for marine mammals is highlighted in orange. 27
Figure 11. *Site 5, Scenario 2,tow azimuth 0°, SPL*: Sound level contours (vertical slice), perpendicular to (broadside, top) and along the tow direction (endfire, bottom). For context the behavioural response threshold for marine mammals is highlighted in orange. 28
Figure 12. *Scenario 1*: Sound level contour map showing unweighted maximum-over-depth SEL_{24h}, along with thresholds for LF-cetaceans and fish. 3
Figure 13. Scenario 2: Sound level contour map showing unweighted maximum-over-depth SEL_{24h}, along with thresholds for LF-cetaceans and fish. 3

Figure A-1. Decidecade frequency bands (vertical lines) shown on a linear frequency scale and a logarithmic scale. A-3
Figure A-2. Sound pressure spectral density levels and the corresponding decidecade band sound pressure levels of example ambient noise shown on a logarithmic frequency scale. A-4
Figure A-3. Auditory weighting functions for functional marine mammal hearing groups used in this project as recommended by Southall et al. (2019). A-6
Figure B-1. Layout of the modelled 2495 in³ array. B-2
Figure B-2. Predicted source level details for the 2495 in³ seismic source with a 6 m towed depth. B-3
Figure B-3. Directionality of the predicted horizontal source levels for the 2495 in³ seismic source, 5 Hz to 2 kHz. B-4
Figure C-1. The N×2-D and maximum-over-depth modelling approach used by MONM. C-1
Figure D-1. Sample areas ensonified to an arbitrary sound level with R_{max} and $R_{95\%}$ ranges shown for two scenarios. D-1

Figure D-2. *Site 3*: Range-and-depth-dependent conversion offsets for converting sound exposure level (SEL) to sound pressure level (SPL) for seismic pulses. D-2
Figure D-3. *Site 5*: Range-and-depth-dependent conversion offsets for converting sound exposure level (SEL) to sound pressure level (SPL) for seismic pulses. D-3
Figure D-4. Bathymetry map of the modelling area for the Eureka Marine Seismic Survey. D-4
Figure D-5. The sound speed profile used for sound propagation modelling at all sites (August). D-5

Tables

Table 1. Maximum horizontal distance (R_{max}) for behavioural response thresholds, permanent threshold shift (PTS) and temporary threshold shift (TTS) for marine mammals. Maximum extents are in the broadside direction. 1
Table 2. Maximum horizontal distance (in km) to turtle behavioural response criteria, temporary threshold shift (TTS), and permanent threshold shift (PTS). 2
Table 3. Maximum onset distances for single impulse and 24 hour sound exposure level (SEL_{24h}) for fish, fish eggs, and larvae injury and temporary threshold shift (TTS). 2
Table 4. Parameters for modelled scenarios 5
Table 5. Location details for the single impulse modelled sites. 5
Table 6. Unweighted sound pressure level (SPL), weighted 24-hour sound exposure level (SEL_{24h}), and peak pressure (PK) thresholds for acoustic effects on marine mammals. 8
Table 7. Criteria for seismic noise exposure for fish, adapted from Popper et al. (2014). 9
Table 8. Acoustic effects of impulsive noise on sea turtles: Unweighted sound pressure level (SPL), 24 hour sound exposure level (SEL_{24h}), and peak pressure (PK) thresholds 10
Table 9. Far-field source levels for 2495 in^3 source 17
Table 10. Maximum (R_{max}) and 95% ($R_{95\%}$) horizontal distances (in km) from the seismic source to modelled maximum-over-depth (also maximised over tow modelled tow direction) unweighted per-pulse sound exposure level (SEL) isopleths from the modelled single impulse sites, with water depth indicated. 18
Table 11. Maximum (R_{max}) and 95% ($R_{95\%}$) horizontal distances (in km) from the seismic source to modelled maximum-over-depth (also maximised over tow modelled tow direction) per-pulse sound pressure level (SPL) isopleths from the modelled single impulse sites, with water depth indicated. 19
Table 12. Maximum (R_{max}) horizontal distances (in km) from the seismic source to modelled maximum-over-depth (also maximised over tow modelled tow direction) peak pressure level (PK) thresholds based on Southall et al. (2019) for marine mammals, and Popper et al. (2014) for fish and Finneran et al. (2017) for sea turtles, Sites 3 and 5), with water depth indicated. 19
Table 13. Maximum (R_{max}) horizontal distances (in m) from the seismic source to modelled seafloor (receiver located 50 cm above seafloor) peak pressure level thresholds (PK) at three water depths within the Operational Area. 20
Table 14. Maximum (R_{max}) horizontal distances (in m) from the seismic source to modelled seafloor (receiver located 5 cm above seafloor) peak-peak pressure levels (PK-PK) at three water depths within the Active Source Area. Results included in relation to benthic invertebrates. 20
Table 15. Maximum (R_{max}) horizontal distances (in m) from the 2495 in^3 to particle motion threshold: Peak acceleration magnitude level (m/s^2) threshold for benthic invertebrates 5 cm above the seafloor, with water depth indicated. Results included in relation to benthic invertebrates (Section 2.4.1) 21
Table 16. Marine mammal and sea turtle criteria: Maximum (R_{max}) horizontal distances (in km) and ensonified area (km^2) from the survey lines to permanent threshold shift (PTS) and temporary threshold shift (TTS) thresholds considering 24 hours of survey activity (maximum-over-depth). 1

Table 17. *Fish criteria*: Maximum horizontal distances (R_{max}, in km) from the survey lines and area (km^2) to injury and temporary threshold shift (TTS) thresholds considering 24 h of survey activity. 2
Table 18. Summary of maximum horizontal distance (R_{max}) for behavioural response thresholds, permanent threshold shift (PTS) and temporary threshold shift (TTS) for marine mammals. Maximum extents are in the broadside direction. 5
Table 19. Summary of maximum horizontal distance (in km) to turtle behavioural response criteria, temporary threshold shift (TTS), and permanent threshold shift (PTS). 6
Table 20. Summary of maximum onset distances for single impulse and 24 hour sound exposure level (SEL_{24h}) for fish, fish eggs, and larvae injury and temporary threshold shift (TTS). 6

Table A-1. Parameters for the auditory weighting functions used in this project as recommended by Southall et al. (2019). A-6
Table B-1. Layout of the modelled 2495 in^3 array. Tow depth is 6 m. Firing pressure for all guns is 2000 psi. Also see Figure B-1. ..... B-2
Table D-1. Geoacoustic profile for modelled sites. D-6

Executive Summary

JASCO Applied Sciences (JASCO) performed numerical modelling to derive underwater sound levels for the proposed Eureka 3D Marine Seismic Survey (MSS) to predict the potential impacts on key regional receptors including marine mammals, fish, turtles, benthic invertebrates, sponges, coral, and plankton. JASCO's specialised Airgun Array Source Model (AASM) was used along with complementary underwater acoustic propagation models to estimate sound levels at six sites, to account for variable coastal features and water depth.

The modelling considered source directivity and range-dependent environmental properties likely to be encountered within the survey area. Estimated acoustic levels are presented as sound pressure levels (SPL, L_p), zero-to-peak pressure levels (PK, L_{pk}), peak-to-peak pressure levels (PK-PK; $L_{pk\text{-}pk}$), and either single-impulse or accumulated sound exposure levels (SEL, L_E) as appropriate for different noise effect criteria.

For the accumulated sound exposure scenarios, the SEL_{24h} is a cumulative metric that reflects the dosimetric effect of noise levels within 24 hours. It assumes a receiver (e.g., an animal) is consistently exposed to the noise at a fixed position. More realistically, marine animals would not stay in the same location for 24 hours. Therefore, a radius for the SEL_{24h} criteria does not mean that marine fauna within this radius will be impaired, but rather that the animal could be exposed to the sound level associated with impairment, either Permanent Threshold Shift (PTS) or Temporary Threshold Shift (TTS), if it remained at that location for 24 hours.

Marine mammals – Results

- Maximum distance for behavioural response based on NOAA (2019) criterion of 160 dB re 1 µPa (SPL) varied between 9.20 and 6.51 km depending on the site.
- The results for marine mammal injury considered the criteria from Southall et al. (2019). These criteria contain two metrics (PK and SEL_{24h}), both required for the assessment of marine mammal PTS and TTS. The longest distance associated with either metric is required to be applied for assessment; Table 1 summarises the maximum distances, along with the relevant metric.

Table 1. Maximum horizontal distance (R_{max}) for behavioural response thresholds, permanent threshold shift (PTS) and temporary threshold shift (TTS) for marine mammals. Maximum extents are in the broadside direction.

Hearing group	Maximum modelled distance to effect threshold (R_{max})		
	Behavioural response[1]	Impairment (km): PTS[2]	Impairment (km): TTS[2]
LF cetaceans (Baleen whales)	9.20	3.08 (SEL_{24h})	43.0 (SEL_{24h})
HF cetaceans (Dolphins, plus toothed, beaked, and bottlenose whales)		–	–
VHF cetaceans (*Kogia*, cephalorhynchid, and *L. australis*)		0.41 (PK)	0.84 (PK)
Other Carnivores in Water (Australian sea lion, Australian fur seal)		–	0.06

Noise exposure criteria: [1] NOAA (2019) and [2] Southall et al. (2019).
A dash indicates the threshold was not reached within the limits of the modelling resolution (20 m).

Sea turtles

- The PK sea turtle impairment criteria from Finneran et al. (2017) were not exceeded beyond the modelled resolution of 20 m.

- The maximum distance for PTS onset was 0.06 and 2.10 km for TTS onset for the seismic source (Finneran et al. 2017).
- Behavioural response of turtles are shown in Table 2, based on 166 dB re 1 µPa and 175 dB re 1 µPa (SPL) (McCauley et al. 2000).

Table 2. Maximum horizontal distance (in km) to turtle behavioural response criteria, temporary threshold shift (TTS), and permanent threshold shift (PTS).

Hearing group	Maximum modelled distance (in km) to effect threshold (R_{max})			
	Behavioural response[1]	Behavioural disturbance[1]	Impairment: TTS[2]	Impairment: PTS[2]
Sea turtles	4.90 (166 dB re 1 µPa - SPL)	1.58 (175 dB re 1 µPa - SPL)	2.10 (SEL_{24h})	0.06 (SEL_{24h})

Noise exposure criteria: [1] McCauley et al. (2000) and [2] Finneran et al. (2017).

Fish, fish eggs, and fish larvae

This modelling study assessed the ranges for quantitative criteria based on Popper et al. (2014) and considered both PK (seafloor and water column) and SEL_{24h} metrics (water column) associated with mortality and potential mortal injury as well as impairment in the following groups:

- Fish without a swim bladder (also appropriate for sharks in the absence of other information),
- Fish with a swim bladder that do not use it for hearing,
- Fish that use their swim bladders for hearing,
- Fish eggs and fish larvae.

Table 3 summarises distances to effect criteria for fish, fish eggs, and fish larvae along with the relevant metric. Seafloor sound levels were assessed at nine different depths within the survey area. Assessment was based on Popper et al. (2014) and considered both PK (seafloor and water column) and SEL_{24h} metrics (water column) associated with mortality, potential mortal injury and impairment.

Table 3. Maximum onset distances for single impulse and 24 hour sound exposure level (SEL_{24h}) for fish, fish eggs, and larvae injury and temporary threshold shift (TTS).

Relevant hearing group	Effect criteria	Metric associated with longest distance to criteria	R_{max} (km)
Fish: No swim bladder	Recoverable injury	PK	0.15
	TTS	SEL_{24h}	4.06
Fish: Swim bladder not involved in hearing and Swim bladder involved in hearing	Recoverable injury	PK	0.27
	TTS	SEL_{24h}	4.06
Fish eggs, and larvae (relevant to plankton)	Injury	PK	0.27

Benthic invertebrates, Cephalopods, Sponges, and Coral

To assist with assessing the potential effects on these receptors, the following results were determined:

- Crustaceans (representative of southern rock lobsters and crabs): The distance to no effect was reached between 206 and 292 m, based on 202 dB re 1 µPa PK-PK level from Payne et al. (2008).

- Bivalves (representative of scallops and mussels): The distance to no effect was reached between 58 and 7 m, based on a particle acceleration limit of 37.57 ms^{-2} at the seafloor as presented in Day et al. (2016a).
- Squid: The distance to the per–pulse SEL (L_E) startle (inking) response level of 162 dB re 1 μPa^2s for squid (Fewtrell and McCauley 2012) was reached between 2.90 and 2.03 km.
- Sponges and coral: The threshold was reached at a maximum of 15 m, based on the PK sound level criteria of 226 dB re 1 µPa PK for sponges and corals (Heyward et al. 2018).

Divers

An SPL human health assessment of 145 dB re 1 µPa (SPL; L_p) derived from Parvin (2005) was considered for people swimming and diving. The sound level was reached at ranges between 36.4 and 24.1 km depending on the modelled site. This is the maximum range over all modelled azimuths, and it is typically in orientated offshore. This maximum range should not be used as an offset distance to the coast and the sound field contour maps should be used to inform any such offset.

1. Introduction

JASCO Applied Sciences (JASCO) performed numerical modelling to calculate underwater sound levels for the proposed Eureka 3D Marine Seismic Survey (MSS) to predict the potential impacts on key regional receptors including marine mammals, fish, turtles, benthic invertebrates, sponges, coral, and plankton. In total, six sites were used for modelling across the proposed survey area to account for variable coastal features and for small changes in sound propagation that could occur in the shallow coastal waters.

JASCO's specialised Airgun Array Source Model (AASM) was used to predict acoustic signatures and spectra for the source. AASM accounts for individual airgun volumes, airgun bubble interactions, and array geometry to yield accurate source predictions.

Complementary underwater acoustic propagation models were used in conjunction with the selected array signature to estimate sound levels considering environmental effects. Single-impulse sound fields were predicted at each of the defined locations, and accumulated sound exposure fields were predicted for each scenario. A worst-case sound speed profile that would be most supportive of sound propagation conditions for the potential survey period was defined and applied throughout.

The modelling considered source directivity and range-dependent environmental properties. Estimated underwater acoustic levels are presented as sound pressure levels (SPL, L_p), zero-to-peak pressure levels (PK, L_{pk}), peak-to-peak pressure levels (PK-PK; $L_{pk\text{-}pk}$), peak acceleration magnitude, and either single-impulse (i.e., per-pulse) or accumulated sound exposure levels (SEL, L_E) as appropriate for different noise effect criteria.

1. Modelling Scenarios

Two nominal acquisition scenarios were considered using both acoustic propagation modelling, are presented in Table 4. Acoustic source and propagation modelling was conducted at six individual single-impulse sites. The single impulse sites and the accumulated SEL scenarios were determined based on proposed survey line plans with lines orientated either at 0/180°. The locations of the modelled sites are provided in Table 5 and presented in Figure 1 . This study considered a 2495 in^3 seismic source towed in a double array configuration at an assumed speed of ~4.5 knots with an impulse interval (inter-pulse interval) of 12.5 m and a crossline array separation of 50 m. The acoustic propagation modelling utilised an August sound speed profile as this month will likely result in favourable propagation conditions within potential acquisition time periods for the proposed survey.

The single impulse sites and accumulated SEL scenarios were chosen to be representative of the range of water depths and the potential sound propagation characteristics within the Active Source Area. Seafloor sound levels were assessed at eight different representative water depths within the Active Source Area (10,12.5,15, 20, 25, 30, 40, and 50 m).

Table 4. Parameters for modelled scenarios

Scenario	Source volume (in^3)	Tow depth (m)	Tow direction (°)	Source configuration	Impulse interval (m)	Discharged impulses
1	2495	6	0 & 180	Double	12.5	11351
2						8558

Table 5. Location details for the single impulse modelled sites.

Site	Latitude (°S)	Longitude (°E)	MGA[1] Zone 50		Water depth (m)
			X (m)	Y (m)	
1	29° 28' 49.64"	114° 51' 05.04"	291676	6736859	25.0
2	29° 31' 38.47"	114° 51' 01.47"	291676	6731659	33.0
3	29° 37' 54.69"	114° 50' 53.49"	291676	6720072	30.0
4	29° 23' 08.13"	114° 40' 10.60"	273835	6747035	45.0
5	29° 30' 13.53"	114° 40' 17.24"	274276	6733941	47.0
6	29° 22' 53.53"	114° 38' 08.87"	270544	6747419	48.0

[1] Map Grid of Australia (MGA)

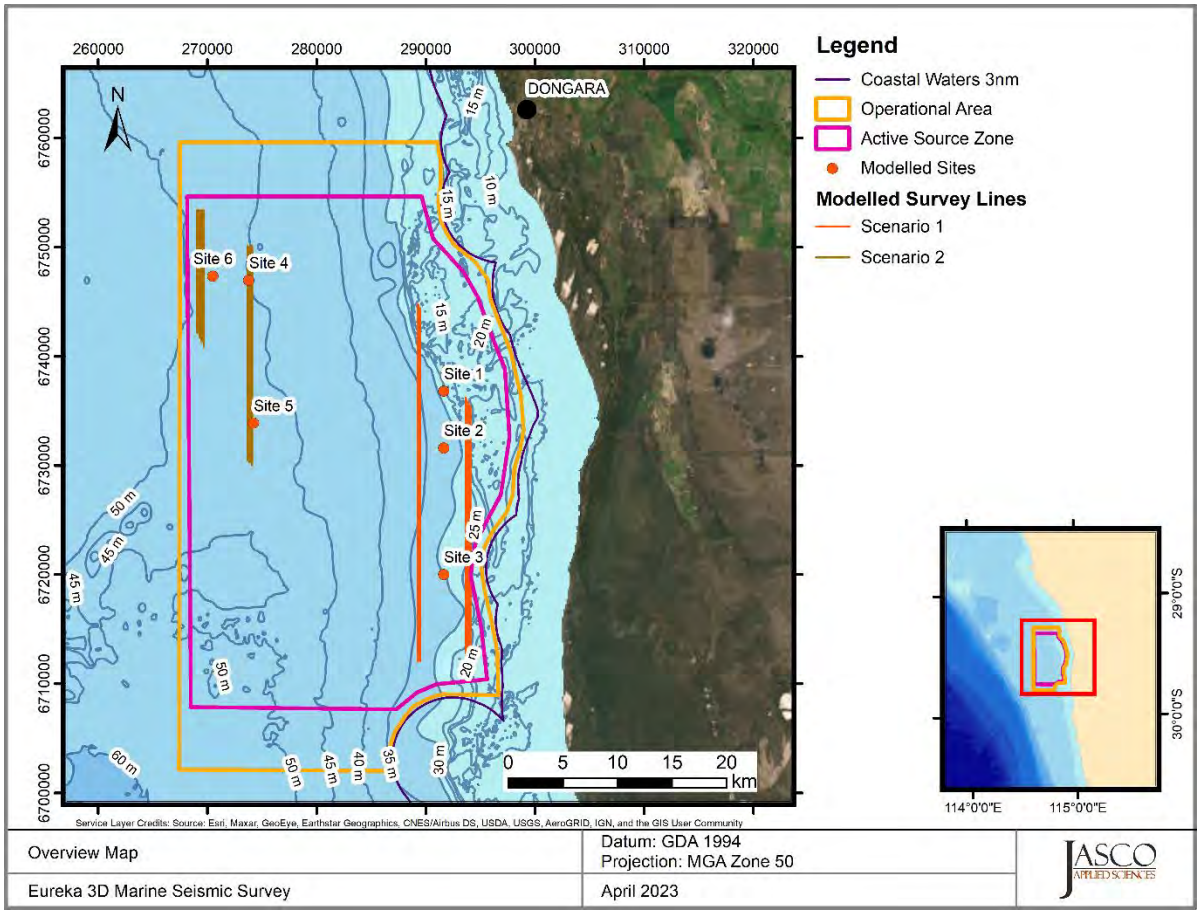


Figure 1. Overview of key survey features, modelled locations and the two survey scenarios.

2. Noise Effect Criteria

The perceived loudness of sound, especially impulsive noise such as that from seismic airguns, is not generally proportional to the instantaneous acoustic pressure. Rather, perceived loudness depends on the pulse rise-time and duration, and the frequency content. Several sound level metrics, such as PK, SPL, and SEL, are commonly used to evaluate noise and its effects on marine life (Appendix A). The period of accumulation associated with SEL is defined, with this report referencing either a "per pulse" assessment or over 24 hours. The acoustic metrics in this report reflect the updated ISO standard for acoustic terminology, ISO/DIS 18405:2017 (2017).

Whether acoustic exposure levels might injure or disturb marine mammals is an active research topic. Since 2007, several expert groups have developed SEL-based assessment approaches for evaluating auditory injury, with key works including Southall et al. (2007), Finneran and Jenkins (2012), Popper et al. (2014), United States National Marine Fisheries Service (NMFS 2018) and Southall et al. (2019). The number of studies that have investigated the level of behavioural disturbance to marine fauna by anthropogenic sound has also increased substantially.

The following noise criteria and sound levels for this study were chosen because they include standard thresholds, thresholds suggested by the best available science, and sound levels presented in literature for species with no suggested thresholds (Sections 2.1–2.4 and Appendix A):

1. Peak pressure levels (PK; L_{pk}) and frequency-weighted accumulated sound exposure levels (SEL; $L_{E,24h}$) from Southall et al. (2019) for the onset of Permanent Threshold Shift (PTS) and Temporary Threshold Shift (TTS) in marine mammals.
2. Marine mammal behavioural threshold based on the current US National Oceanic and Atmospheric Administration (NOAA 2019) criterion for marine mammals of 160 dB re 1 µPa (SPL; L_p) for impulsive sound sources.
3. Sound exposure guidelines for fish, fish eggs and larvae (including plankton) (Popper et al. 2014).
4. Peak pressure levels (PK; L_{pk}) and frequency-weighted accumulated sound exposure levels (SEL; $L_{E,24h}$) from Finneran et al. (2017) for the onset of permanent threshold shift (PTS) and temporary threshold shift (TTS) in turtles.
5. Sea turtle behavioural response threshold of 166 dB re 1 µPa (SPL; L_p) for impulsive noise, along with a sound level associated with behavioural disturbance 175 dB re 1 µPa (SPL; L_p) (McCauley et al. 2000).
6. Peak-peak pressure levels (PK-PK; $L_{pk\text{-}pk}$) and peak particle acceleration magnitude (ms^{-2}) at the seafloor to help assess effects of noise on crustaceans through comparing to results in Day et al. (2016a), Day et al. (2019), Day et al. (2016b), Day et al. (2017) and Payne et al. (2008).
7. A sound level of 226 dB re 1 µPa (PK; L_{pk}) reported for comparing to Heyward et al. (2018) for sponges and corals.
8. A startle (inking) response sound level of 162 dB re 1 μPa^2s per–pulse SEL (L_E) for squid from Fewtrell and McCauley (2012).
9. An SPL human health assessment threshold of 145 dB re 1 µPa (SPL; L_p) for sound exposure to people swimming and diving derived from Parvin (2005), and considering Ainslie (2008).

Additionally, to assess the size of the low-power zone required under the Australian Environment Protection and Biodiversity Conservation (EPBC) Act Policy Statement 2.1, Department of the Environment, Water, Heritage and the Arts (DEWHA 2008), the distance to an unweighted per-pulse SEL of 160 dB re 1 $\mu Pa^2 \cdot s$ (L_E) is reported.

2.1. Marine Mammals

There are two categories of auditory threshold shifts or hearing loss: permanent threshold shift (PTS), a physical injury to an animal's hearing organs; and Temporary Threshold Shift (TTS), a temporary reduction in an animal's hearing sensitivity as the result of receptor hair cells in the cochlea fatigue.

To help assess the potential for the possible injury and hearing sensitivity changes in marine mammals, this report applies the criteria recommended be Southall et al. (2019), considering both PTS and TTS. These criteria, along with the applied behavioural criteria (NOAA 2019), are summarised in Table 6, with descriptions included in Appendix A.4.1 (auditory impairment) and Appendix A.4.2 (behavioural response), with frequency weighting explained in Appendix A.5. Whilst the newly published Southall et al. (2021) includes recommendations and discusses the nuances of assessing behavioural response, the authors do not recommend new numerical thresholds for onset of behavioural responses for marine mammals.

Table 6. Unweighted sound pressure level (SPL), weighted 24-hour sound exposure level (SEL_{24h}), and peak pressure (PK) thresholds for acoustic effects on marine mammals.

Hearing group	NOAA (2019)	Southall et al. (2019)			
	Behaviour	PTS onset thresholds[1] (received level)		TTS onset thresholds[1] (received level)	
	SPL (L_p; dB re 1 µPa)	Weighted SEL (L_E; dB re 1 µPa^2 s)	PK (L_{pk}; dB re 1 µPa)	Weighted SEL (L_E; dB re 1 µPa^2 s)	PK (L_{pk}; dB re 1 µPa)
Low-frequency cetaceans (baleen whales)	160	183	219	168	213
High-frequency cetaceans (dolphins, plus toothed, beaked, and bottlenose whales)		185	230	170	224
Very-high-frequency cetaceans (*Kogia*, cephalorhynchid, and *L. australis*)		155	202	140	196
Pinnipeds[2] (Australian sea lion, Australian fur seal, New Zealand fur seal)		203	232	188	226

[1] Dual metric acoustic thresholds for impulsive sounds: Use whichever results in the largest isopleth for calculating PTS and TTS onset.

[2] Listed as pinnipeds but equivalent to other marine carnivores in water in the Southall et al. (2019) criteria.

L_p-denotes sound pressure level period and has a reference value of 1 µPa.

L_{pk}, flat–peak sound pressure is flat weighted or unweighted and has a reference value of 1 µPa.

L_E - denotes cumulative sound exposure over a 24-hour period and has a reference value of 1 µPa^{2}s.

Subscripts indicate the designated marine mammal auditory weighting.

2.2. Fish, Fish Eggs, and Fish Larvae

In 2006, the Working Group on the Effects of Sound on Fish and Turtles was formed to continue developing noise exposure criteria for fish and turtles, work begun by a panel convened by NOAA two years earlier. The resulting guidelines included specific thresholds for different levels of effects and for different groups of species (Popper et al. 2014). These guidelines defined quantitative thresholds for three types of immediate effects:

- Mortality, including injury leading to death.
- Recoverable injury, including injuries unlikely to result in mortality, such as hair cell damage and minor haematoma.

- TTS.

Masking and behavioural effects can be assessed qualitatively, by assessing relative risk rather than by specific sound level thresholds. However, as these depend upon activity-based subjective ranges, these effects are not addressed in this report and are included in Table 7 for completeness only. Because the presence or absence of a swim bladder has a role in hearing, a fish's susceptibility to injury from noise exposure varies depending on the species and the presence and possible role of a swim bladder in hearing. Thus, different thresholds were proposed for fish without a swim bladder (also appropriate for sharks and applied to whale sharks in the absence of other information), fish with a swim bladder not used for hearing, and fish that use their swim bladders for hearing. Turtles, fish eggs, and fish larvae are considered separately. Table 7 lists relevant effects thresholds from Popper et al. (2014).

The SEL metric integrates noise intensity over some period of exposure. Because the period of integration for regulatory assessments is not well defined for sounds that do not have a clear start or end time, or for very long-lasting exposures, it is required to define a time. Popper et al. (2014) recommend applying a standard period, where this is either defined as a justified fixed period or the duration of the activity; however Popper et al. (2014) also included caveats about how long the fish will be exposed because they can move (or remain in location) and so can the source. Popper et al. (2014) summarises that in all TTS studies considered, fish that showed TTS recovered to normal hearing levels within 18–24 hours. Due to this, a period of accumulation of 24 hours has been applied in this study for SEL, which is similar to that applied for marine mammals in NMFS (2016, 2018).

Additional information is provided in Appendix A.4.

Table 7. Criteria for seismic noise exposure for fish, adapted from Popper et al. (2014).

Type of animal	Mortality and Potential mortal injury	Impairment			Behaviour
		Recoverable injury	TTS	Masking	
Fish: No swim bladder (particle motion detection)	>219 dB SEL_{24h} or >213 dB PK	>216 dB SEL_{24h} or >213 dB PK	>>186 dB SEL_{24h}	(N) Low (I) Low (F) Low	(N) High (I) Moderate (F) Low
Fish: Swim bladder not involved in hearing (particle motion detection)	210 dB SEL_{24h} or >207 dB PK	203 dB SEL_{24h} or >207 dB PK	>>186 dB SEL_{24h}	(N) Low (I) Low (F) Low	(N) High (I) Moderate (F) Low
Fish: Swim bladder involved in hearing (primarily pressure detection)	207 dB SEL_{24h} or >207 dB PK	203 dB SEL_{24h} or >207 dB PK	186 dB SEL_{24h}	(N) Low (I) Low (F) Moderate	(N) High (I) High (F) Moderate
Fish eggs and fish larvae (relevant to plankton)	>210 dB SEL_{24h} or >207 dB PK	(N) Moderate (I) Low (F) Low	(N) Moderate (I) Low (F) Low	(N) Low (I) Low (F) Low	(N) Moderate (I) Low (F) Low

Peak sound level (PK) dB re 1 µPa; SEL_{24h} dB re 1µPa^2·s. All criteria are presented as sound pressure, even for fish without swim bladders, since no data for particle motion exist. Relative risk (high, moderate, or low) is given for animals at three distances from the source defined in relative terms as near (N), intermediate (I), and far (F).

2.3. Sea Turtles

There is a paucity of data regarding responses of turtles to acoustic exposure, and no studies of hearing loss due to exposure to loud sounds. Popper et al. (2014) suggested thresholds for onset of mortal injury (including PTS) and mortality for sea turtles and, in absence of taxon-specific information, adopted the levels for fish that do not hear well (suggesting that this likely would be conservative for sea turtles).

Finneran et al. (2017) presented revised thresholds for sea turtle injury and hearing impairment (TTS and PTS). Their rationale is that sea turtles have best sensitivity at low frequencies and are known to

have poor auditory sensitivity (Bartol and Ketten 2006, Dow Piniak et al. 2012). Accordingly, TTS and PTS thresholds for turtles are likely more similar to those of fishes than to marine mammals (Popper et al. 2014).

McCauley et al. (2000) observed the behavioural response of caged sea turtles—green (*Chelonia mydas*) and loggerhead (*Caretta caretta*)—to an approaching seismic airgun. For received levels above 166 dB re 1 µPa (SPL), the sea turtles increased their swimming activity, and above 175 dB re 1 µPa they began to behave erratically, which was interpreted as an agitated state. The Recovery Plan for Marine Turtles in Australia (Department of the Environment and Energy et al. 2017) acknowledges the 166 dB re 1 µPa SPL reported (McCauley et al. 2000) as the level that may result in a behavioural response to marine turtles. The 175 dB re 1 µPa level from (McCauley et al. 2000) is recommended as a criterion for behavioural disturbance. These are shown in Table 8.

Table 8. Acoustic effects of impulsive noise on sea turtles: Unweighted sound pressure level (SPL), 24 hour sound exposure level (SEL_{24h}), and peak pressure (PK) thresholds.

Effect type	Criterion	SPL (L_p; dB re 1 µPa)	Weighted SEL_{24h} ($L_{E,24h}$; dB re 1 $\mu Pa^2 \cdot s$)	PK (L_{pk}; dB re 1 µPa)
Behavioural response	McCauley et al. (2000)	166	NA	
Behavioural disturbance		175		
PTS onset thresholds[1] (received level)	Finneran et al. (2017)	NA	204	232
TTS onset thresholds[1] (received level)			189	226

[1] Dual metric acoustic thresholds for impulsive sounds: Use whichever results in the largest isopleth for calculating PTS and TTS onset. If a non-impulsive sound has the potential of exceeding the peak sound pressure level thresholds associated with impulsive sounds, these thresholds should also be considered.

L_p denotes sound pressure level period and has a reference value of 1 µPa.

$L_{pk,flat}$ denotes peak sound pressure is flat weighted or unweighted and has a reference value of 1 µPa.

L_E denotes cumulative sound exposure over a 24 h period and has a reference value of 1 $\mu Pa^2 s$.

2.4. Invertebrates

2.4.1. Benthic Invertebrates (Crustaceans and Bivalves)

Research is ongoing into the relationship between sound and its effects on crustaceans (including southern rock lobsters and crabs), including the relevant metrics for effect and impact. Available literature suggests particle motion, rather than sound pressure, is a more important factor for crustacean and bivalve hearing. Water depth and seismic source size are related to the particle motion levels at the seafloor, with larger arrays and shallower water being related to higher particle motion levels, more likely relevant to effects on crustaceans and bivalves (including scallops, abalone, mussels, squid, and octopus).

At the seafloor interface, crustaceans and bivalves are subject to particle motion stimuli from several acoustic or acoustically induced waves. These include the particle motion associated with an impinging sound pressure wave in the water column (the incident, reflected, and transmitted portions), substrate acoustic waves, and interface waves of the Scholte type. However, it is unclear which aspect(s) of these waves is/are most relevant to the animals, either when they normally sense the environment or their physiological responses to loud sounds so there is not enough information to establish similar criteria and thresholds as done for marine mammals and fish. Including recent research, such as Day et al. (2016b), current literature does not clearly define an appropriate metric or identify relevant levels (pressure or particle motion) for an assessment. This includes the consideration of what particle motion levels lead to a behavioural response, or mortality. Therefore, at

this stage, we cannot propose authoritative thresholds to inform the impact assessment. However, levels can be determined for pressure metrics presented in literature to assist the assessment.

The pressure and acceleration examples provided in Day et al. (2016a) (Figures 11 and 12 in report) indicate that the acceleration and pressure signals occurred simultaneously, which was interpreted as an indication that the waterborne sounds were responsible for the accelerations measured by the geophones. For clarity, it is important to distinguish that the acceleration from waterborne sound energy is *not* ground roll, which Day et al. (2016a) correctly define as the sound that propagates along the interface at a speed lower than the shear wave speed of the sediment. However, the report subsequently uses ground roll for all further discussions of particle acceleration. While Day et al. (2016a) discuss that they chose the simplest measure of ground roll, it should have been referring to as 'the acceleration from waterborne sound energy', or 'waterborne acceleration' for short.

For crustaceans, a PK-PK sound level of 202 dB re 1 µPa (Payne et al. 2008) is considered to be associated with no effect, and therefore applied in the assessment. Additionally for context related to different levels of potential impairment, the PK-PK sound levels determined for crustaceans in Day et al. (2016b), 209–212 dB re 1 µPa and 213 dB re 1 µPa from Day et al. (2019), are also included.

For bivalves, PK-PK sound levels of 212, and 213 are presented to allow comparison to the maximum sound levels measured in Day et al. (2016a) and Day et al. (2017) for scallops and pearl shell oyster.

Literature does not present a sound level associated with no impact, and as particle motion is the more relevant metric, particle acceleration from the seismic source has been presented for comparing the results in Table 7 of Day et al. (2016a). The maximum particle acceleration assessed for scallops was 37.57 ms^{-2}.

2.4.2. Plankton

To assess effects on plankton, there are only a few studies to base threshold criteria on. Popper et al. (2014) cites many of the references and studies on potential impacts of noise emissions on fish eggs and larvae prior to 2014. Results presented in Day et al. (2016b) for embryonic lobsters and Fields et al. (2019) for copepods align with those presented in Popper et al. (2014), which is that mortality and sub-lethal injury are limited to within tens of metres of seismic sources. Additionally, the Popper et al. (2014) criteria (Table 7), are extrapolated from simulated pile driving signals which have a more rapid rise time and greater potential for trauma than pulses from a seismic source.

Other research, such as McCauley et al. (2017), has indicated the potential for effects at longer range and at levels of 178 dB PK-PK, however, Fields et al. (2019) noted that it was difficult to reconcile the high mortality reported by McCauley et al. (2017) with the low mortalities reported in the greater previous body of earlier research and their experiment. They recommended further research into whether it is the sound pulse itself (i.e., the energy, peak pressures, or particle acceleration), the (turbulent) fluid flow occurring more slowly (i.e., not related to the sound pulse), or other effects such as the bubble cloud that which might cause higher mortality near the seismic source.

2.4.3. Squid

The responses of squid to airgun signals were investigated by Fewtrell and McCauley (2012). The authors conducted a number of experiments and examined the received per–pulse SEL for caged squid. They found that in one trial, where the received level of the first airgun impulse was 162 dB re 1 $\mu Pa^2 \cdot s$, the squid inked. This response was not observed again within this trial, however the authors stated that it was unknown if this was due to depleted ink reserves or habituation. In two other trials, the initial received levels were lower (132 and 146 dB re 1 $\mu Pa^2 \cdot s$ per–pulse SEL), and although the cumulative received levels did exceed 162 dB re 1 $\mu Pa^2 s$, no inking behaviour was observed. The authors hypothesised that the results also suggest that a gradual increase in received

levels and prior exposure to air gun impulses decreases the severity of the alarm responses in this species. This aligns with findings of general habituation in response to predators in squid (Long et al. 1989). Recent work (Jones et al. 2020) supports these findings as well, indicating potential rapid, short–term habituation by squid to impulsive noise, however, similar response rates were seen 24 h later, which indicated that squid might re–sensitise to the noise.

The results presented in by Fewtrell and McCauley (2012) were stated by the authors to be preliminary, and while they stated that while it is possible that noise levels greater than 147 dB re 1 $\mu Pa^2 \cdot s$ are required to induce avoidance behaviour, the level associated with inking, of 162 dB re 1 $\mu Pa^2 \cdot s$ per–pulse SEL, has been considered as a startle response level for squid. In the absence of additional studies and thresholds this level may be considered for other cephalopods; however, it may be limited when applied to other species.

2.5. Human Health Assessment Threshold

Underwater, the human ear is about 20 dB less sensitive than it is in air at low frequencies (20 Hz), increasing to 40 dB at mid–frequencies (less than 1 kHz), and increasing to 70–80 dB less sensitive at higher frequencies (Parvin 1998). Divers who wear neoprene hoods have even higher hearing thresholds (lower sensitivity) above 500 Hz because the hood material absorbs high–frequency sounds (Sims et al. 1999). Exposure studies related to divers have typically focused on military sonar exposure, with little information on seismic surveys, and as such care is required when considering thresholds for recreational divers and swimmers, particularly for impulsive sounds such as seismic surveys (Ainslie 2008).

The auditory threshold of hearing under water was lowest at 1 kHz (70 dB re 1 µPa SPL) and increased for lower and higher frequencies to around 120 dB re 1 µPa at 20 Hz and at 20 kHz (Parvin 1998). Fothergill et al. (2000) and Fothergill et al. (2001) conducted controlled acoustic exposure experiments on military divers under fully controlled conditions at a US Ocean Simulation Facility and an US Open water test facility; in all tests, the diver were covered with soft or hard shell dive suits and their position and distance relative to sound source, signal characteristics and received levels were controlled and documented (Pestorius et al. 2009). A total of 89 male Navy divers were exposed to pure tone signals and sweeps between 160–320 Hz at SPLs up to 160 dB re 1 µPa. The divers were exposed to these sounds over 100 seconds at depths from 10 to 40 metres. The divers rated the sounds on a severity scale. For frequencies between 100 and 500 Hz, at a received SPL of 130 dB re 1 µPa, divers and swimmers detected body vibration. None of the divers tested rated levels of 140 dB re 1 µPa as “very severe”; however, at 157 dB re 1 µPa, sound was rated as “very severe” 19 % of the time. No physiological damage was observed at the highest levels tested: 160 dB re 1 µPa (Fothergill et al. 2001). In a subsequent study, recreational divers were exposed to tonal signals or 30 Hz sweeps at frequencies between 100 and 500 Hz at received levels of 130–157 dB re 1 µPa (Pestorius et al. 2009). Each exposure lasted for 7 s. Nine female and 17 male scuba divers were tested, all wearing full body neoprene wetsuits. Diver aversion and perception of body vibration were used as test parameters. The results showed no sex–specific differences. The results differed as a function of frequency – while test results showed a strong overall variation between subjects, signals at 100 Hz elicited the strongest aversion in all tests and even at 148 dB a few diver ratings indicated extreme aversion. Due to this and the strong variation between test subjects, the following exposure limit for both military and recreational divers was suggested as a conservative measure: For frequencies between 100 and 500 Hz, the maximum SPL should be 145 dB re 1 µPa over a maximum continuous exposure of 100 seconds or with a maximum duty cycle of 20 % and a maximum daily cumulative total of 3 h. The trading relation between the maximum SPL and duration was 4 dB per doubling of duration (e.g., 141 dB SPL for a 200 second exposure) (Pestorius et al. 2009).

Considering only frequencies between 100 and 500 Hz, Parvin (2005) suggested 145 dB re 1 µPa as a safety criterion for recreational divers and swimmers. Seismic impulses are broadband sources, and

therefore, to be precautionary, the 145 dB re 1 µPa SPL suggested by Fothergill et al. (2001) and Parvin (2005) has been applied in this study as a broadband SPL and as a human health assessment threshold for recreational divers and swimmers. This does not imply that this level is associated with the onset of injury.

3. Methods

3.1. Parameter Overview

The specifications of the seismic source and the environmental parameters used in the propagation models are described in detail in Appendix D. A single sound speed profile for August was considered in this modelling study; this was identified as the seasonal period that would provide the farthest propagation (Appendix D.3.2); as such it was selected to as part of a conservative approach to estimating distances to received sound level thresholds.

The propagation models used in this study consider a single geoacoustic profile. Several papers describe potential geoacoustic models estimated via acoustic inversion (Duncan et al. 2008, Fan et al. 2009). These models consist of a thin sand layer underlain by a semi-cemented limestone/calcarenite bottom. A nominal three layer representation of the seabed has been proposed based on this information; however, the studies all give slightly different geoacoustic values and layer thicknesses. The seabed model consists of sand/calcarenite/limestone basement where the geoacoustic parameters were averaged to obtain representative geoacoustic values.

3.2. Acoustic Source Model

The pressure signature of the individual airguns and the composite decidecade-band point-source equivalent directional levels (i.e., source levels) of the 2495 in^3 seismic source was modelled with JASCO's Airgun Array Source Model (AASM). Although AASM accounts for notional pressure signatures of each seismic source with respect to the effects of surface-reflected signals on bubble oscillations and inter-bubble interactions, the surface-reflected signal (known as surface ghost) is not included in the far-field source signatures. The acoustic propagation models account for those surface reflections, which are a property of the propagating medium rather than the source.

AASM considers:

- Array layout.
- Volume, tow depth, and firing pressure of each airgun.
- Interactions between different airguns in the array.

All seismic sources considered were modelled over AASM's full frequency range, up to 25 kHz. Appendix B.1 details this model.

3.3. Sound Propagation Models

Three sound propagation models were used to predict the acoustic field around the seismic source:

- Combined range-dependent parabolic equation and Gaussian beam acoustic ray-trace model (MONM-BELLHOP, 10 Hz to 25 kHz).
- Full Waveform Range-dependent Acoustic Model (FWRAM, 10 to 1024 Hz).
- Wavenumber integration model (VSTACK, 10 to 1024 Hz).

The models were used in combination to characterise the acoustic fields at short and long ranges in terms of SEL, SPL, PK, and PK-PK. Appendix C details each model. MONM-BELLHOP was used to calculate SEL of a 360° area around each source location. FWRAM was used to model synthetic seismic pulses and to generate a generalised range-dependent SEL to SPL conversion function. The

range-dependent conversion function was applied to predicted per-pulse SEL results from MONM-BELLHOP to estimate SPL values. FWRAM was also used to calculate water column PK and PK-PK levels.

VSTACK was used to calculate close range PK, PK-PK, and particle motion levels along 4 transects at the seafloor along the endfire and broadside directions at 15, 20, 25, 30, 40, and 50 m water depths.

3.4. Geometry and Modelled Regions

To assess sound levels with MONM-BELLHOP, the sound field modelling calculated propagation losses up to distances of 80 km from the source in each cardinal direction, with a horizontal separation of 20 m between receiver points along the modelled radials. The sound fields were modelled with a horizontal angular resolution of $\Delta\theta = 2.5°$ for a total of $N = 144$ radial planes. Receiver depths were chosen to span the entire water column over the modelled areas, from 2 m to a maximum of 2600 m, with step sizes that increased with depth. To supplement the MONM results, high-frequency results for propagation loss were modelled using BELLHOP for frequencies from 1.25 to 25 kHz. The MONM and Bellhop results were combined to produce results for the full frequency range of interest.

FWRAM was run to 80 km along four radials (fore and aft endfire, and port and starboard broadside) for computational efficiency. This was done to compute SEL-to-SPL conversions (Appendix D.2) but also to quantify water column PK and PK-PK. The horizontal range step begins at 20 m and increases with range from the source.

The maximum modelled range for VSTACK was 1000 m, and a variable receiver range increment that increased away from the source was used, which increased from 10 to 25 m. Received levels were computed for receivers at 5 and 50 cm above the seafloor to assist in the assessment on invertebrates and fish respectively.

3.5. Accumulated SEL

New sound energy is introduced into an environment with each pulse from the seismic source. While some impact criteria are based on the per-pulse energy released, others, such as the marine mammal and fish SEL criteria (Section 2), account for the total acoustic energy marine fauna is subjected to over a specified duration, defined in this report as 24 h. An accurate assessment of the accumulated sound energy depends not only on the parameters of each seismic impulse but also on the number of impulses delivered in a duration and the relative positions of the impulses.

When there are many seismic impulses, it becomes computationally prohibitive to perform sound propagation modelling for every single event. The distance between the consecutive seismic impulses is small enough, such that the environmental parameters that influence sound propagation are virtually the same for many impulse points. The acoustic fields can, therefore, be modelled for a subset of seismic pulses and estimated at several adjacent ones. After sound fields from representative impulse locations are calculated, they are adjusted to account for the source position for nearby impulses.

Although estimating the cumulative sound field with the described approach is not as precise as modelling sound propagation at every impulse location, small-scale, site-specific sound propagation features tend to blur and become less relevant when sound fields from adjacent impulses are summed. Larger scale sound propagation features, primarily dependent on water depth, dominate the cumulative field. The accuracy of the present method acceptably reflects those large-scale features, thus providing a meaningful estimate of a wide area SEL field in a computationally feasible framework.

To produce the map of accumulated received sound level distributions and calculate distances to specified sound level thresholds, the maximum-over-depth were calculated at each sampling point

within the modelled region. The radial grids of maximum-over-depth and seafloor sound levels for each impulse were then resampled (by linear triangulation) to produce a regular Cartesian grid. The sound field grids from all impulses were summed (see Equation A-5) to produce the cumulative sound field grid with cell sizes of 20 m. The contours and threshold ranges were calculated from these flat Cartesian projections of the modelled acoustic fields.

The unweighted (fish) and frequency-weighted SEL_{24h} results were rendered as contour maps, including contours that focus on the relevant criteria-based thresholds. Only contours at ranges larger than the nearfield of the seismic source were rendered.

4. Results

4.1. Acoustic Source Levels and Directivity

AASM (Section 3.2) was used to predict the horizontal and vertical overpressure signatures and corresponding power spectrum levels for the 2495 in^3 source array (Table 9), with additional results provided in Appendix B.3 along with the horizontal directivity plots for this source.

Table 9. Far-field source levels for 2495 in^3 source at 2 m depth. Source levels are for a point-like acoustic source with equivalent far-field acoustic output in the specified direction. Sound level metrics are per-pulse and unweighted.

Direction	Peak source pressure level ($L_{s,pk}$; dB re 1 µPa m)	Per-pulse source SEL ($L_{s,E}$; dB 1 µPa^{2}m^{2}s)	
		10–2000 Hz	2000–25000 Hz
Broadside	249.2	224.5	184.0
Endfire	245.3	222.4	187.3
Vertical	255.2	228.0	194.6
Vertical (surface affected source level)	255.2	230.5	197.6

4.2. Per-pulse Sound Fields

This section presents the per-pulse sound fields in terms of maximum-over-depth SPL, SEL, PK, and seafloor PK and PK-PK. The different metrics are presented for the following reasons:

- SPL sound fields were used to determine the distances to marine mammal and turtle behavioural thresholds.
- Per-pulse SEL sound fields are used as inputs into the 24 h SEL scenario and to provide context for the range to 160 dB re 1 µPa^2·s, relevant for the EPBC Act Policy Statement 2.1 (DEWHA 2008).
- Per-pulse SEL sound fields are used as inputs into the 24 h SEL scenario and to provide context for the range to 160 dB re 1 µPa^2·s, relevant for the EPBC Act Policy Statement 2.1 (DEWHA 2008).
- Per-pulse SEL sound fields to determine the distances to the level associated with squid startle (inking) response (Fewtrell and McCauley 2012).
- PK metrics within the water column are relevant to thresholds and guidelines for marine mammals, sea turtles, fish, fish eggs and larvae (as well as plankton)
- PK metrics at the seafloor are relevant to guidelines for fish, fish eggs and larvae and the sound level for no effect on corals and sponges.
- PK-PK metrics at the seafloor are relevant to sound levels used in the assessment of effect on benthic invertebrates.

The maximum and 95% distances to per-pulse SEL and SPL metrics are presented in Tables 10 and 18. The SPL sound fields, and distances to relevant isopleths can be visualised on the contour maps presented in Figures 2–7. The SPL sound fields are also presented as vertical slices for selected azimuths along the endfire and broadside directions out to 20 km, with the airgun array in the centre (Figures 8–11).

Maximum distances to maximum-over-depth water column PK thresholds were calculated for three modelled single impulse sites, Sites 1, 4, and 6, and presented in Table 12. Seafloor sound levels were assessed at eight different representative depths and Tables 13–14 present the PK and PK-PK results. At these eight depths particle motion was also calculated.

4.2.1. Tabulated Results

4.2.1.1. Entire Water Column

Table 10. Maximum (R_{max}) and 95% ($R_{95\%}$) horizontal distances (in km) from the seismic source to modelled maximum-over-depth (also maximised over tow modelled tow direction) unweighted per-pulse sound exposure level (SEL) isopleths from the modelled single impulse sites, with water depth indicated.

Per-pulse SEL (L_E, dB re 1 µPa²·s)	Site 1 (25 m)		Site 2 (33 m)		Site 3 (30 m)		Site 4 (45 m)		Site 5 (47 m)		Site 6 (48 m)	
	R_{max}	$R_{95\%}$	R_{max}	$R_{95\%}$	R_{max}	$R_{95\%}$	R_{max}	$R_{95\%}$	R_{max}	$R_{95\%}$	R_{max}	$R_{95\%}$
190	0.08	0.07	0.07	0.06	0.07	0.06	0.06	0.06	0.06	0.06	0.06	0.06
180	0.30	0.26	0.30	0.26	0.30	0.26	0.28	0.22	0.30	0.23	0.26	0.23
170	1.10	0.87	1.20	0.95	1.22	1.00	1.14	0.91	1.06	0.92	1.12	0.92
162[1]	2.80	2.18	2.66	2.03	2.56	2.03	2.90	2.36	2.62	2.09	2.58	2.06
160[2]	3.38	2.70	3.24	2.44	3.20	2.38	3.38	2.80	3.22	2.54	3.20	2.52
150	7.70	6.21	8.12	6.72	8.31	6.74	9.52	7.44	8.08	6.28	8.21	6.27
140	19.2	14.9	17.8	14.6	19.1	15.7	22.9	17.7	23.8	19.0	23.2	18.7
130	54.4	48.4	49.6	40.9	51.2	43.2	48.0	36.8	46.9	40.7	49.7	41.5
120	73.1	61.0	98.6	62.4	75.8	61.6	82.4	65.8	99.2	72.9	99.4	69.7

[1] Startle response level for squid (Fewtrell and McCauley 2012).
[2] Low power zone assessment criteria DEWHA (2008).

Table 11. Maximum (R_{max}) and 95% ($R_{95\%}$) horizontal distances (in km) from the seismic source to modelled maximum-over-depth (also maximised over tow modelled tow direction) per-pulse sound pressure level (SPL) isopleths from the modelled single impulse sites, with water depth indicated.

SPL (L_p; dB re 1 µPa)	Site 1 (25 m)		Site 2 (33 m)		Site 3 (30 m)		Site 4 (45 m)		Site 5 (47 m)		Site 6 (48 m)	
	R_{max}	$R_{95\%}$	R_{max}	$R_{95\%}$	R_{max}	$R_{95\%}$	R_{max}	$R_{95\%}$	R_{max}	$R_{95\%}$	R_{max}	$R_{95\%}$
200	0.06	0.06	0.06	0.06	0.06	0.06	0.06	0.05	0.06	0.06	0.06	0.06
190	0.28	0.23	0.26	0.22	0.26	0.22	0.22	0.20	0.24	0.20	0.24	0.20
180	0.90	0.76	0.90	0.76	0.94	0.78	0.86	0.68	0.80	0.70	0.82	0.68
175[1]	1.52	1.19	1.56	1.24	1.58	1.25	1.28	1.03	1.26	1.06	1.28	1.01
170	2.86	2.30	2.72	2.17	2.74	2.16	2.18	1.70	2.02	1.64	2.00	1.59
166[2]	4.90	4.02	4.26	3.22	4.14	3.14	3.78	3.07	3.50	2.71	3.34	2.63
160[3]	9.20	7.68	7.64	6.32	7.65	6.32	8.04	6.54	6.51	5.10	6.58	5.05
150	19.9	16.6	16.7	13.6	17.7	14.6	20.7	16.2	20.7	16.0	20.5	16.4
145[4]	30.0	25.0	24.1	19.2	27.9	22.1	29.8	23.8	36.4	31.2	35.4	29.7
140	53.6	45.1	41.1	33.1	48.3	39.9	46.5	33.3	44.8	40.1	47.9	40.8
130	98.4	65.2	70.8	60.0	70.6	58.2	72.9	58.5	98.7	61.7	99.0	62.1

[1] Threshold for turtle behavioural disturbance from impulsive noise.
[2] Threshold for turtle behavioural response to impulsive noise (NSF 2011).
[3] Marine mammal behavioural threshold for impulsive sound sources (NOAA 2019).
[4] Human health assessment threshold derived from (Parvin 2005).

Table 12. Maximum (R_{max}) horizontal distances (in km) from the seismic source to modelled maximum-over-depth (also maximised over tow modelled tow direction) peak pressure level (PK) thresholds based on Southall et al. (2019) for marine mammals, and Popper et al. (2014) for fish and Finneran et al. (2017) for sea turtles, Sites 3 and 5), with water depth indicated.

Hearing group	PK threshold (L_{pk}; dB re 1 µPa)	Distance R_{max} (km)	
		Site 4 (30 m)	Site 6 (47 m)
Low-frequency cetaceans (PTS)	219	0.06	0.04
Low-frequency cetaceans (TTS)	213	0.15	0.11
High-frequency cetaceans (PTS)	230	–	–
High-frequency cetaceans (TTS)	224	–	–
Very-high-frequency cetaceans (PTS)	202	0.41	0.39
Very-high-frequency cetaceans (TTS)	196	0.84	0.76
Other Carnivores in Water (PTS)	232	–	–
Other Carnivores in Water (TTS)	226	–	–
Sea Turtles (PTS)	232	–	–
Sea Turtles (TTS)	226	–	–
Fish: No swim bladder (also applied to sharks)	213	0.15	0.11
Fish: Swim bladder not involved in hearing, Swim bladder involved in hearing Fish eggs, and larvae	207	0.27	0.24

A dash indicates the threshold is not reached within the limits of the modelling resolution (20 m).

4.2.1.2. Seafloor

Ranges presented at the seafloor (50 and 5 cm above the interface) provided in Tables 13 and 14 are different to those for the maximum-over-depth modelling results presented in Table 12. This is because the model used for the water column results, calculated using FWRAM do not represent the maximum sound levels at the seafloor close to the array. This is because FWRAM is based on a wide-angle parabolic equation (PE) algorithm which is valid to only approximately 70° down angle from the horizontal, and while it provides accurate predictions in the horizontal direction, it cannot predict sound levels directly under the array. The VSTACK model is used to determine the levels at the seafloor directly under the array, and due to seafloor interactions, these can be greater than those elsewhere in the water column.

Table 13. Maximum (R_{max}) horizontal distances (in m) from the seismic source to modelled seafloor (receiver located 50 cm above seafloor) peak pressure level thresholds (PK) at three water depths within the Operational Area.

Hearing group/animal type	PK threshold (L_{pk}; dB re 1 µPa)	Water Depth							
		10 m	12.5 m	15 m	20 m	25 m	30 m	40 m	50 m
		Distance R_{max} (m)							
Sound levels for sponges and corals[1]	226	6	7	9	15	13	13	*	*
Fish: No swim bladder (also applied to sharks)	213	50	48	59	66	70	57	65	71
Fish: Swim bladder not involved in hearing, Swim bladder involved in hearing Fish eggs, and larvae	207	98	126	93	104	113	105	117	120

[1] Heyward et al. (2018)
An asterisk indicates that the sound level was not reached.

Table 14. Maximum (R_{max}) horizontal distances (in m) from the seismic source to modelled seafloor (receiver located 5 cm above seafloor) peak-peak pressure levels (PK-PK) at three water depths within the Active Source Area. Results included in relation to benthic invertebrates.

PK-PK ($L_{pk\text{-}pk}$; dB re 1 µPa)	Water Depth							
	10 m	12.5 m	15 m	20 m	25 m	30 m	40 m	50 m
	Distance R_{max} (m)							
213[1,2,3]	83	73	85	90	92	94	103	86
212[2,3]	86	88	89	103	100	100	111	121
210[1,2]	101	130	123	110	122	136	120	133
209[1,2]	112	132	150	124	126	141	167	145
202[4]	206	251	292	228	247	254	276	228

[1] Day et al. (2019), lobster
[2] Day et al. (2016a), lobster and scallops
[3] Day et al. (2017), scallops.
[4] Payne et al. (2008), lobster

4.2.1.2.1. Particle Motion Metrics

Table 15. Maximum (R_{max}) horizontal distances (in m) from the 2495 in^3 to particle motion threshold: Peak acceleration magnitude level (m/s^2) threshold for benthic invertebrates 5 cm above the seafloor, with water depth indicated. Results included in relation to benthic invertebrates (Section 2.4.1).

Hearing group/animal type	Peak Acceleration Magnitude (m/s^2)	Water Depth							
		10 m	12.5 m	15 m	20 m	25 m	30 m	40 m	50 m
		Distance R_{max} (m)							
Benthic invertebrates	37.57	58	48	44	40	43	47	54	7

4.2.2. Sound Field Maps and Graphs

4.2.2.1. Sound Level Contour Maps

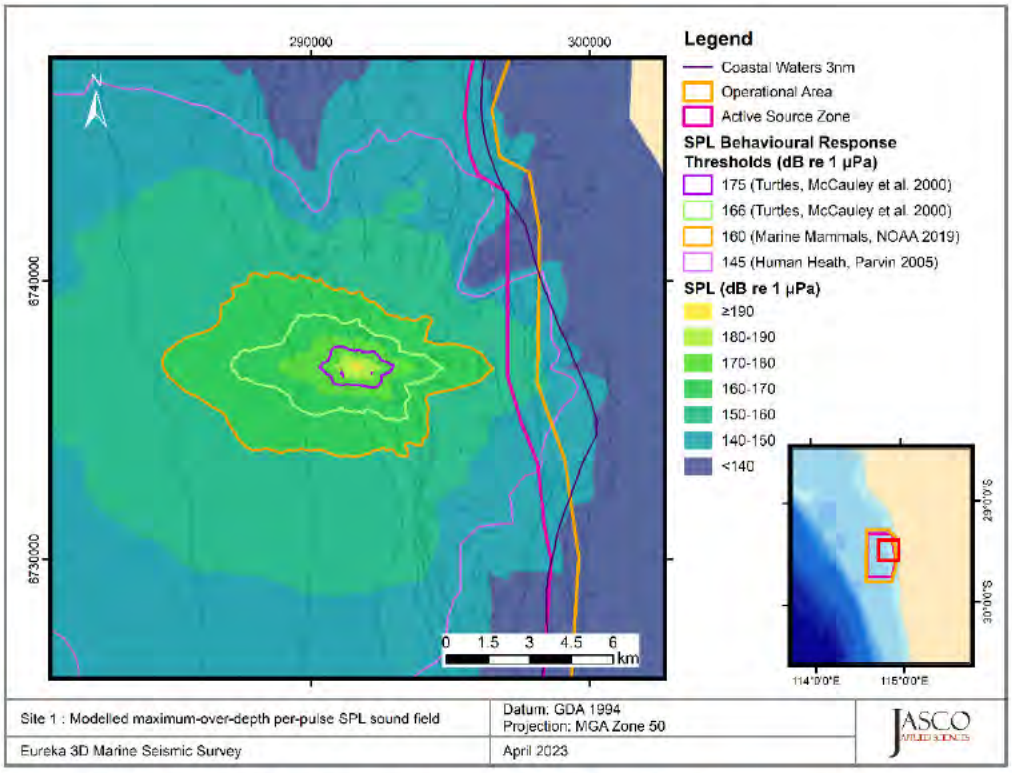


Figure 2. *Site 1, SPL, 2495 in^3 source, tow azimuth 0°*. Sound level contour map of unweighted maximum-over-depth sound field in 10 dB steps, and the isopleths for behavioural response thresholds for marine mammals and turtles.

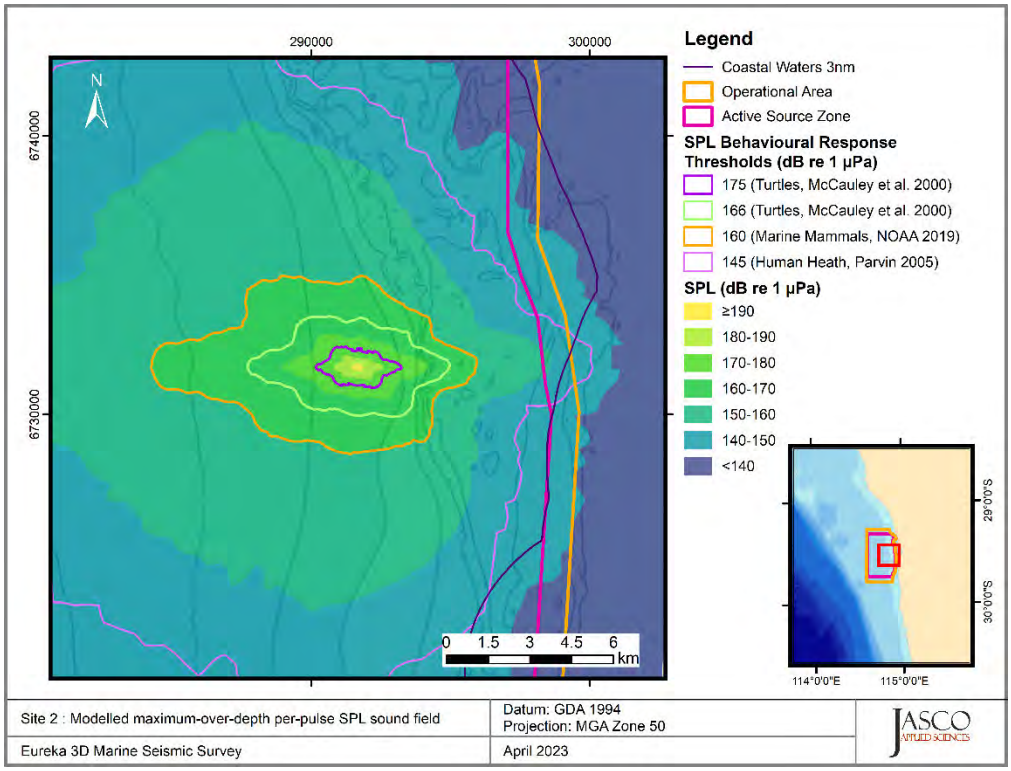


Figure 3. *Site 2, SPL, 2495 in³ source, tow azimuth 0°*: Sound level contour map of unweighted maximum-over-depth sound field in 10 dB steps, and the isopleths for behavioural response thresholds for marine mammals and turtles.

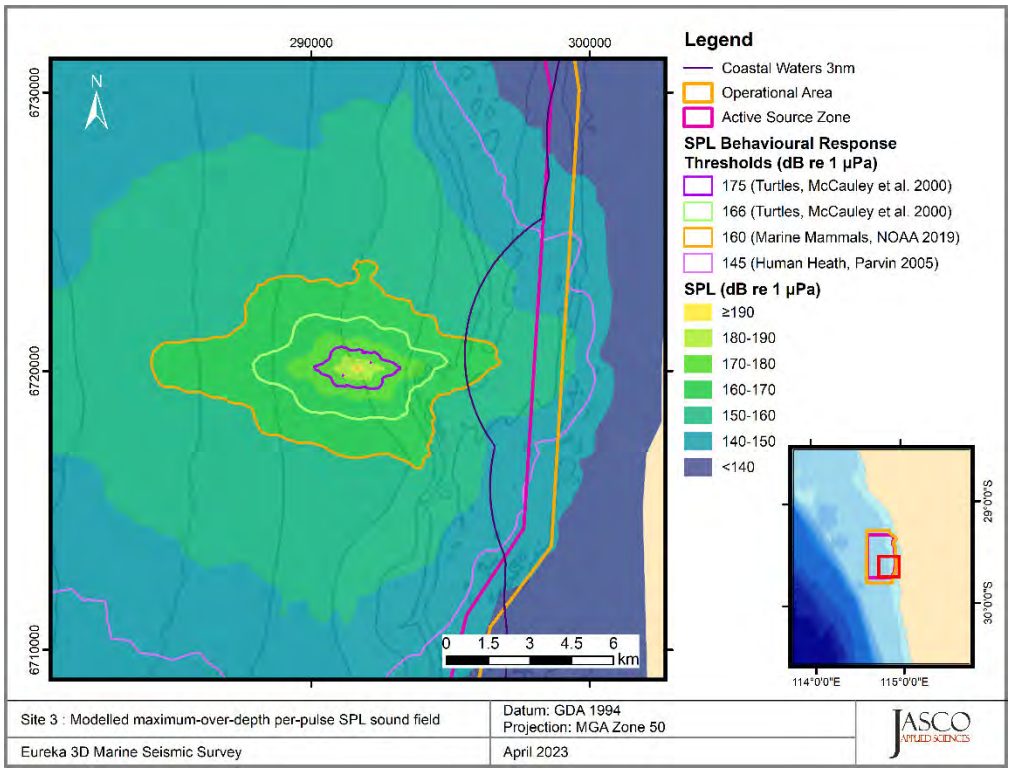


Figure 4. *Site 3, SPL, 2495 in³ source, tow azimuth 0°*: Sound level contour map of unweighted maximum-over-depth sound field in 10 dB steps, and the isopleths for behavioural response thresholds for marine mammals and turtles.

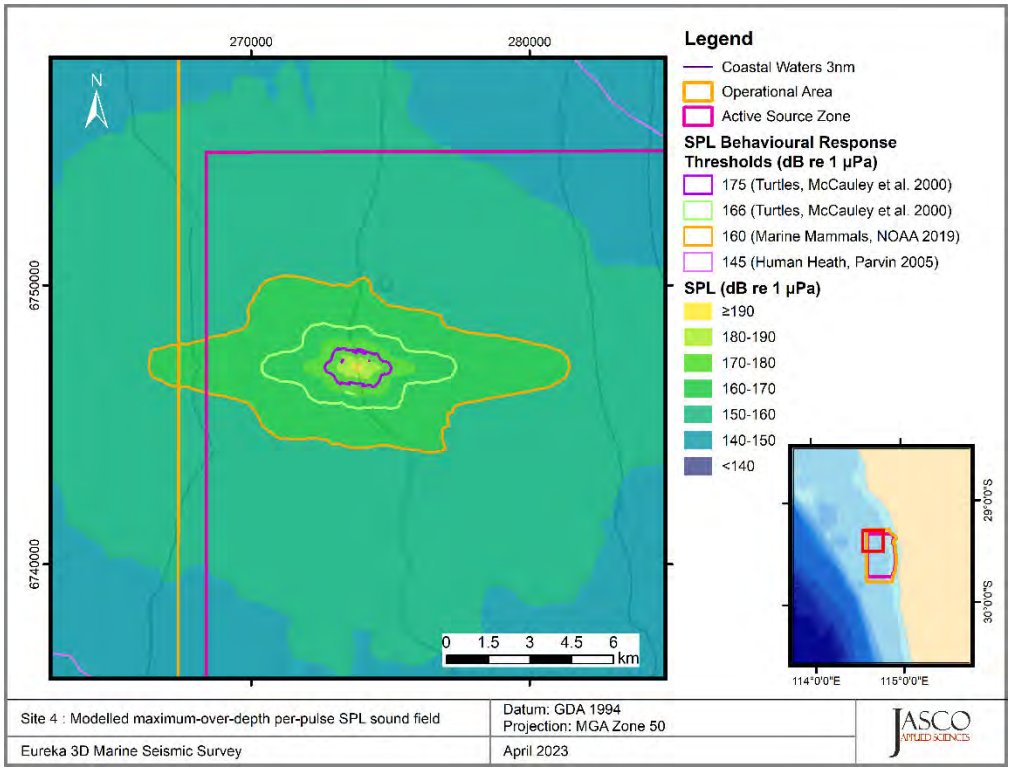


Figure 5. *Site 4, SPL, 2495 in³ source, tow azimuth 0°*: Sound level contour map of unweighted maximum-over-depth sound field in 10 dB steps, and the isopleths for behavioural response thresholds for marine mammals and turtles.

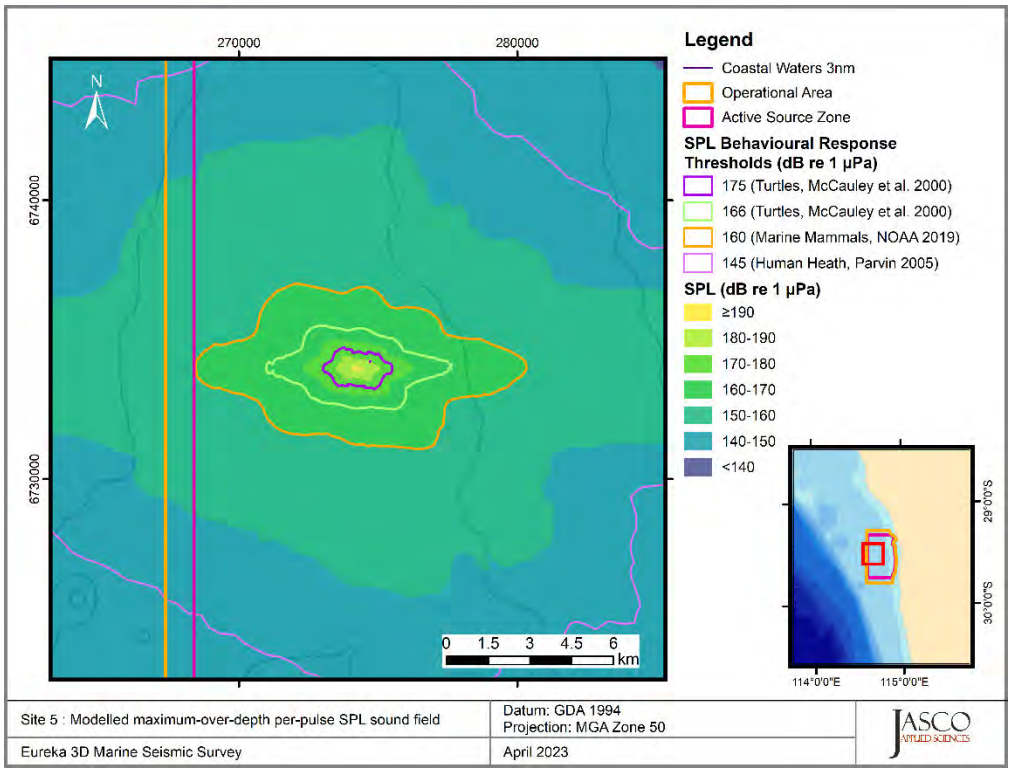


Figure 6. *Site 5, SPL, 2495 in³ source, tow azimuth 0°*: Sound level contour map of unweighted maximum-over-depth sound field in 10 dB steps, and the isopleths for behavioural response thresholds for marine mammals and turtles.

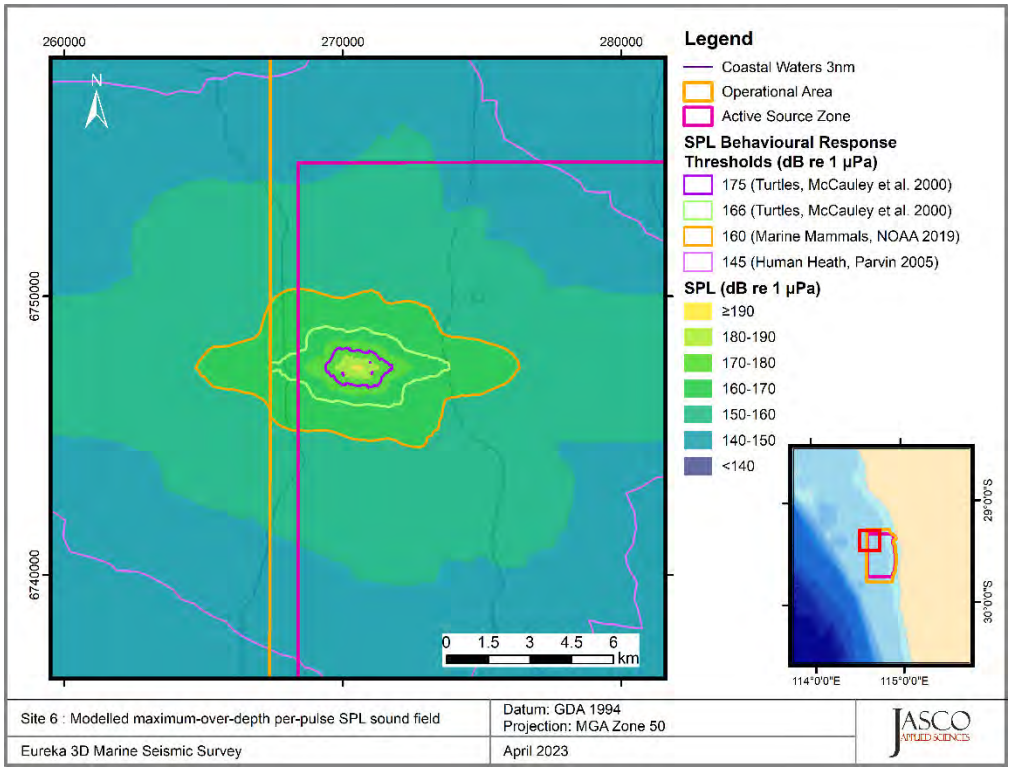


Figure 7. *Site 6, SPL, 2495 in³ source, tow azimuth 0°*: Sound level contour map of unweighted maximum-over-depth sound field in 10 dB steps, and the isopleths for behavioural response thresholds for marine mammals and turtles.

4.2.2.2. Sound Level Vertical Slices

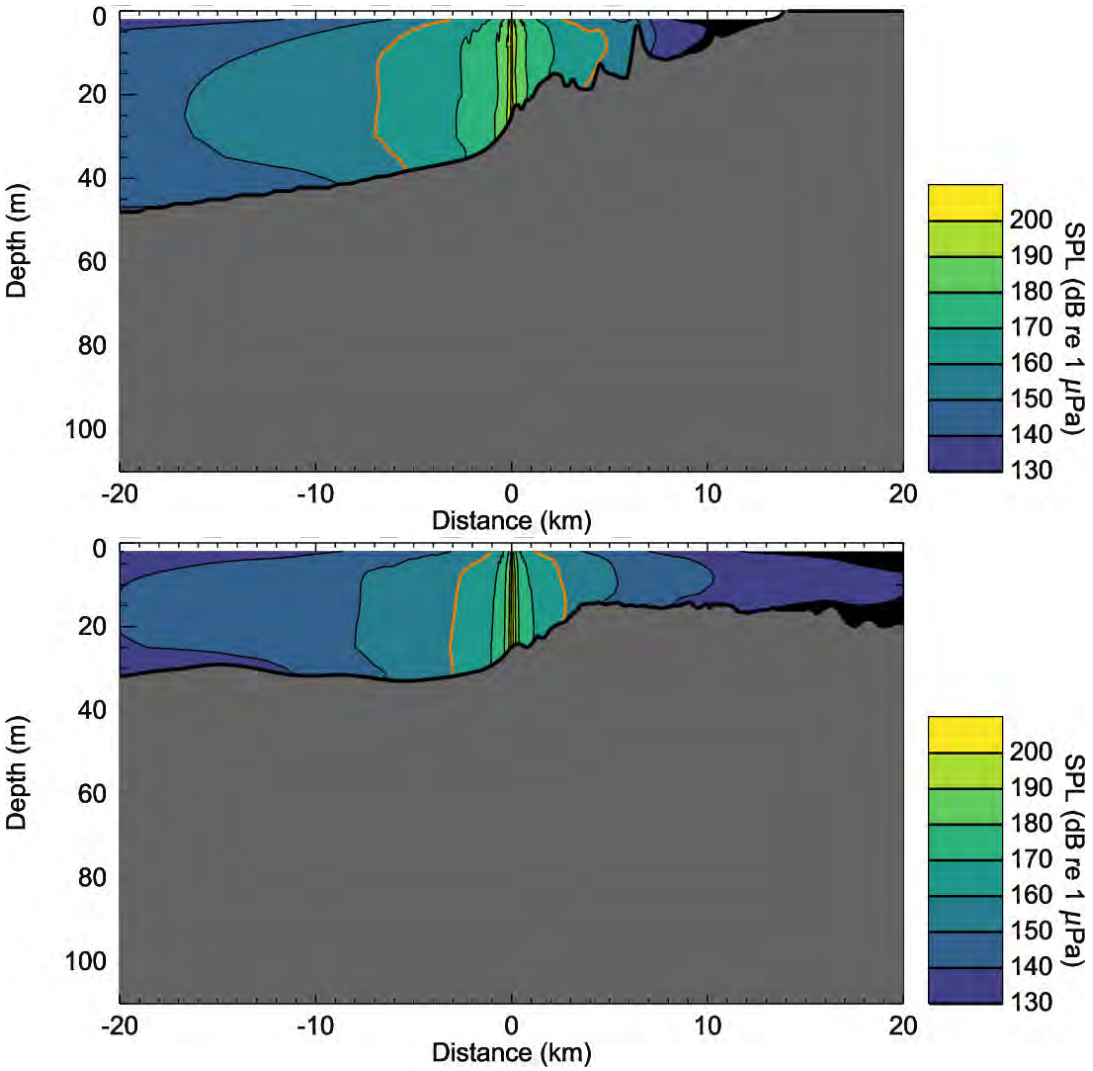


Figure 8. *Site 1, Scenario 1, tow azimuth 0°, SPL*: Sound level contours (vertical slice), perpendicular to (broadside, top) and along the tow direction (endfire, bottom). For context the behavioural response threshold for marine mammals is highlighted in orange. The positive distance direction in each slice is 90° clockwise from the tow azimuth for broadside, and the tow azimuth for the endfire slice.

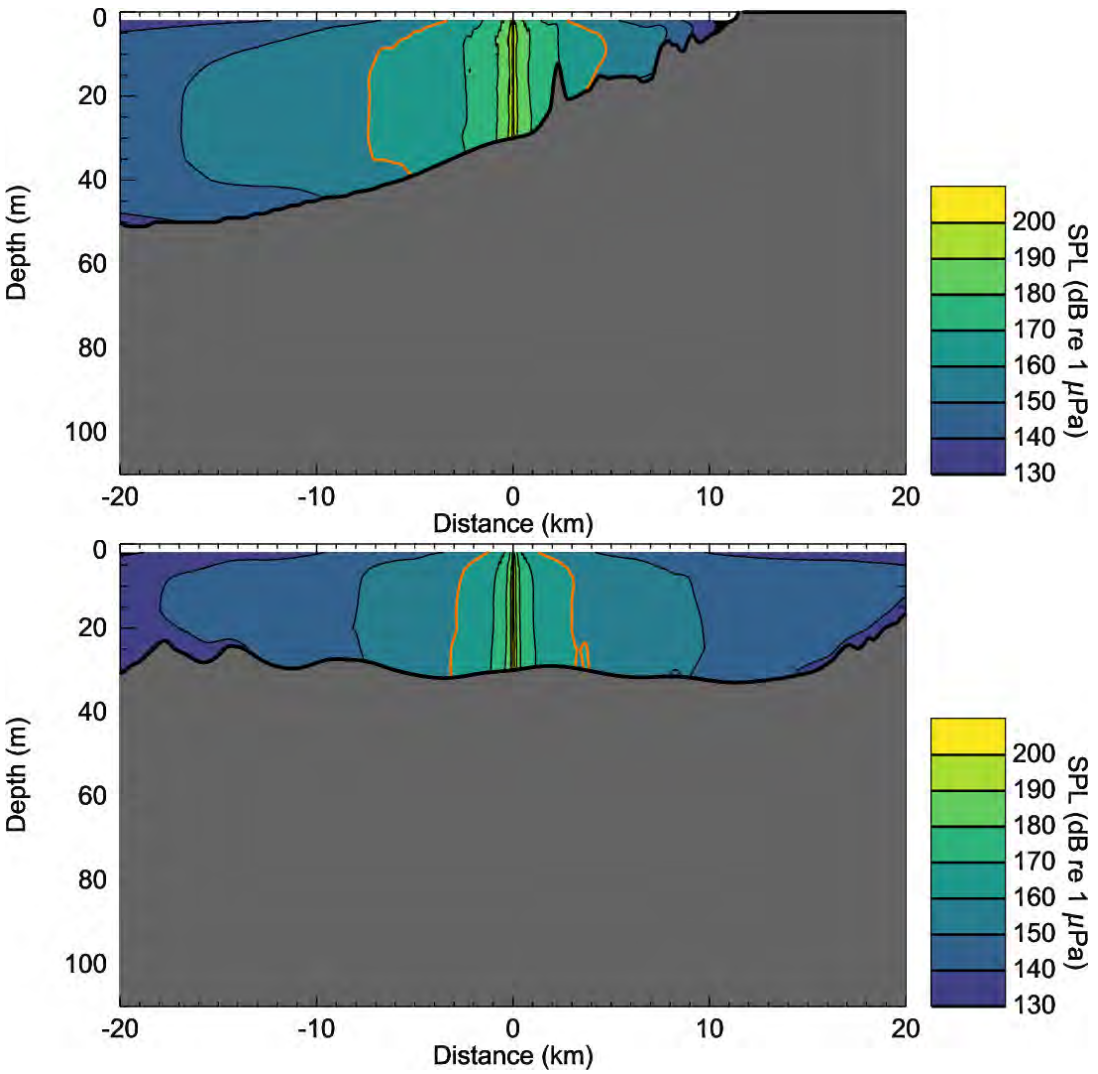


Figure 9. *Site 3, Scenario 1,tow azimuth 0°, SPL*: Sound level contours (vertical slice), perpendicular to (broadside, top) and along the tow direction (endfire, bottom). For context the behavioural response threshold for marine mammals is highlighted in orange. The positive distance direction in each slice is 90° clockwise from the tow azimuth for broadside, and the tow azimuth for the endfire slice.

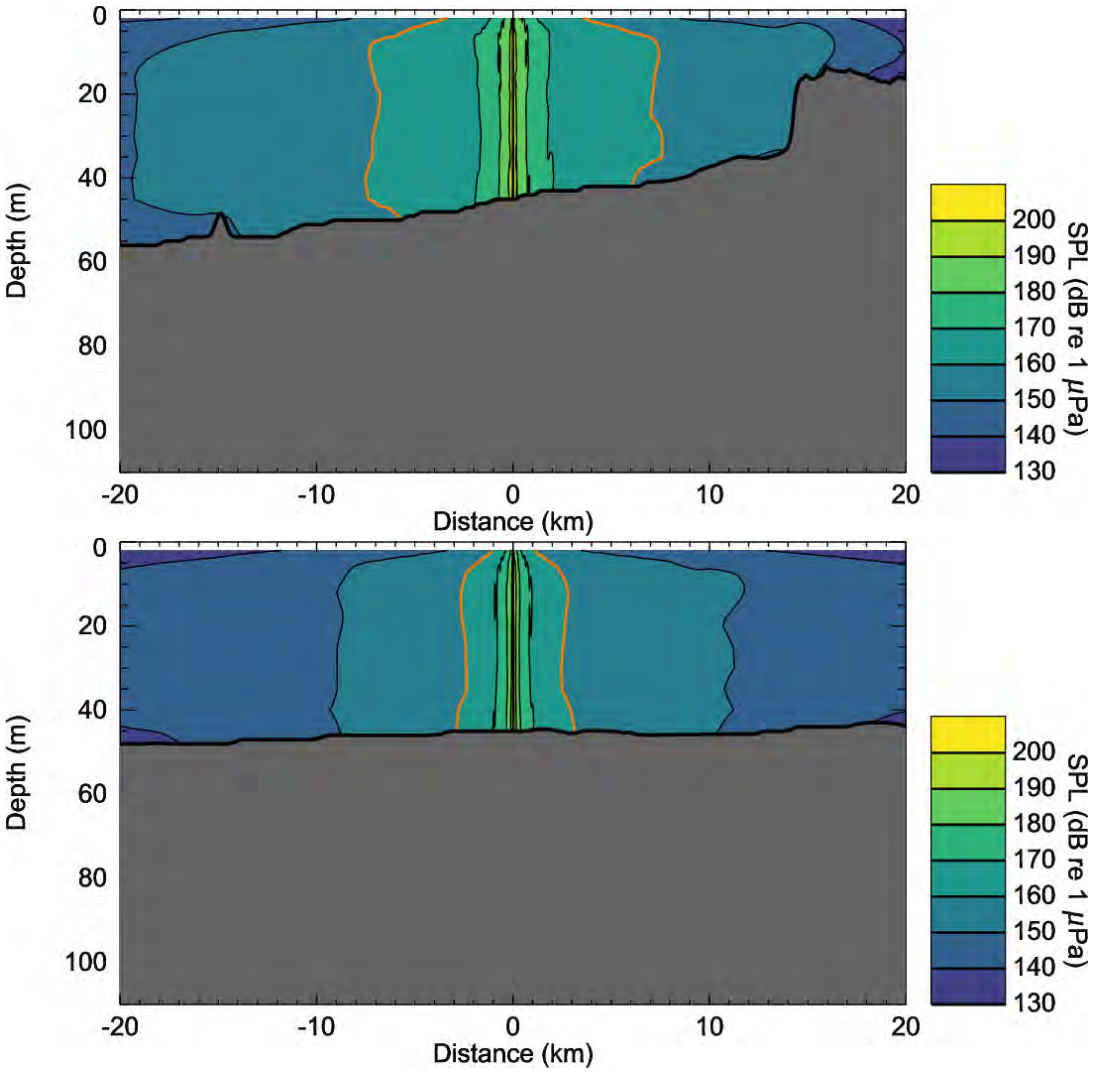


Figure 10. *Site 4, Scenario 2,tow azimuth 0°, SPL*: Sound level contours (vertical slice), perpendicular to (broadside, top) and along the tow direction (endfire, bottom). For context the behavioural response threshold for marine mammals is highlighted in orange. The positive distance direction in each slice is 90° clockwise from the tow azimuth for broadside, and the tow azimuth for the endfire slice.

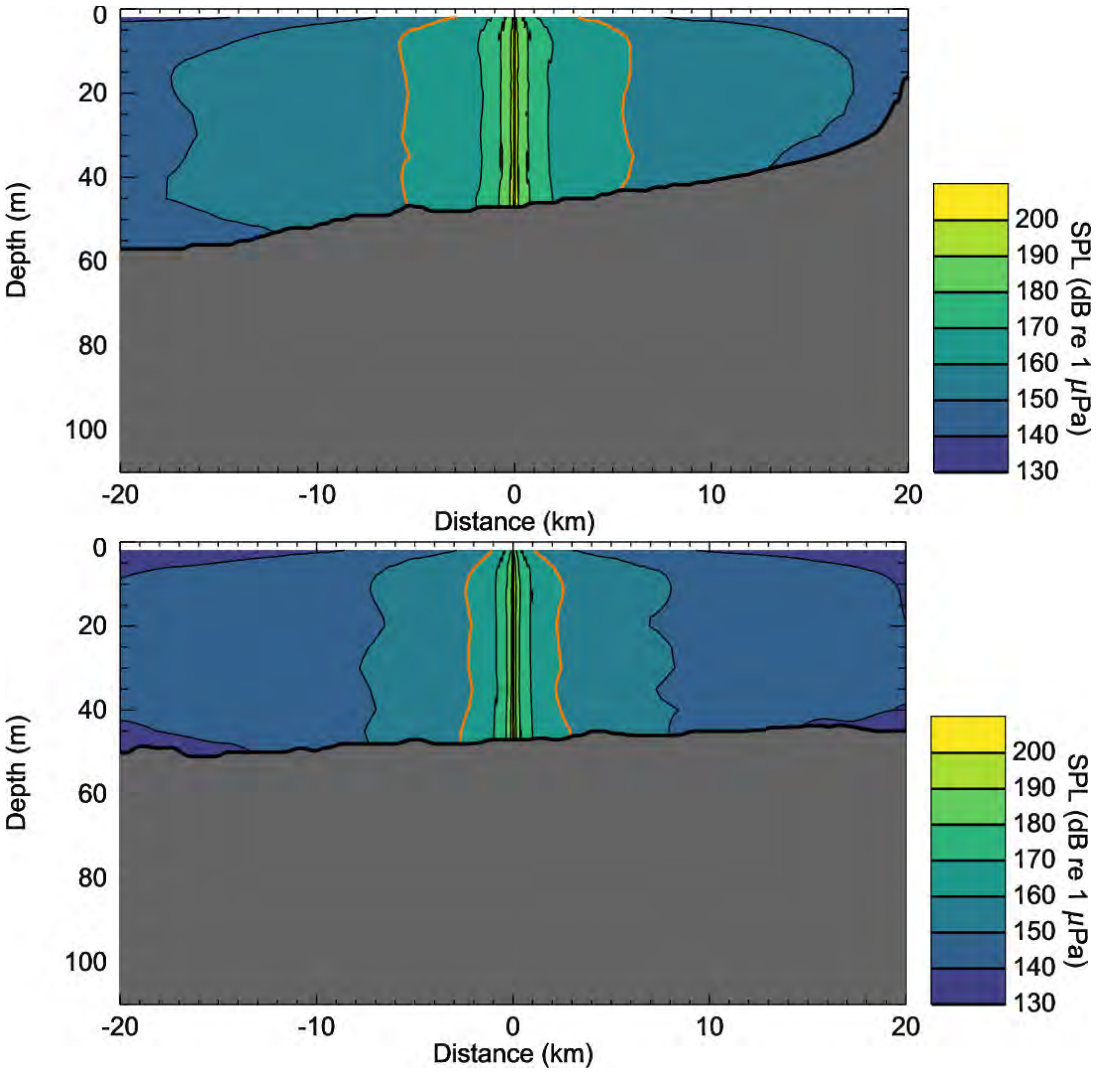


Figure 11. *Site 5, Scenario 2,tow azimuth 0°, SPL*: Sound level contours (vertical slice), perpendicular to (broadside, top) and along the tow direction (endfire, bottom). For context the behavioural response threshold for marine mammals is highlighted in orange. The positive distance direction in each slice is 90° clockwise from the tow azimuth for broadside, and the tow azimuth for the endfire slice.

4.3. Multiple Source Fields

This section presents the sound fields in terms of SEL accumulated over 24 hours of survey, for the two modelled scenarios (Section 1). Frequency-weighted SEL_{24h} sound fields were used to estimate the maximum horizontal distances (R_{max}) to marine mammal and sea turtle PTS and TTS thresholds (listed in Table 6), and to estimate maximum distance and the area for injury and TTS guidelines for fish (Tables 16–17).

The SEL_{24h} sound fields are presented as contour maps in Figures 12 and 13. These figures present the unweighted SEL_{24h} in 10 dB steps, as well as the isopleths corresponding to thresholds or guidelines for which R_{max} is greater than 20 m.

4.3.1. Tabulated Results

Table 16. Marine mammal and sea turtle criteria: Maximum (R_{max}) horizontal distances (in km) and ensonified area (km^2) from the survey lines to permanent threshold shift (PTS) and temporary threshold shift (TTS) thresholds considering 24 hours of survey activity (maximum-over-depth).

Hearing group	Weighted SEL thresholds ($L_{E,24h}$; dB re 1 $\mu Pa^2 \cdot s$)	Scenario 1		Scenario 2	
		R_{max} (km)	Area (km^2)	R_{max} (km)	Area (km^2)
PTS					
Low-frequency cetaceans	183	2.72	272	3.08	167
High-frequency cetaceans	185	-	-	–	–
Very-high-frequency cetaceans	155	0.06	5.68	0.06	6.19
Pinnipeds	203	-	-	–	–
Sea Turtles	204	0.06	5.68	0.06	6.19
TTS					
Low-frequency cetaceans	168	34.8	1884	43.0	2220
High-frequency cetaceans	170	0.06	3.91	0.06	5.56
Very-high-frequency cetaceans	140	0.44	58.7	0.42	37.2
Pinnipeds	188	0.06	4.71	0.06	5.56
Sea turtles	189	2.10	204	2.00	119.8

A dash indicates the threshold was not reached within the limits of the modelling resolution (20 m).

Table 17. *Fish criteria*: Maximum horizontal distances (R_{max}, in km) from the survey lines and area (km²) to injury and temporary threshold shift (TTS) thresholds considering 24 h of survey activity.

Marine fauna group	Threshold for SEL_{24h} ($L_{E,24h}$; dB re 1 µPa²·s)	Scenario 1		Scenario 2	
		R_{max} (km)	Area (km²)	R_{max} (km)	Area (km²)
Mortality and potential mortal injury					
I	219	0.06	4.71	0.06	4.75
II, fish eggs and larvae	210	0.06	5.68	0.06	6.19
III	207	0.06	5.68	0.06	6.19
Fish recoverable injury					
I	216	0.06	5.31	0.06	5.8
II, III	203	0.10	25.8	0.10	19.3
Fish TTS					
I, II, III	186	4.06	339	4.66	256

Fish I–No swim bladder; Fish II–Swim bladder not involved with hearing; Fish III–Swim bladder involved with hearing. An asterisk indicates that the sound level was not reached.

4.3.2. Sound Level Contour Maps

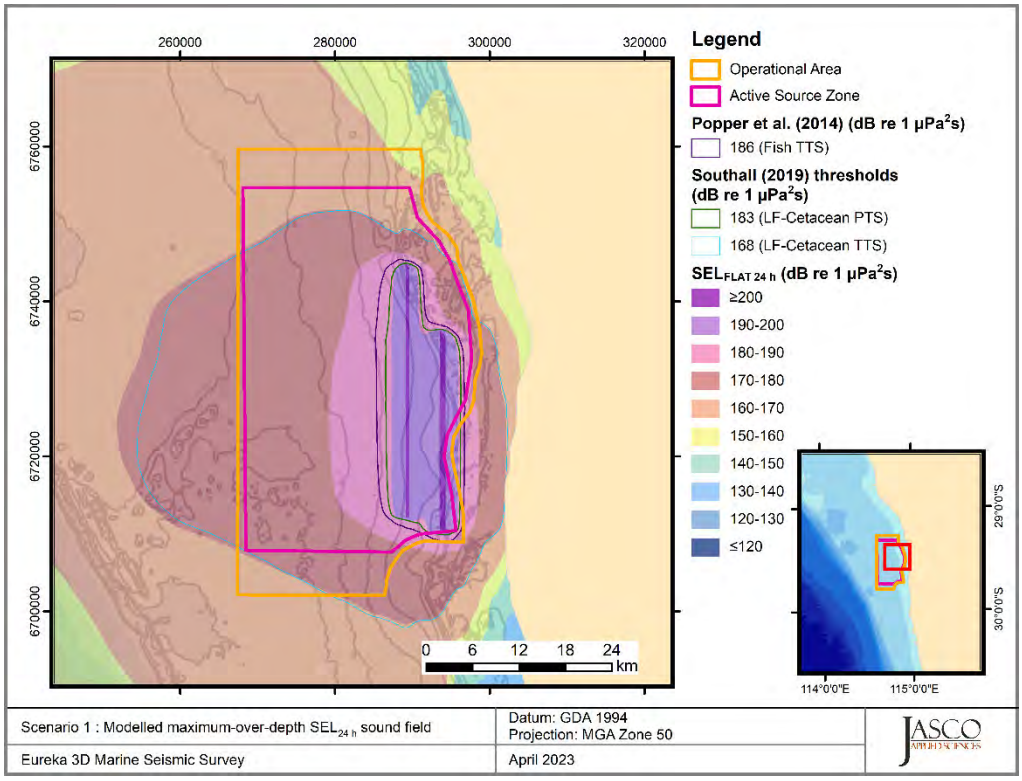


Figure 12. *Scenario 1*: Sound level contour map showing unweighted maximum-over-depth SEL_{24h}, along with thresholds for LF-cetaceans and fish. Thresholds omitted here were not reached or not large enough to display graphically. Refer to Tables 16 and 17 for tabulated radii.

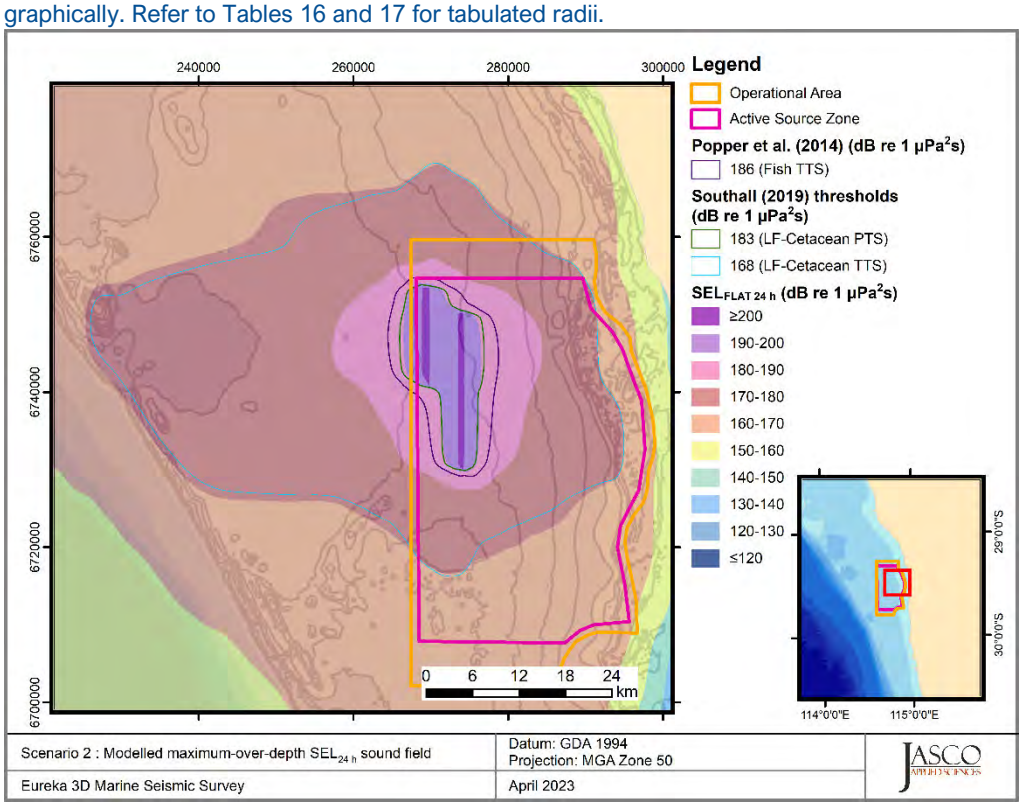


Figure 13. Scenario 2: Sound level contour map showing unweighted maximum-over-depth SEL_{24h}, along with thresholds for LF-cetaceans and fish. Thresholds omitted here were not reached or not large enough to display graphically. Refer to Tables 16 and 17 for tabulated radii.

5. Discussion and Summary

The modelling study predicted underwater sound levels associated with the planned Eureka 3D MSS. The underwater sound field was modelled for a 2495 in^3 seismic source within the active source area.

Most acoustic energy from a seismic source is output at lower frequencies, in the tens to hundreds of hertz. Most acoustic energy from a seismic source is output at lower frequencies, in the tens to hundreds of hertz. The modelled array had a pronounced broadside directivity for decidecade bands between ~100 to 400 Hz (Appendix B.3), which caused a noticeable axial bulge in the modelled acoustic footprints.

5.1. Per-Pulse Sound Fields

The Eureka 3D MSS covers an area that is close to the Western Australia coastline; this required specifically selected sites to capture the propagation effects associated with shallow water depths and bathymetric features. The per-pulse modelled sites span water depths from about 25 to 48 m across an assumed single geological region. Seafloor sound levels were assessed at eight different representative water depths. The bathymetry within vicinity of the active source area varied approximately between 10–60 m; however, along a westward transect the environment generally transitions from coastal shallow waters to relatively deeper waters of the continental shelf and then the continental slope. The frequency content of the seismic source coupled with the bathymetry had a considerable effect on propagation at longer distances, with larger lobes of sound energy extending into the deeper waters. The maximum-over-depth sound footprint maps and vertical slice plots (Sections 4.2.2.1 and 4.2.2.2) assist in demonstrating the influence of the bathymetry and seabed interactions on the sound field.

Furthermore, sites located in deeper water have a lower "cut-off frequency (f_c)" than sites in shallower coast water. The cut-off frequency is a single number that describes how much acoustic energy can propagate with minimal loss between the sea-surface and seafloor interfaces. For a given acoustic signal, frequencies below f_c are subject to higher loss compared to frequencies above the f_c (Jensen et al. 2011). For sources in waters greater than 30 m deep (i.e. sites associated with Scenario 2) the cut off frequency was less than 20 Hz. For these sites a comparatively larger amount of low-frequency energy can propagate in the water column compared to sources in shallow water below 30 m (i.e. sites associated with Scenario 1).

Based on available literature of the area, the seabed was modelled as a sand layer underlain by semi-cemented limestone/calcarenite. Acoustic propagation over calcarenite seabeds generally displayed higher rates of loss at distance away from the source as compared to seabeds that contain thick packages of unconsolidated sediments (Duncan et al. 2009). Literature suggests that the thickness of this layer is variable and could be on the order of several metres thick or in some locations non-existent(Duncan et al. 2008, Duncan et al. 2009, Fan et al. 2009). The distribution of sand layer is not well known and if the thickness of the sand layer is not as uniform as modelled then this variability could potentially lead to smaller radii if thinner or larger radii if thicker.

5.2. Multiple Pulse Sound Fields

The accumulated SEL over 24 hours of seismic source operation was modelled considering representative scenarios with a realistic acquisition pattern for the marine portion of the Eureka 3D MSS. The model methodology predicted the accumulation of sound energy, considering the change in location and the azimuth of the source at each pulse point, which was used to assess possible injury in marine mammals and the SEL_{24h} based fish and marine mammal criteria. The results were

presented as maps of the accumulated exposure levels and tabulated values of ranges to threshold levels and exposure areas for the given effects criteria (Section 2).

The footprints and range maxima for all SEL_{24h} criteria are substantially influenced by the location of single impulse modelled sites. As discussed above, the footprints and range maxima for all accumulated SEL thresholds within the survey area are primarily influenced by the high levels in the offshore direction due to deepening waters. This results in generally different isopleth and threshold distances for Scenarios 1 and 2.

5.3. Summary

A summary of predicted distances to criteria from acoustic modelling are presented below.

Marine mammals

The maximum distance for behavioural response based on NOAA (2019) criterion of 160 dB re 1 µPa (SPL) varied between 9.20 and 6.51 km depending on the site. All results can be found in Section 4.2.1.1. The results for marine mammal injury considered the criteria from Southall et al. (2019). These criteria contain two metrics (PK and SEL_{24h}), both required for the assessment of marine mammal PTS and TTS. The longest distance associated with either metric is required to be applied for assessment; Table 18 summarises the maximum distances, along with the relevant metric. Results for PK thresholds can be found in Section 4.2.1.1 and SEL_{24h} can be found in Section 4.3.1.

Table 18. Summary of maximum horizontal distance (R_{max}) for behavioural response thresholds, permanent threshold shift (PTS) and temporary threshold shift (TTS) for marine mammals. Maximum extents are in the broadside direction.

Hearing group	Maximum modelled distance to effect threshold (R_{max})		
	Behavioural response[1]	Impairment (km): PTS[2]	Impairment (km): TTS[2]
LF cetaceans (Baleen whales)	9.20	3.08 (SEL_{24h})	43.0 (SEL_{24h})
HF cetaceans (Dolphins, plus toothed, beaked, and bottlenose whales)		–	–
VHF cetaceans (*Kogia*, cephalorhynchid, and *L. australis*)		0.41 (PK)	0.84 (PK)
Pinnipeds (Australian sea lion, Australian fur seal, New Zealand fur seal)		–	0.06

Noise exposure criteria: [1] NOAA (2019) and [2] Southall et al. (2019).
A dash indicates the threshold was not reached within the limits of the modelling resolution (20 m).

Sea turtles

The PK sea turtle impairment criteria from Finneran et al. (2017) were not exceeded beyond the modelled resolution of 20 m. The maximum distance for PTS and TTS onset associated with the SEL_{24h} (Finneran et al. 2017) were respectively 0.06 and 2.10 km, and the behavioural response of turtles (McCauley et al. 2000) are summarised in Table 19. Results for PK and behavioural response thresholds can be found in Section 4.2.1.1 and SEL_{24h} can be found in Section 4.3.1.

Table 19. Summary of maximum horizontal distance (in km) to turtle behavioural response criteria, temporary threshold shift (TTS), and permanent threshold shift (PTS).

Hearing group	Maximum modelled distance (in km) to effect threshold (R_{max})			
	Behavioural response[1]	Behavioural disturbance[1]	Impairment: TTS[2]	Impairment: PTS[2]
Sea turtles	4.90 (166 dB re 1 µPa - SPL)	1.58 (175 dB re 1 µPa - SPL)	2.10 (SEL_{24h})	0.06 (SEL_{24h})

Noise exposure criteria: [1] McCauley et al. (2000) and [2] Finneran et al. (2017).

Fish, fish eggs, and fish larvae

This modelling study assessed the ranges for quantitative criteria based on Popper et al. (2014) and considered both PK (seafloor and water column) and SEL_{24h} metrics (water column) associated with mortality and potential mortal injury as well as impairment in the following groups:

- Fish without a swim bladder (also appropriate for sharks in the absence of other information),
- Fish with a swim bladder that do not use it for hearing,
- Fish that use their swim bladders for hearing,
- Fish eggs and fish larvae.

Table 20 summarises distances to effect criteria for fish, fish eggs, and fish larvae along with the relevant metric. Seafloor sound levels were assessed at nine different depths within the survey area. Assessment was based on Popper et al. (2014) and considered both PK (seafloor and water column, Sections 4.2.1.1 and 4.2.1.2) and SEL_{24h} metrics (water column, Section 4.3.1) associated with mortality, potential mortal injury and impairment.

Table 20. Summary of maximum onset distances for single impulse and 24 hour sound exposure level (SEL_{24h}) for fish, fish eggs, and larvae injury and temporary threshold shift (TTS).

Relevant hearing group	Effect criteria	Metric associated with longest distance to criteria	R_{max} (km)
Fish: No swim bladder	Recoverable injury	PK	0.15
	TTS	SEL_{24h}	4.06
Fish: Swim bladder not involved in hearing and Swim bladder involved in hearing	Recoverable injury	PK	0.27
	TTS	SEL_{24h}	4.06
Fish eggs, and larvae (relevant to plankton)	Injury	PK	0.27

Benthic invertebrates, Cephalopods, Sponges, and Coral

A full set of tabulated results can be found in Section 4.2.1.2; however, to summarise the potential effects on these receptors, the following results are provided:

- Crustaceans (representative of southern rock lobsters and crabs): The distance to no effect was reached between 206 and 292 m, based on 202 dB re 1 µPa PK-PK level from Payne et al. (2008).
- Bivalves (representative of scallops and mussels): The distance to no effect was reached between 54 and 7 m, based on a particle acceleration limit of 37.57 ms^{-2} at the seafloor as presented in Day et al. (2016a).
- Squid: The distance to the per–pulse SEL (L_E) startle (inking) response level of 162 dB re 1 μPa^2s for squid (Fewtrell and McCauley 2012) was reached between 2.90 and 2.03 km.
- Sponges and coral: The threshold was reached at a maximum of 15 m, based on the PK sound level criteria of 226 dB re 1 µPa PK for sponges and corals (Heyward et al. 2018).

Divers

An SPL human health assessment of 145 dB re 1 µPa (SPL; L_p) derived from Parvin (2005) was considered for people swimming and diving. The sound level was reached at ranges between 36.4 and 24.1 km depending on the modelled site. This is the maximum range over all modelled azimuths, and it is typically in orientated offshore. This maximum range should not be used as an offset distance to the coast and the sound field contour maps should be used to inform any such offset.

Glossary

1/3-octave

One third of an octave. *Note*: A one-third octave is approximately equal to one decidecade (1/3 oct ≈ 1.003 ddec).

1/3-octave-band

Frequency band whose bandwidth is one one-third octave. *Note*: The bandwidth of a one-third octave-band increases with increasing centre frequency.

absorption

The reduction of acoustic pressure amplitude due to acoustic particle motion energy converting to heat in the propagation medium.

attenuation

The gradual loss of acoustic energy from absorption and scattering as sound propagates through a medium.

audiogram

A graph or table of hearing threshold as a function of frequency that describes the hearing sensitivity of an animal over its hearing range.

auditory frequency weighting

The process of applying an auditory frequency weighting function. In human audiometry, C-weighting is the most commonly used function, an example for marine mammals are the auditory frequency weighting functions published by Southall et al. (2007).

auditory frequency weighting function

Frequency weighting function describing a compensatory approach accounting for a species' (or functional hearing group's) frequency-specific hearing sensitivity. Example hearing groups are low-, mid-, and high-frequency cetaceans, phocid and otariid pinnipeds.

azimuth

A horizontal angle relative to a reference direction, which is often magnetic north or the direction of travel. In navigation it is also called bearing.

bandwidth

The range of frequencies over which a sound occurs. Broadband refers to a source that produces sound over a broad range of frequencies (e.g., seismic airguns, vessels) whereas narrowband sources produce sounds over a narrow frequency range (e.g., sonar) (ANSI S1.13-2005 (R2010)).

bar

Unit of pressure equal to 100 kPa, which is approximately equal to the atmospheric pressure on Earth at sea level. 1 bar is equal to 10^5 Pa or 10^{11} µPa.

broadband level

The total level measured over a specified frequency range.

broadside direction

Perpendicular to the travel direction of a source. Compare with endfire direction.

cetacean

Any animal in the order Cetacea. These are aquatic species and include whales, dolphins, and porpoises.

compressional wave

A mechanical vibration wave in which the direction of particle motion is parallel to the direction of propagation. Also called primary wave or P-wave.

conductivity-temperature-depth (CTD)

Measurement data of the ocean's conductivity, temperature, and depth; used to compute sound speed and salinity.

decade

Logarithmic frequency interval whose upper bound is ten times larger than its lower bound (ISO 80000-3:2006).

decidecade

One tenth of a decade. *Note*: An alternative name for decidecade (symbol ddec) is "one-tenth decade". A decidecade is approximately equal to one third of an octave (1 ddec ≈ 0.3322 oct) and for this reason is sometimes referred to as a "one-third octave".

decidecade band

Frequency band whose bandwidth is one decidecade. *Note*: The bandwidth of a decidecade band increases with increasing centre frequency.

decibel (dB)

Unit of level used to express the ratio of one value of a power quantity to another on a logarithmic scale. Unit: dB.

endfire direction

Parallel to the travel direction of a source. Also see **broadside direction**.

energy source level

A property of a sound source obtained by adding to the sound exposure level measured in the far field the propagation loss from the acoustic centre of the source to the receiver position. Unit: decibel (dB). Reference value: 1 μPa^2m^2s.

energy spectral density

Ratio of energy (time-integrated square of a specified field variable) to bandwidth in a specified frequency band f_1 to f_2. In equation form, the energy spectral density E_f is given by:

$$E_f = \frac{2\int_{f_1}^{f_2} |X(f)|^2 \, \mathrm{d}f}{f_2 - f_1},$$

where $X(f)$ is the Fourier transform of the field variable $x(t)$

$$X(f) = \int_{-\infty}^{+\infty} x(t) \exp(-2\pi \mathrm{i} f t) \, \mathrm{d}t \, .$$

The field variable $x(t)$ is a scalar quantity, such as sound pressure. It can also be the magnitude or a specified component of a vector quantity such as sound particle displacement, sound particle velocity,

or sound particle acceleration. The unit of energy spectral density depends on the nature of x, as follows:

- If x = sound pressure: Pa^2 s/Hz
- If x = sound particle displacement: m^2 s/Hz
- If x = sound particle velocity: $(m/s)^2$ s/Hz
- If x = sound particle acceleration: $(m/s^2)^2$ s/Hz

The factor of two on the right-hand side of the equation for E_f is needed to express a spectrum that is symmetric about $f = 0$, in terms of positive frequencies only. See entry 3.1.3.9 of ISO 18405 (2017).

energy spectral density level

The level ($L_{E,f}$) of the **energy spectral density** (E_f). Unit: decibel (dB).

$$L_{E,f} := 10 \log_{10}\left(E_f / E_{f,0}\right) \text{dB} .$$

The frequency band and integration time should be specified.

As with **energy spectral density**, energy spectral density level can be expressed in terms of various field variables (e.g., sound pressure, sound particle displacement). The reference value ($E_{f,0}$) for energy spectral density level depends on the nature of field variable.

energy spectral density source level

A property of a sound source obtained by adding to the energy spectral density level of the sound pressure measured in the far field the propagation loss from the acoustic centre of the source to the receiver position. Unit: decibel (dB). Reference value: 1 $\mu Pa^2 m^2 s/Hz$.

ensonified

Exposed to sound.

far field

The zone where, to an observer, sound originating from an array of sources (or a spatially distributed source) appears to radiate from a single point.

Fourier transform (or Fourier synthesis)

A mathematical technique which, although it has varied applications, is referenced in the context of this report as a method used in the process of deriving a spectrum estimate from time-series data (or the reverse process, termed the inverse Fourier transform). A computationally efficient numerical algorithm for computing the Fourier transform is known as fast Fourier transform (FFT).

flat weighting

Term indicating that no frequency weighting function is applied. Synonymous with unweighted.

frequency

The rate of oscillation of a periodic function measured in cycles-per-unit-time. The reciprocal of the period. Unit: hertz (Hz). Symbol: f. 1 Hz is equal to 1 cycle per second.

frequency weighting

The process of applying a frequency weighting function.

frequency-weighting function

The squared magnitude of the sound pressure transfer function. For sound of a given frequency, the frequency weighting function is the ratio of output power to input power of a specified filter, sometimes expressed in decibels. Examples include the following:

- *Auditory frequency weighting function*: compensatory frequency weighting function accounting for a species' (or functional hearing group's) frequency-specific hearing sensitivity.
- *System frequency weighting function*: frequency weighting function describing the sensitivity of an acoustic acquisition system, typically consisting of a hydrophone, one or more amplifiers, and an analogue to digital converter.

functional hearing group

Category of animal species when classified according to their hearing sensitivity, hearing anatomy, and susceptibility to sound. For marine mammals, initial groupings were proposed by Southall et al. (2007), and revised groupings are developed as new research/data becomes available. Revised groupings proposed by Southall et al. (2019) include low-frequency cetaceans, high-frequency cetaceans, very high-frequency cetaceans, phocid carnivores in water, other carnivores in water, and sirenians. See auditory frequency weighting functions, which are often applied to these groups. Example hearing groups for fish include species for which the swim bladder is involved in hearing, species for which the swim bladder is not involved in hearing, and species without a swim bladder (Popper et al. 2014).

geoacoustic

Relating to the acoustic properties of the seabed.

hearing threshold

The sound pressure level for any frequency of the hearing group that is barely audible for a given individual for specified background noise during a specific percentage of experimental trials.

hertz (Hz)

A unit of frequency defined as one cycle per second.

high-frequency (HF) cetacean

See **functional hearing** group.

impulsive sound

Qualitative term meaning sounds that are typically transient, brief (less than 1 s), broadband, with rapid rise time and rapid decay. They can occur in repetition or as a single event. Examples of impulsive sound sources include explosives, seismic airguns, and impact pile drivers.

isopleth

A line drawn on a map through all points having the same value of some quantity.

knot

One nautical mile per hour. Symbol: kn.

level

A measure of a quantity expressed as the logarithm of the ratio of the quantity to a specified reference value of that quantity. Examples include sound pressure level, sound exposure level, and peak sound pressure level. For example, a value of sound exposure level with reference to 1 μPa^2 s can be written in the form *x* dB re 1 μPa^2 s.

low-frequency (LF) cetacean

See **functional hearing** group.

Monte Carlo simulation

The method of investigating the distribution of a non-linear multi-variate function by random sampling of all of its input variable distributions.

mysticete

A suborder of cetaceans that use baleen plates to filter food from water. Members of this group include rorquals (Balaenopteridae), right whales (Balaenidae), and grey whales (*Eschrichtius robustus*).

octave

The interval between a sound and another sound with double or half the frequency. For example, one octave above 200 Hz is 400 Hz, and one octave below 200 Hz is 100 Hz.

odontocete

The presence of teeth, rather than baleen, characterizes these whales. Members of the Odontoceti are a suborder of cetaceans, a group comprised of whales, dolphins, and porpoises. The skulls of toothed whales are mostly asymmetric, an adaptation for their echolocation. This group includes sperm whales, killer whales, belugas, narwhals, dolphins, and porpoises.

otariid

A common term used to describe members of the Otariidae, eared seals, commonly called sea lions and fur seals. Otariids are adapted to a semi-aquatic life; they use their large fore flippers for propulsion. Their ears distinguish them from phocids. Otariids are one of the three main groups in the superfamily Pinnipedia; the other two groups are phocids and walrus.

otariid pinnipeds in water (OPW)

See **functional hearing** group.

other marine carnivores in air (OCA)

See **functional hearing** group.

other marine carnivores in water (OCW)

See **functional hearing** group.

parabolic equation method

A computationally efficient solution to the acoustic wave equation that is used to model propagation loss. The parabolic equation approximation omits effects of back-scattered sound, simplifying the computation of propagation loss. The effect of back-scattered sound is negligible for most ocean-acoustic propagation problems.

particle acceleration

See **sound particle acceleration**.

particle displacement

See **sound particle displacement**.

particle motion

See **sound particle motion**.

particle velocity

See **sound particle velocity**.

peak sound pressure level (zero-to-peak sound pressure level)

The level ($L_{p,pk}$ or L_{pk}) of the squared maximum magnitude of the sound pressure (p_{pk}^2). Unit: decibel (dB). Reference value (p_0^2) for sound in water: 1 μPa^2.

$$L_{p,\mathrm{pk}} := 10\log_{10}\left(p_{\mathrm{pk}}^2/p_0^2\right)\mathrm{dB} = 20\log_{10}\left(p_{\mathrm{pk}}/p_0\right)\mathrm{dB}$$

The frequency band and time window should be specified. Abbreviation: PK or Lpk.

peak-to-peak sound pressure

The difference between the maximum and minimum sound pressure over a specified frequency band and time window. Unit: pascal (Pa).

permanent threshold shift (PTS)

An irreversible loss of hearing sensitivity caused by excessive noise exposure. PTS is considered auditory injury.

phocid

A common term used to describe all members of the family Phocidae. These true/earless seals are more adapted to in-water life than are otariids, which have more terrestrial adaptations. Phocids use their hind flippers to propel themselves. Phocids are one of the three main groups in the superfamily Pinnipedia; the other two groups are otariids and walrus.

phocid pinnipeds in water (PPW)

See **functional hearing** group.

pinniped

A common term used to describe all three groups that form the superfamily Pinnipedia: phocids (true seals or earless seals), otariids (eared seals or fur seals and sea lions), and walrus.

point source

A source that radiates sound as if from a single point.

power spectral density

Generic term, formally defined as power in a unit frequency band. Unit: watt per hertz (W/Hz). The term is sometimes loosely used to refer to the spectral density of other parameters such as squared sound pressure. ratio of **energy spectral density**, E_f, to time duration, Δt, in a specified temporal observation window. In equation form, the power spectral density P_f is given by:

$$P_f = \frac{E_f}{\Delta t}.$$

Power spectral density can be expressed in terms of various field variables (e.g., sound pressure, sound particle displacement).

power spectral density level

The level ($L_{P,f}$) of the **power spectral density** (P_f). Unit: decibel (dB).

$$L_{P,f} := 10 \log_{10}\left(P_f / P_{f,0}\right) \text{dB} .$$

The frequency band and integration time should be specified.

As with **power spectral density**, power spectral density level can be expressed in terms of various field variables (e.g., sound pressure, sound particle displacement). The reference value ($P_{f,0}$) for power spectral density level depends on the nature of field variable.

pressure, acoustic

The deviation from the ambient pressure caused by a sound wave. Also called sound pressure. Unit: pascal (Pa).

pressure, hydrostatic

The pressure at any given depth in a static liquid that is the result of the weight of the liquid acting on a unit area at that depth, plus any pressure acting on the surface of the liquid. Unit: pascal (Pa).

propagation loss (PL)

Difference between a source level (SL) and the level at a specified location, PL(x) = SL − L(x).

received level

The level measured (or that would be measured) at a defined location. The type of level should be specified.

reference values

standard underwater references values used for calculating sound **levels**, e.g., the reference value for expressing sound pressure level in decibels is 1 µPa.

Quantity	Reference value
Sound pressure	1 µPa
Sound exposure	1 µPa² s
Sound particle displacement	1 pm
Sound particle velocity	1 nm/s
Sound particle acceleration	1 µm/s²

shear wave

A mechanical vibration wave in which the direction of particle motion is perpendicular to the direction of propagation. Also called a secondary wave or S-wave. Shear waves propagate only in solid media, such as sediments or rock. Shear waves in the seabed can be converted to compressional waves in water at the water-seabed interface.

sound

A time-varying disturbance in the **pressure, stress, or material displacement** of a medium propagated by **local compression and expansion of the medium.**

sound exposure

Time integral of squared sound pressure over a stated time interval. The time interval can be a specified time duration (e.g., 24 h) or from start to end of a specified event (e.g., a pile strike, an airgun pulse, a construction operation). Unit: Pa² s.

sound exposure level

The level (L_E) of the sound exposure (E). Unit: decibel (dB). Reference value (E_0) for sound in water: 1 μPa^2 s.

$$L_E := 10 \log_{10}(E/E_0)\,\text{dB} = 20 \log_{10}\left(E^{1/2}/E_0^{1/2}\right)\,\text{dB}$$

The frequency band and integration time should be specified. Abbreviation: SEL.

sound exposure spectral density

Distribution as a function of frequency of the time-integrated squared sound pressure per unit bandwidth of a sound having a continuous spectrum. Unit: Pa^2 s/Hz.

sound field

Region containing sound waves.

sound intensity

Product of the sound pressure and the sound particle velocity. The magnitude of the sound intensity is the sound energy flowing through a unit area perpendicular to the direction of propagation per unit time.

sound particle acceleration

The rate of change of sound particle velocity. Unit: metre per second squared (m/s^2). Symbol: *a*.

sound particle motion

smallest volume of a medium that represents its mean physical properties.

sound particle displacement

Displacement of a material element caused by the action of sound, where a material element is the smallest element of the medium that represents the medium's mean density.

sound particle velocity

The velocity of a particle in a material moving back and forth in the direction of the pressure wave. Unit: metre per second (m/s). Symbol: *v*.

sound pressure

The contribution to total pressure caused by the action of sound.

sound pressure level (rms sound pressure level)

The level ($L_{p,\text{rms}}$) of the time-mean-square sound pressure (p^2_{rms}). Unit: decibel (dB). Reference value (p_0^2) for sound in water: 1 μPa^2.

$$L_{p,\text{rms}} := 10 \log_{10}(p^2_{\text{rms}}/p_0^2)\,\text{dB} = 20 \log_{10}(p_{\text{rms}}/p_0)\,\text{dB}$$

The frequency band and averaging time should be specified. Abbreviation: SPL or Lrms.

sound speed profile

The speed of sound in the water column as a function of depth below the water surface.

source level (SL)

A property of a sound source obtained by adding to the sound pressure level measured in the far field the propagation loss from the acoustic centre of the source to the receiver position. Unit: decibel (dB). Reference value: 1 μPa^2m^2.

spectrum

An acoustic signal represented in terms of its power, energy, mean-square sound pressure, or sound exposure distribution with frequency.

surface duct

The upper portion of a water column within which the sound speed profile gradient causes sound to refract upward and therefore reflect off the surface resulting in relatively long-range sound propagation with little loss.

temporary threshold shift (TTS)

Reversible loss of hearing sensitivity. TTS can be caused by noise exposure.

thermocline

The depth interval near the ocean surface that experiences temperature gradients due to warming or cooling by heat conduction from the atmosphere and by warming from solar heating.

unweighted

Term indicating that no frequency weighting function is applied. Synonymous with flat weighting.

very high-frequency (VHF) cetacean

See **functional hearing** group.

wavelength

Distance over which a wave completes one cycle of oscillation. Unit: metre (m). Symbol: λ.

Literature Cited

[ANSI] American National Standards Institute and [ASA] Acoustical Society of America. S1.13-2005 (R2010). *American National Standard: Measurement of Sound Pressure Levels in Air*. NY, USA. https://webstore.ansi.org/Standards/ASA/ANSIASAS1132005R2010.

[DEWHA] Department of the Environment, Water, Heritage, and the Arts (Australia). 2008. *EPBC Act Policy Statement 2.1 - Interaction Between Offshore Seismic Exploration and Whales*. 14 p. http://www.environment.gov.au/resource/epbc-act-policy-statement-21-interaction-between-offshore-seismic-exploration-and-whales.

[HESS] High Energy Seismic Survey. 1999. *High Energy Seismic Survey Review Process and Interim Operational Guidelines for Marine Surveys Offshore Southern California*. Prepared for the California State Lands Commission and the United States Minerals Management Service Pacific Outer Continental Shelf Region by the High Energy Seismic Survey Team, Camarillo, CA, USA. 98 p. https://ntrl.ntis.gov/NTRL/dashboard/searchResults/titleDetail/PB2001100103.xhtml.

[ISO] International Organization for Standardization. 2006. *ISO 80000-3:2006 Quantities and units – Part 3: Space and time*. https://www.iso.org/standard/31888.html.

[ISO] International Organization for Standardization. 2017. *ISO 18405:2017. Underwater acoustics – Terminology*. Geneva. https://www.iso.org/standard/62406.html.

[NMFS] National Marine Fisheries Service (US). 1998. *Acoustic Criteria Workshop*. Dr. Roger Gentry and Dr. Jeanette Thomas Co-Chairs.

[NMFS] National Marine Fisheries Service (US). 2016. *Technical Guidance for Assessing the Effects of Anthropogenic Sound on Marine Mammal Hearing: Underwater Acoustic Thresholds for Onset of Permanent and Temporary Threshold Shifts*. US Department of Commerce, NOAA. NOAA Technical Memorandum NMFS-OPR-55. 178 p.

[NMFS] National Marine Fisheries Service (US). 2018. *2018 Revision to: Technical Guidance for Assessing the Effects of Anthropogenic Sound on Marine Mammal Hearing (Version 2.0): Underwater Thresholds for Onset of Permanent and Temporary Threshold Shifts*. US Department of Commerce, NOAA. NOAA Technical Memorandum NMFS-OPR-59. 167 p. https://www.fisheries.noaa.gov/webdam/download/75962998.

[NOAA] National Oceanic and Atmospheric Administration (US). 2013. *Draft guidance for assessing the effects of anthropogenic sound on marine mammals: Acoustic threshold levels for onset of permanent and temporary threshold shifts*. National Oceanic and Atmospheric Administration, US Department of Commerce, and NMFS Office of Protected Resources, Silver Spring, MD, USA. 76 p.

[NOAA] National Oceanic and Atmospheric Administration (US). 2015. *Draft guidance for assessing the effects of anthropogenic sound on marine mammal hearing: Underwater acoustic threshold levels for onset of permanent and temporary threshold shifts*. NMFS Office of Protected Resources, Silver Spring, MD, USA. 180 p.

[NOAA] National Oceanic and Atmospheric Administration (US). 2016. *Document Containing Proposed Changes to the NOAA Draft Guidance for Assessing the Effects of Anthropogenic Sound on Marine Mammal Hearing: Underwater Acoustic Threshold Levels for Onset of Permanent and Temporary Threshold Shifts*. National Oceanic and Atmospheric Administration and US Department of Commerce. 24 p.

[NOAA] National Oceanic and Atmospheric Administration (US). 2018. Takes of Marine Mammals Incidental to Specified Activities; Taking Marine Mammals Incidental to Marine Site Characterization Surveys off of Delaware. *Federal Register* 83(65): 14417-14443. https://www.federalregister.gov/d/2018-12225.

[NOAA] National Oceanic and Atmospheric Administration (US). 2019. *ESA Section 7 Consultation Tools for Marine Mammals on the West Coast* (webpage), 27 Sep 2019. https://www.fisheries.noaa.gov/west-coast/endangered-species-conservation/esa-section-7-consultation-tools-marine-mammals-west.

[NSF] National Science Foundation (US). 2011. *Final Programmatic Environmental Impact Statement/Overseas. Environmental Impact Statement for Marine Seismic Research Funded by the National Science Foundation or Conducted by the US Geological Survey*. National Science Foundation, Arlington, VA, USA. https://www.nsf.gov/geo/oce/envcomp/usgs-nsf-marine-seismic-research/nsf-usgs-final-eis-oeis_3june2011.pdf.

[ONR] Office of Naval Research. 1998. *ONR Workshop on the Effect of Anthropogenic Noise in the Marine Environment*. Dr. R. Gisiner Chair.

Aerts, L.A.M., M. Blees, S.B. Blackwell, C.R. Greene, Jr., K.H. Kim, D.E. Hannay, and M.E. Austin. 2008. *Marine mammal monitoring and mitigation during BP Liberty OBC seismic survey in Foggy Island Bay, Beaufort Sea, July-August 2008: 90-day report*. Document Number P1011-1. Report by LGL Alaska Research Associates Inc., LGL Ltd., Greeneridge Sciences Inc., and JASCO Applied Sciences for BP Exploration Alaska. 199 p. ftp://ftp.library.noaa.gov/noaa_documents.lib/NMFS/Auke%20Bay/AukeBayScans/Removable%20Disk/P1011-1.pdf.

Ainslie, M.A. 2008. *Review of Published Safety Thresholds for Human Divers Exposed to Underwater Sound (Veilige maximale geluidsniveaus voor duikers-beoordeling van publicaties)*. Report Number TNO-DV-

2007-A598. DTIC Document, TNO Defence Security and Safety, The Hague (Netherlands). 17 p. http://www.dtic.mil/dtic/tr/fulltext/u2/a485758.pdf

ANSI S1.1-2013. R2013. *American National Standard Acoustical Terminology*. American National Standards Institute, NY, USA.

Austin, M.E. and G.A. Warner. 2012. *Sound Source Acoustic Measurements for Apache's 2012 Cook Inlet Seismic Survey*. Version 2.0. Technical report by JASCO Applied Sciences for Fairweather LLC and Apache Corporation.

Austin, M.E. and L. Bailey. 2013. *Sound Source Verification: TGS Chukchi Sea Seismic Survey Program 2013*. Document Number 00706, Version 1.0. Technical report by JASCO Applied Sciences for TGS-NOPEC Geophysical Company.

Austin, M.E., A. McCrodan, C. O'Neill, Z. Li, and A.O. MacGillivray. 2013. *Marine mammal monitoring and mitigation during exploratory drilling by Shell in the Alaskan Chukchi and Beaufort Seas, July–November 2012: 90-Day Report*. *In*: Funk, D.W., C.M. Reiser, and W.R. Koski (eds.). Underwater Sound Measurements. LGL Rep. P1272D–1. Report from LGL Alaska Research Associates Inc. and JASCO Applied Sciences, for Shell Offshore Inc., National Marine Fisheries Service (US), and US Fish and Wildlife Service. 266 pp plus appendices.

Austin, M.E. 2014. Underwater noise emissions from drillships in the Arctic. *In*: Papadakis, J.S. and L. Bjørnø (eds.). *UA2014 - 2nd International Conference and Exhibition on Underwater Acoustics*. 22-27 Jun 2014, Rhodes, Greece. pp. 257-263.

Austin, M.E., H. Yurk, and R. Mills. 2015. *Acoustic Measurements and Animal Exclusion Zone Distance Verification for Furie's 2015 Kitchen Light Pile Driving Operations in Cook Inlet*. Version 2.0. Technical report by JASCO Applied Sciences for Jacobs LLC and Furie Alaska.

Austin, M.E. and Z. Li. 2016. *Marine Mammal Monitoring and Mitigation During Exploratory Drilling by Shell in the Alaskan Chukchi Sea, July–October 2015: Draft 90-day report*. *In*: Ireland, D.S. and L.N. Bisson (eds.). Underwater Sound Measurements. LGL Rep. P1363D. Report from LGL Alaska Research Associates Inc., LGL Ltd., and JASCO Applied Sciences Ltd. For Shell Gulf of Mexico Inc, National Marine Fisheries Service, and US Fish and Wildlife Service. 188 pp + appendices.

Bartol, S.M. and D.R. Ketten. 2006. *Turtle and tuna hearing*. *In*: Swimmer, Y. and R. Brill. Volume December 2006. NOAA Technical Memorandum NMFS-PIFSC-7. 98-103 p. http://www.sefsc.noaa.gov/turtles/TM_NMFS_PIFSC_7_Swimmer_Brill.pdf#page=108.

Carnes, M.R. 2009. *Description and Evaluation of GDEM-V 3.0*. US Naval Research Laboratory, Stennis Space Center, MS. NRL Memorandum Report 7330-09-9165. 21 p. https://apps.dtic.mil/dtic/tr/fulltext/u2/a494306.pdf.

Collins, M.D. 1993. A split-step Padé solution for the parabolic equation method. *Journal of the Acoustical Society of America* 93(4): 1736-1742. https://doi.org/10.1121/1.406739.

Collins, M.D., R.J. Cederberg, D.B. King, and S. Chin-Bing. 1996. Comparison of algorithms for solving parabolic wave equations. *Journal of the Acoustical Society of America* 100(1): 178-182. https://doi.org/10.1121/1.415921.

Coppens, A.B. 1981. Simple equations for the speed of sound in Neptunian waters. *Journal of the Acoustical Society of America* 69(3): 862-863. https://doi.org/10.1121/1.382038.

Day, R.D., R.D. McCauley, Q.P. Fitzgibbon, K. Hartmann, J.M. Semmens, and Institute for Marine and Antarctic Studies. 2016a. *Assessing the Impact of Marine Seismic Surveys on Southeast Australian Scallop and Lobster Fisheries*. Impacts of Marine Seismic Surveys on Scallop and Lobster Fisheries. Fisheries Ressearch & Development Corporation. FRDC Project No 2012/008, University of Tasmania, Hobart. 159 p.

Day, R.D., R.D. McCauley, Q.P. Fitzgibbon, and J.M. Semmens. 2016b. Seismic air gun exposure during early-stage embryonic development does not negatively affect spiny lobster *Jasus edwardsii larvae* (Decapoda:Palinuridae). *Scientific Reports* 6: 1-9. https://doi.org/10.1038/srep22723.

Day, R.D., R.D. McCauley, Q.P. Fitzgibbon, K. Hartmann, and J.M. Semmens. 2017. Exposure to seismic air gun signals causes physiological harm and alters behavior in the scallop *Pecten fumatus*. *Proceedings of the National Academy of Sciences* 114(40): E8537-E8546. https://doi.org/10.1073/pnas.1700564114.

Day, R.D., R.D. McCauley, Q.P. Fitzgibbon, K. Hartmann, and J.M. Semmens. 2019. Seismic air guns damage rock lobster mechanosensory organs and impair righting reflex. *Proceedings of the Royal Society B* 286(1907). https://doi.org/10.1098/rspb.2019.1424.

Department of the Environment and Energy, NSW Government, and Queensland Government. 2017. *Recovery Plan for Marine Turtles in Australia*. https://www.environment.gov.au/marine/publications/recovery-plan-marine-turtles-australia-2017.

Dow Piniak, W.E., S.A. Eckert, C.A. Harms, and E.M. Stringer. 2012. *Underwater hearing sensitivity of the leatherback sea turtle (Dermochelys coriacea): Assessing the potential effect of anthropogenic noise*. Document Number 2012-01156. US Dept. of the Interior, Bureau of Ocean Energy Management, Headquarters. 35 p.

Dragoset, W.H. 1984. A comprehensive method for evaluating the design of airguns and airgun arrays. *16th Annual Offshore Technology Conference* Volume 3, 7–9 May 1984. OTC 4747, Houston, TX, USA. pp. 75–84. https://doi.org/10.4043/4783-MS.

Duncan, A., A. Gavrilov, and F. Li. 2009. Acoustic propagation over limestone seabeds. *ACOUSTICS*. University of Adelaide. pp. 1-6.
Duncan, A.J., A. Gavrilov, and T. Hu. 2008. Using offshore seismic surveys as acoustic sources of opportunity for geoacoustic inversion. *Journal of the Acoustical Society of America* 123(5): 3365.
Ellison, W.T. and P.J. Stein. 1999. *SURTASS LFA High Frequency Marine Mammal Monitoring (HF/M3) Sonar: Sustem Description and Test & Evaluation*. Under US Navy Contract N66604-98-D-5725. http://www.surtass-lfa-eis.com/wp-content/uploads/2018/02/HF-M3-Ellison-Report-2-4a.pdf.
Ellison, W.T. and A.S. Frankel. 2012. A common sense approach to source metrics. *In* Popper, A.N. and A.D. Hawkins (eds.). *The Effects of Noise on Aquatic Life*. Volume 730. Springer, New York. pp. 433-438. https://doi.org/10.1007/978-1-4419-7311-5_98.
Fan, L., A.J. Duncan, and A. Gavrilov. 2009. *Propagation and inversion of airgun signals in shallow water over a limestone seabed*. *Proceedings of the 3rd International Conference" Underwater Acoustic Measurements: Technologies and Results*. Citeseer.
Fewtrell, J.L. and R.D. McCauley. 2012. Impact of air gun noise on the behaviour of marine fish and squid. *Marine Pollution Bulletin* 64(5): 984-993. https://doi.org/10.1016/j.marpolbul.2012.02.009.
Fields, D.M., N.O. Handegard, J. Dalen, C. Eichner, K. Malde, Ø. Karlsen, A.B. Skiftesvik, C.M.F. Durif, and H.I. Browman. 2019. Airgun blasts used in marine seismic surveys have limited effects on mortality, and no sublethal effects on behaviour or gene expression, in the copepod *Calanus finmarchicus*. *ICES Journal of Marine Science*. https://doi.org/10.1093/icesjms/fsz126.
Finneran, J.J. and C.E. Schlundt. 2010. Frequency-dependent and longitudinal changes in noise-induced hearing loss in a bottlenose dolphin (*Tursiops truncatus*). *Journal of the Acoustical Society of America* 128(2): 567-570. https://doi.org/10.1121/1.3458814.
Finneran, J.J. and A.K. Jenkins. 2012. *Criteria and thresholds for U.S. Navy acoustic and explosive effects analysis*. SPAWAR Systems Center Pacific, San Diego, CA, USA. 64 p.
Finneran, J.J. 2015. *Auditory weighting functions and TTS/PTS exposure functions for cetaceans and marine carnivores*. Technical report by SSC Pacific, San Diego, CA, USA.
Finneran, J.J. 2016. *Auditory weighting functions and TTS/PTS exposure functions for marine mammals exposed to underwater noise*. Technical Report for Space and Naval Warfare Systems Center Pacific, San Diego, CA, USA. 49 p. http://www.dtic.mil/dtic/tr/fulltext/u2/1026445.pdf.
Finneran, J.J., E. Henderson, D.S. Houser, K. Jenkins, S. Kotecki, and J. Mulsow. 2017. *Criteria and Thresholds for U.S. Navy Acoustic and Explosive Effects Analysis (Phase III)*. Technical report by Space and Naval Warfare Systems Center Pacific (SSC Pacific). 183 p.
Fisher, F.H. and V.P. Simmons. 1977. Sound absorption in sea water. *Journal of the Acoustical Society of America* 62(3): 558-564. https://doi.org/10.1121/1.381574.
Fothergill, D.M., J.R. Sims, and M.D. Curley. 2001. Recreational SCUBA divers' aversion to low frequency underwater sound. *Undersea and Hyperbaric Medicine* 28(1): 9-18.
Funk, D., D.E. Hannay, D.S. Ireland, R. Rodrigues, and W.R. Koski (eds.). 2008. *Marine mammal monitoring and mitigation during open water seismic exploration by Shell Offshore Inc. in the Chukchi and Beaufort Seas, July–November 2007: 90-day report*. LGL Report P969-1. Prepared by LGL Alaska Research Associates Inc., LGL Ltd., and JASCO Research Ltd. for Shell Offshore Inc., National Marine Fisheries Service (US), and US Fish and Wildlife Service. 218 p.
Hannay, D.E. and R.G. Racca. 2005. *Sakhalin Energy: Acoustic Model Validation*. Technical report by JASCO Research Ltd. Version 1.3.
Heyward, A., J. Colquhoun, E. Cripps, D. McCorry, M. Stowar, B. Radford, K. Miller, I. Miller, and C. Battershill. 2018. No evidence of damage to the soft tissue or skeletal integrity of mesophotic corals exposed to a 3D marine seismic survey. *Marine Pollution Bulletin* 129(1): 8-13. https://doi.org/10.1016/j.marpolbul.2018.01.057.
Ireland, D.S., R. Rodrigues, D. Funk, W.R. Koski, and D.E. Hannay. 2009. *Marine mammal monitoring and mitigation during open water seismic exploration by Shell Offshore Inc. in the Chukchi and Beaufort Seas, July–October 2008: 90-Day Report*. Document Number P1049-1. 277 p.
James, N.P. and Y. Bone. 2010. *Neritic carbonate sediments in a temperate realm: southern Australia*. Springer Science & Business Media.
Jensen, F.B., W.A. Kuperman, M.B. Porter, and H. Schmidt. 2011. *Computational Ocean Acoustics*. 2nd edition. AIP Series in Modern Acourics and Signal Processing. AIP Press - Springer, New York. 794 p.
Jones, I.T., J.A. Stanley, and T.A. Mooney. 2020. Impulsive pile driving noise elicits alarm responses in squid (*Doryteuthis pealeii*). *Marine Pollution Bulletin* 150: 110792. https://doi.org/10.1016/j.marpolbul.2019.110792.
Landro, M. 1992. Modeling of GI gun signatures. *Geophysical Prospecting* 40: 721–747. https://doi.org/10.1111/j.1365-2478.1992.tb00549.x
Laws, R.M., L. Hatton, and M. Haartsen. 1990. Computer modeling of clustered airguns. *First Break* 8(9): 331–338.
Long, T.M., R.T. Hanlon, A. Ter Maat, and H.M. Pinsker. 1989. Non-associative learning in the squid Lolliguncula brevis (Mollusca, Cephalopoda). *Marine Behaviour and Physiology* 16: 1-9.

Lucke, K., U. Siebert, P. Lepper, A., and M.-A. Blanchet. 2009. Temporary shift in masked hearing thresholds in a harbor porpoise (*Phocoena phocoena*) after exposure to seismic airgun stimuli. *Journal of the Acoustical Society of America* 125(6): 4060-4070. https://doi.org/10.1121/1.3117443.

Lurton, X. 2002. *An Introduction to Underwater Acoustics: Principles and Applications*. Springer, Chichester, UK. 347 p.

MacGillivray, A.O. and N.R. Chapman. 2012. Modeling underwater sound propagation from an airgun array using the parabolic equation method. *Canadian Acoustics* 40(1): 19-25. https://jcaa.caa-aca.ca/index.php/jcaa/article/view/2502/2251.

MacGillivray, A.O. 2018. Underwater noise from pile driving of conductor casing at a deep-water oil platform. *Journal of the Acoustical Society of America* 143(1): 450-459. https://doi.org/10.1121/1.5021554.

Malme, C.I., P.R. Miles, C.W. Clark, P.L. Tyack, and J.E. Bird. 1984. *Investigations of the Potential Effects of Underwater Noise from Petroleum Industry Activities on Migrating Gray Whale Behavior. Phase II: January 1984 migration*. Report Number 5586. Report prepared by Bolt, Beranek and Newman Inc. for the US Department of the Interior, Minerals Management Service, Cambridge, MA, USA. 357 p. https://www.boem.gov/BOEM-Newsroom/Library/Publications/1983/rpt5586.aspx.

Martin, B., K. Bröker, M.-N.R. Matthews, J.T. MacDonnell, and L. Bailey. 2015. Comparison of measured and modeled air-gun array sound levels in Baffin Bay, West Greenland. *OceanNoise 2015*. 11-15 May 2015, Barcelona, Spain.

Martin, B., J.T. MacDonnell, and K. Bröker. 2017a. Cumulative sound exposure levels—Insights from seismic survey measurements. *Journal of the Acoustical Society of America* 141(5): 3603-3603. https://doi.org/10.1121/1.4987709.

Martin, S.B. and A.N. Popper. 2016. Short- and long-term monitoring of underwater sound levels in the Hudson River (New York, USA). *Journal of the Acoustical Society of America* 139(4): 1886-1897. https://doi.org/10.1121/1.4944876.

Martin, S.B., M.-N.R. Matthews, J.T. MacDonnell, and K. Bröker. 2017b. Characteristics of seismic survey pulses and the ambient soundscape in Baffin Bay and Melville Bay, West Greenland. *Journal of the Acoustical Society of America* 142(6): 3331-3346. https://doi.org/10.1121/1.5014049.

Matthews, M.-N.R. and A.O. MacGillivray. 2013. Comparing modeled and measured sound levels from a seismic survey in the Canadian Beaufort Sea. *Proceedings of Meetings on Acoustics* 19(1): 1-8. https://doi.org/10.1121/1.4800553

Mattsson, A. and M. Jenkerson. 2008. Single Airgun and Cluster Measurement Project. *Joint Industry Programme (JIP) on Exploration and Production Sound and Marine Life Proramme Review*. 28-30 Oct. International Association of Oil and Gas Producers, Houston, TX, USA.

McCauley, R.D., J. Fewtrell, A.J. Duncan, C. Jenner, M.-N. Jenner, J.D. Penrose, R.I.T. Prince, A. Adhitya, J. Murdoch, et al. 2000. *Marine seismic surveys: Analysis and propagation of air-gun signals; and effects of air-gun exposure on humpback whales, sea turtles, fishes and squid*. Report Number R99-15. Prepared for Australian Petroleum Production Exploration Association by Centre for Maine Science and Technology, Western Australia. 198 p. https://cmst.curtin.edu.au/wp-content/uploads/sites/4/2016/05/McCauley-et-al-Seismic-effects-2000.pdf.

McCauley, R.D., R.D. Day, K.M. Swadling, Q.P. Fitzgibbon, R.A. Watson, and J.M. Semmens. 2017. Widely used marine seismic survey air gun operations negatively impact zooplankton. *Nature Ecology & Evolution* 1(7): 1-8. https://doi.org/10.1038/s41559-017-0195.

McCrodan, A., C.R. McPherson, and D.E. Hannay. 2011. *Sound Source Characterization (SSC) Measurements for Apache's 2011 Cook Inlet 2D Technology Test*. Version 3.0. Technical report by JASCO Applied Sciences for Fairweather LLC and Apache Corporation. 51 p.

McPherson, C.R. and G.A. Warner. 2012. *Sound Sources Characterization for the 2012 Simpson Lagoon OBC Seismic Survey 90-Day Report*. Document Number 00443, Version 2.0. Technical report by JASCO Applied Sciences for BP Exploration (Alaska) Inc. http://www.nmfs.noaa.gov/pr/pdfs/permits/bp_openwater_90dayreport_appendices.pdf.

McPherson, C.R., K. Lucke, B.J. Gaudet, B.S. Martin, and C.J. Whitt. 2018. *Pelican 3-D Seismic Survey Sound Source Characterisation*. Document Number 001583. Version 1.0. Technical report by JASCO Applied Sciences for RPS Energy Services Pty Ltd.

McPherson, C.R. and B. Martin. 2018. *Characterisation of Polarcus 2380 in^3 Airgun Array*. Document Number 001599, Version 1.0. Technical report by JASCO Applied Sciences for Polarcus Asia Pacific Pte Ltd.

Nedwell, J.R. and A.W. Turnpenny. 1998. The use of a generic frequency weighting scale in estimating environmental effect. *Workshop on Seismics and Marine Mammals*. 23–25 Jun 1998, London, UK.

Nedwell, J.R., A.W. Turnpenny, J. Lovell, S.J. Parvin, R. Workman, J.A.L. Spinks, and D. Howell. 2007. *A validation of the dB$_{ht}$ as a measure of the behavioural and auditory effects of underwater noise*. Document Number 534R1231 Report prepared by Subacoustech Ltd. for the UK Department of Business, Enterprise and Regulatory Reform under Project No. RDCZ/011/0004. 74 p. https://tethys.pnnl.gov/sites/default/files/publications/Nedwell-et-al-2007.pdf.

O'Neill, C., D. Leary, and A. McCrodan. 2010. Sound Source Verification. (Chapter 3) *In* Blees, M.K., K.G. Hartin, D.S. Ireland, and D.E. Hannay (eds.). *Marine mammal monitoring and mitigation during open water seismic exploration by Statoil USA E&P Inc. in the Chukchi Sea, August-October 2010: 90-day report*.

LGL Report P1119. Prepared by LGL Alaska Research Associates Inc., LGL Ltd., and JASCO Applied Sciences Ltd. for Statoil USA E&P Inc., National Marine Fisheries Service (US), and US Fish and Wildlife Service. pp. 1-34.

Parvin, S. 2005. *Limits for underwater noise exposure of human divers and swimmers*. Subacoustech. Presented at the National Physics Laboratory Seminar on Underwater Acoustics, Teddington, UK. http://www.subacoustech.com/wp-content/uploads/NPLDiverNoisePresentation.pdf.

Parvin, S.J. 1998. The effects of low frequency underwater sound on divers. *Undersea Defence Technology*. Wembley, UK. pp. 227-232.

Payne, J.F., C. Andrews, L. Fancey, D. White, and J. Christian. 2008. *Potential Effects of Seismic Energy on Fish and Shellfish: An Update since 2003*. Report Number 2008/060. Canadian Science Advisory Secretariat. 22 p.

Payne, R. and D. Webb. 1971. Orientation by means of long range acoustic signaling in baleen whales. *Annals of the New York Academy of Sciences* 188: 110-141. https://doi.org/10.1111/j.1749-6632.1971.tb13093.x.

Pestorius, F.M., E.A. Cudahy, and D.M. Fothergill. 2009. Evolution of navy diver exposure standards for deterministic underwater sound in the 100-500 Hz band. *Meetings on Acoustics*. Volume 8(070002), 26-30 Oct 2009. Journal of the Acoustical Society of America, San Antonio, Texas. https://doi.org/10.1121/1.3280165.

Popper, A.N., A.D. Hawkins, R.R. Fay, D.A. Mann, S. Bartol, T.J. Carlson, S. Coombs, W.T. Ellison, R.L. Gentry, et al. 2014. *Sound Exposure Guidelines for Fishes and Sea Turtles: A Technical Report prepared by ANSI-Accredited Standards Committee S3/SC1 and registered with ANSI*. ASA S3/SC1.4 TR-2014. SpringerBriefs in Oceanography. ASA Press and Springer. https://doi.org/10.1007/978-3-319-06659-2.

Porter, M.B. and Y.-C. Liu. 1994. Finite-element ray tracing. *In*: Lee, D. and M.H. Schultz (eds.). *International Conference on Theoretical and Computational Acoustics*. Volume 2. World Scientific Publishing Co. pp. 947-956.

Racca, R.G., A.N. Rutenko, K. Bröker, and M.E. Austin. 2012a. A line in the water - design and enactment of a closed loop, model based sound level boundary estimation strategy for mitigation of behavioural impacts from a seismic survey. *11th European Conference on Underwater Acoustics*. Volume 34(3), Edinburgh, UK.

Racca, R.G., A.N. Rutenko, K. Bröker, and G. Gailey. 2012b. Model based sound level estimation and in-field adjustment for real-time mitigation of behavioural impacts from a seismic survey and post-event evaluation of sound exposure for individual whales. *In*: McMinn, T. (ed.). *Acoustics 2012*. Fremantle, Australia. http://www.acoustics.asn.au/conference_proceedings/AAS2012/papers/p92.pdf.

Racca, R.G., M.E. Austin, A.N. Rutenko, and K. Bröker. 2015. Monitoring the gray whale sound exposure mitigation zone and estimating acoustic transmission during a 4-D seismic survey, Sakhalin Island, Russia. *Endangered Species Research* 29(2): 131-146. https://doi.org/10.3354/esr00703.

Sims, J.R., D.M. Fothergill, and M.D. Curley. 1999. *Effects of a neoprene wetsuit hood on low-frequency underwater hearing thresholds*. *The Journal of the Acoustical Society of America*. Volume 105(2). 2, pp. 1298-1298. https://asa.scitation.org/doi/abs/10.1121/1.426183.

Southall, B.L., A.E. Bowles, W.T. Ellison, J.J. Finneran, R.L. Gentry, C.R. Greene, Jr., D. Kastak, D.R. Ketten, J.H. Miller, et al. 2007. Marine Mammal Noise Exposure Criteria: Initial Scientific Recommendations. *Aquatic Mammals* 33(4): 411-521. https://doi.org/10.1578/AM.33.4.2007.411.

Southall, B.L., D.P. Nowaceck, P.J.O. Miller, and P.L. Tyack. 2016. Experimental field studies to measure behavioral responses of cetaceans to sonar. *Endangered Species Research* 31: 293-315. https://doi.org/10.3354/esr00764.

Southall, B.L., J.J. Finneran, C. Reichmuth, P.E. Nachtigall, D.R. Ketten, A.E. Bowles, W.T. Ellison, D.P. Nowacek, and P.L. Tyack. 2019. Marine Mammal Noise Exposure Criteria: Updated Scientific Recommendations for Residual Hearing Effects. *Aquatic Mammals* 45(2): 125-232. https://doi.org/10.1578/AM.45.2.2019.125.

Southall, B.L., D.P. Nowacek, A.E. Bowles, V. Senigaglia, L. Bejder, and P.L. Tyack. 2021. Marine Mammal Noise Exposure Criteria: Assessing the Severity of Marine Mammal Behavioral Responses to Human Noise. *Aquatic Mammals* 47(5): 421-464. https://doi.org/10.1578/AM.47.5.2021.421.

Teague, W.J., M.J. Carron, and P.J. Hogan. 1990. A comparison between the Generalized Digital Environmental Model and Levitus climatologies. *Journal of Geophysical Research* 95(C5): 7167-7183. https://doi.org/10.1029/JC095iC05p07167.

Warner, G.A., C. Erbe, and D.E. Hannay. 2010. Underwater Sound Measurements. (Chapter 3) *In* Reiser, C.M., D. Funk, R. Rodrigues, and D.E. Hannay (eds.). *Marine Mammal Monitoring and Mitigation during Open Water Shallow Hazards and Site Clearance Surveys by Shell Offshore Inc. in the Alaskan Chukchi Sea, July-October 2009: 90-Day Report*. LGL Report P1112-1. Report by LGL Alaska Research Associates Inc. and JASCO Applied Sciences for Shell Offshore Inc., National Marine Fisheries Service (US), and Fish and Wildlife Service (US). pp. 1-54.

Warner, G.A., M.E. Austin, and A.O. MacGillivray. 2017. Hydroacoustic measurements and modeling of pile driving operations in Ketchikan, Alaska [Abstract]. *Journal of the Acoustical Society of America* 141(5): 3992. https://doi.org/10.1121/1.4989141.

Whiteway, T. 2009. *Australian Bathymetry and Topography Grid, June 2009*. GeoScience Australia, Canberra. http://pid.geoscience.gov.au/dataset/ga/67703.

Wood, J., B.L. Southall, and D.J. Tollit. 2012. *PG&E offshore 3-D Seismic Survey Project Environmental Impact Report–Marine Mammal Technical Draft Report*. SMRU Ltd. 121 p. https://www.coastal.ca.gov/energy/seismic/mm-technical-report-EIR.pdf.

Zhang, Z.Y. and C.T. Tindle. 1995. Improved equivalent fluid approximations for a low shear speed ocean bottom. *Journal of the Acoustical Society of America* 98(6): 3391-3396. https://doi.org/10.1121/1.413789.

Ziolkowski, A. 1970. A method for calculating the output pressure waveform from an air gun. *Geophysical Journal of the Royal Astronomical Society* 21(2): 137-161. https://doi.org/10.1111/j.1365-246X.1970.tb01773.x.

Zykov, M.M. and J.T. MacDonnell. 2013. *Sound Source Characterizations for the Collaborative Baseline Survey Offshore Massachusetts Final Report: Side Scan Sonar, Sub-Bottom Profiler, and the R/V Small Research Vessel experimental*. Document Number 00413, Version 2.0. Technical report by JASCO Applied Sciences for Fugro GeoServices, Inc. and the (US) Bureau of Ocean Energy Management.

Appendix A. Acoustic Metrics

A.1. Pressure Related Acoustic Metrics

Underwater sound pressure amplitude is measured in decibels (dB) relative to a fixed reference pressure of p_0 = 1 µPa. Because the perceived loudness of sound, especially pulsed sound such as from seismic airguns, pile driving, and sonar, is not generally proportional to the instantaneous acoustic pressure, several sound level metrics are commonly used to evaluate sound and its effects on marine life. Here we provide specific definitions of relevant metrics used in the accompanying report. Where possible, we follow the American National Standard Institute and International Organization for Standardization definitions and symbols for sound metrics (e.g., ISO 2017, ANSI R2013), but these standards are not always consistent.

The zero-to-peak sound pressure, or peak sound pressure (PK or $L_{p,pk}$; dB re 1 µPa), is the decibel level of the maximum instantaneous acoustic pressure in a stated frequency band attained by an acoustic pressure signal, $\mathrm{p}(\mathrm{t})$:

$$L_{p,\mathrm{pk}} = 10\log_{10}\frac{\max|p^2(t)|}{p_0^2} = 20\log_{10}\frac{\max|p(t)|}{p_0} \tag{A-1}$$

PK is often included as a criterion for assessing whether a sound is potentially injurious; however, because it does not account for the duration of an acoustic event, it is generally a poor indicator of perceived loudness.

The peak-to-peak sound pressure (PK-PK or $L_{p,pk\text{-}pk}$; dB re 1 µPa) is the difference between the maximum and minimum instantaneous sound pressure, possibly filtered in a stated frequency band, attained by an impulsive sound, $\mathrm{p}(\mathrm{t})$:

$$L_{p,\mathrm{pk\text{-}pk}} = 10\log_{10}\frac{[\max(p(t)) - \min(p(t))]^2}{p_0^2} \tag{A-2}$$

The sound pressure level (SPL or L_p; dB re 1 µPa) is the root-mean-square (rms) pressure level in a stated frequency band over a specified time window (T; s). It is important to note that SPL always refers to an rms pressure level and therefore not instantaneous pressure:

$$L_p = 10\log_{10}\left(\frac{1}{T}\int_T g(t)\,p^2(t)\,dt \Big/ p_0^2\right) \tag{A-3}$$

where $\mathrm{g}(\mathrm{t})$ is an optional time weighting function. In many cases, the start time of the integration is marched forward in small time steps to produce a time-varying SPL function. For short acoustic events, such as sonar pulses and marine mammal vocalizations, it is important to choose an appropriate time window that matches the duration of the signal. For in-air studies, when evaluating the perceived loudness of sounds with rapid amplitude variations in time, the time weighting function $\mathrm{g}(\mathrm{t})$ is often set to a decaying exponential function that emphasizes more recent pressure signals. This function mimics the leaky integration nature of mammalian hearing. For example, human-based fast time-weighted SPL ($L_{p,fast}$) applies an exponential function with time constant 125 ms. A related simpler approach used in underwater acoustics sets $\mathrm{g}(\mathrm{t})$ to a boxcar (unity amplitude) function of width 125 ms; the results can be referred to as $L_{p,boxcar\ 125ms}$. Another approach, historically used to evaluate SPL of impulsive signals underwater, defines $\mathrm{g}(\mathrm{t})$ as a boxcar function with edges set to the times corresponding to 5% and 95% of the cumulative square pressure function encompassing the duration of an impulsive acoustic event. This calculation is applied individually to each impulse signal, and the results are referred to as 90% SPL ($L_{p,90\%}$).

The sound exposure level (SEL or L_E; dB re 1 µPa²·s) is the time-integral of the squared acoustic pressure over a duration (T):

$$L_E = 10 \log_{10} \left(\int_T p^2(t)\, dt \Big/ T_0 p_0^2 \right) \quad \text{(A-4)}$$

where T_0 is a reference time interval of 1 s. SEL continues to increase with time when non-zero pressure signals are present. It is a dose-type measurement, so the integration time applied must be carefully considered for its relevance to impact to the exposed recipients.

SEL can be calculated over a fixed duration, such as the time of a single event or a period with multiple acoustic events. When applied to pulsed sounds, SEL can be calculated by summing the SEL of the N individual pulses. For a fixed duration, the square pressure is integrated over the duration of interest. For multiple events, the SEL can be computed by summing (in linear units) the SEL of the N individual events:

$$L_{E,N} = 10 \log_{10} \sum_{i=1}^{N} 10^{\frac{L_{E,i}}{10}} \quad \text{(A-5)}$$

If applied, the frequency weighting of an acoustic event should be specified, as in the case of weighted SEL (e.g., $L_{E,LF,24h}$; see Appendix A.5) or auditory-weighted SPL ($L_{p,ht}$). The use of fast, slow, or impulse exponential-time-averaging or other time-related characteristics should also be specified.

A.2. Particle Acceleration and Velocity Metrics

Since sound is a mechanical wave, it can also be measured in terms of the vibratory motion of fluid particles. Particle motion can be measured in terms of three different (but related) quantities: displacement, velocity, or acceleration. Acoustic particle velocity is the time derivative of particle displacement, and likewise acceleration is the time derivative of velocity. For the present study, acoustic particle motion has been reported in terms of acceleration and velocity.

The particle velocity (v) is the physical speed of a particle in a material moving back and forth in the direction of the pressure wave. It can be derived from the pressure gradient and Euler's linearised momentum equation where ρ_0 is the density of the medium:

$$v = -\int \nabla p(t) dt / \rho_0 \quad \text{(A-6)}$$

The particle acceleration (a) is the rate of change of the velocity with respect to time, and it can be obtained from equation A-6 as:

$$a = \frac{dv}{dt} = -\frac{\nabla p(t)}{\rho_0} \quad \text{(A-7)}$$

Unlike sound pressure, particle motion is a vector quantity, meaning that it has both magnitude and direction: at any given point in space, acoustic particle motion has three different time-varying components (x, y, and z). Given the particle velocity in the x, y, and z, directions, v_x, v_y, and v_z, the particle velocity magnitude $|v|$ is computed per the Pythagorean equation:

$$|v| = \sqrt{v_x + v_y + v_z} \quad \text{(A-8)}$$

The magnitude of particle acceleration is calculated similarly from the particle acceleration in the *x*, *y*, and *z* directions.

A.3. Decidecade Band Analysis

The distribution of a sound's power with frequency is described by the sound's spectrum. The sound spectrum can be split into a series of adjacent frequency bands. Splitting a spectrum into 1 Hz wide bands, called passbands, yields the power spectral density of the sound. This splitting of the spectrum into passbands of a constant width of 1 Hz, however, does not represent how animals perceive sound.

Because animals perceive exponential increases in frequency rather than linear increases, analysing a sound spectrum with passbands that increase exponentially in size better approximates real-world scenarios. In underwater acoustics, a spectrum is commonly split into decidecade bands, which are one tenth of a decade wide. They are approximately one third of an octave (base 2) wide and are therefore often referred to as 1/3-octave-bands. Each octave represents a doubling in sound frequency. The centre frequency of the ith band, $f_c(i)$, is defined as:

$$f_c(i) = 10^{\frac{i}{10}} \text{ kHz} \tag{A-9}$$

and the low (f_{lo}) and high (f_{hi}) frequency limits of the ith decade band are defined as:

$$f_{lo,i} = 10^{\frac{-1}{20}} f_c(i) \quad \text{and} \quad f_{hi,i} = 10^{\frac{1}{20}} f_c(i) \tag{A-10}$$

The decidecade bands become wider with increasing frequency, and on a logarithmic scale the bands appear equally spaced (Figure A-1). The acoustic modelling spans from band 7 (f_c (7) = 5 Hz) to band 44 ($f_c(44)$ = 25 kHz).

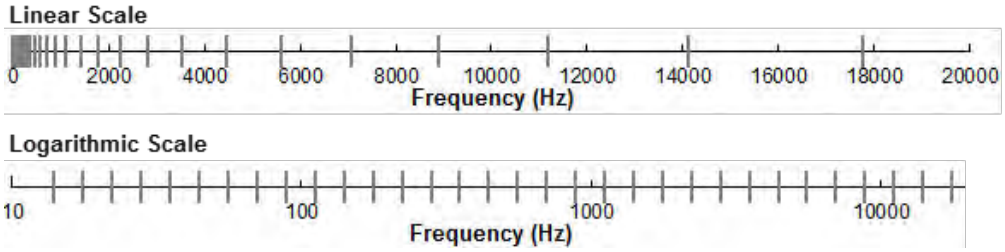


Figure A-1. Decidecade frequency bands (vertical lines) shown on a linear frequency scale and a logarithmic scale.

The sound pressure level in the ith band ($L_{p,i}$) is computed from the spectrum $S(f)$ between $f_{lo,i}$ and $f_{hi,i}$:

$$L_{p,i} = 10 \log_{10} \int_{f_{lo,i}}^{f_{hi,i}} S(f)\, df \tag{A-11}$$

Summing the sound pressure level of all the bands yields the broadband sound pressure level:

$$\text{Broadband SPL} = 10 \log_{10} \sum_i 10^{\frac{L_{p,i}}{10}} \tag{A-12}$$

Figure A-2 shows an example of how the decidecade band sound pressure levels compare to the sound pressure spectral density levels of an ambient noise signal. Because the decidecade bands are wider with increasing frequency, the decidecade band SPL is higher than the spectral levels at higher frequencies. Acoustic modelling of decidecade bands requires less computation time than 1 Hz bands and still resolves the frequency-dependence of the sound source and the propagation environment.

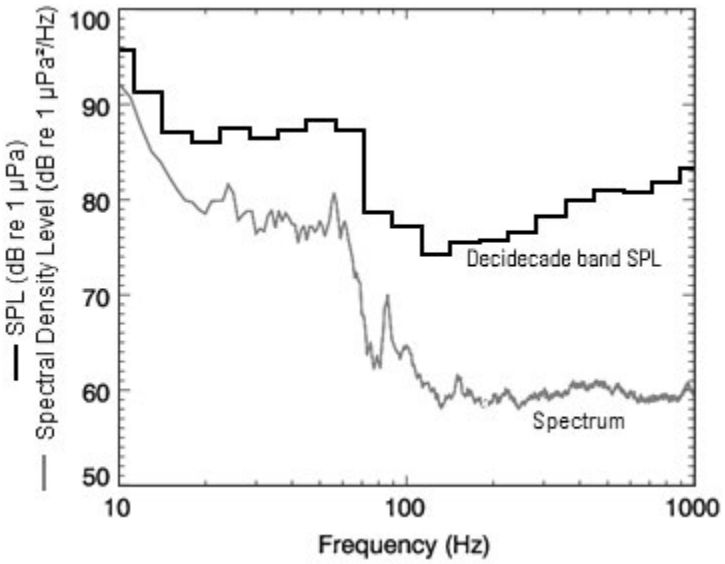


Figure A-2. Sound pressure spectral density levels and the corresponding decidecade band sound pressure levels of example ambient noise shown on a logarithmic frequency scale.

A.4. Marine Mammal Impact Criteria

It has been long recognised that marine mammals can be adversely affected by underwater anthropogenic noise. For example, Payne and Webb (1971) suggested that communication distances of fin whales are reduced by shipping sounds. Subsequently, similar concerns arose regarding effects of other underwater noise sources and the possibility that impulsive sources—primarily airguns used in seismic surveys—could cause auditory injury. This led to a series of workshops held in the late 1990s, conducted to address acoustic mitigation requirements for seismic surveys and other underwater noise sources (NMFS 1998, ONR 1998, Nedwell and Turnpenny 1998, HESS 1999, Ellison and Stein 1999). In the years since these early workshops, a variety of thresholds have been proposed for both injury and disturbance. The following sections summarize the recent development of thresholds; however, this field remains an active research topic.

A.4.1. Injury

In recognition of shortcomings of the SPL-only based injury criteria, in 2005 NMFS sponsored the Noise Criteria Group to review literature on marine mammal hearing to propose new noise exposure criteria. Some members of this expert group published a landmark paper (Southall et al. 2007) that suggested assessment methods similar to those applied for humans. The resulting recommendations introduced dual acoustic injury criteria for impulsive sounds that included peak pressure level thresholds and SEL_{24h} thresholds, where the subscripted 24h refers to the accumulation period for calculating SEL. The peak pressure level criterion is not frequency weighted whereas the SEL_{24h} is frequency weighted according to one of four marine mammal species hearing groups: low-, mid- and high-frequency cetaceans (LF, MF, and HF cetaceans, respectively) and Pinnipeds in Water (PINN). These weighting functions are referred to as M-weighting filters (analogous to the A-weighting filter for human; Appendix A.4). The SEL_{24h} thresholds were obtained by extrapolating measurements of onset levels of Temporary Threshold Shift (TTS) in belugas by the amount of TTS required to produce Permanent Threshold Shift (PTS) in chinchillas. The Southall et al. (2007) recommendations do not specify an exchange rate, which suggests that the thresholds are the same regardless of the duration of exposure (i.e., it implies a 3 dB exchange rate).

Wood et al. (2012) refined Southall et al.'s (2007) thresholds, suggesting lower injury values for LF and HF cetaceans while retaining the filter shapes. Their revised thresholds were based on TTS-onset levels in harbour porpoises from Lucke et al. (2009), which led to a revised impulsive sound PTS threshold for HF cetaceans of 179 dB re 1 $\mu Pa^2 \cdot s$. Because there were no data available for baleen whales, Wood et al. (2012) based their recommendations for LF cetaceans on results obtained from MF cetacean studies. In particular they referenced Finneran and Schlundt (2010) research, which found mid-frequency cetaceans are more sensitive to non-impulsive sound exposure than Southall et al. (2007) assumed. Wood et al. (2012) thus recommended a more conservative TTS-onset level for LF cetaceans of 192 dB re 1 $\mu Pa^2 \cdot s$.

As of present, an optimal approach is not apparent. There is consensus in the research community that an SEL-based method is preferable either separately or in addition to an SPL-based approach to assess the potential for injuries. In August 2016, after substantial public and expert input into three draft versions and based largely on the above-mentioned literature (NOAA 2013, 2015, 2016), NMFS finalised technical guidance for assessing the effect of anthropogenic sound on marine mammal hearing (NMFS 2016). The guidance describes injury criteria with new thresholds and frequency weighting functions for the five hearing groups described by Finneran and Jenkins (2012). The latest revision to this work was published in 2018; with the criteria defined in NMFS (2018). The latest criteria are from Southall et al. (2019) which is applied in this report.

A.4.2. Behavioural Response

Numerous studies on marine mammal behavioural responses to sound exposure have not resulted in consensus in the scientific community regarding the appropriate metric for assessing behavioural reactions. However, it is recognised that the context in which the sound is received affects the nature and extent of responses to a stimulus (Southall et al. 2007, Ellison and Frankel 2012, Southall et al. 2016).

For impulsive noise, NMFS currently uses step function thresholds of 160 dB re 1 µPa SPL (unweighted) to assess and regulate noise-induced behavioural impacts for marine mammals (NOAA 2018, NOAA 2019). The threshold for impulsive sound is derived from the High-Energy Seismic Survey (HESS) panel (HESS 1999) report that, in turn, is based on the responses of migrating mysticete whales to airgun sounds (Malme et al. 1984). The HESS team recognised that behavioural responses to sound may occur at lower levels, but significant responses were only likely to occur above a SPL of 140 dB re 1 µPa. Southall et al. (2007) found varying responses for most marine mammals between a SPL of 140 and 180 dB re 1 µPa, consistent with the HESS (1999) report, but lack of convergence in the data prevented them from suggesting explicit step functions.

A.5. Marine Mammal Frequency Weighting

The potential for noise to affect animals depends on how well the animals can hear it. Noises are less likely to disturb or injure an animal if they are at frequencies that the animal cannot hear well. An exception occurs when the sound pressure is so high that it can physically injure an animal by non-auditory means (i.e., barotrauma). For sound levels below such extremes, the importance of sound components at particular frequencies can be scaled by frequency weighting relevant to an animal's sensitivity to those frequencies (Nedwell and Turnpenny 1998, Nedwell et al. 2007).

A.5.1. Marine Mammal Frequency Weighting Functions

In 2015, a US Navy technical report by Finneran (2015) recommended new auditory weighting functions. The overall shape of the auditory weighting functions is similar to human A-weighting

functions, which follows the sensitivity of the human ear at low sound levels. The new frequency-weighting function is expressed as:

$$G(f) = K + 10\log_{10}\left[\left(\frac{(f/f_{lo})^{2a}}{\left[1+(f/f_{lo})^{2}\right]^{a}\left[1+(f/f_{hi})^{2}\right]^{b}}\right)\right] \quad \text{(A-13)}$$

Finneran (2015)Finneran (2015) proposed five functional hearing groups for marine mammals in water: low-, mid- and high-frequency cetaceans (LF, MF, and HF cetaceans, respectively), phocid pinnipeds, and otariid pinnipeds. The parameters for these frequency-weighting functions were further modified the following year (Finneran 2016) and were adopted in NOAA's technical guidance that assesses acoustic impacts on marine mammals (NMFS 2018), and in the latest guidance by Southall (2019). The updates did not affect the content related to either the definitions of frequency-weighting functions or the threshold values. Table A-1 lists the frequency-weighting parameters for each hearing group. Figure A-3 shows the resulting frequency-weighting curves.

Table A-1. Parameters for the auditory weighting functions used in this project as recommended by Southall et al. (2019).

Hearing group	a	b	f_{lo} (Hz)	f_{hi} (kHz)	K (dB)
Low-frequency cetaceans (baleen whales)	1.0	2	200	19,000	0.13
High-frequency cetaceans (dolphins, plus toothed, beaked, and bottlenose whales)	1.6	2	8,800	110,000	1.20
Very-high-frequency cetaceans (*Kogia*, cephalorhynchid, and *L. australis*)	1.8	2	12,000	140,000	1.36
Other marine carnivores in water (Australian sea lion, Australian fur seal, New Zealand fur seal)	2.0	2	940	25,000	0.64

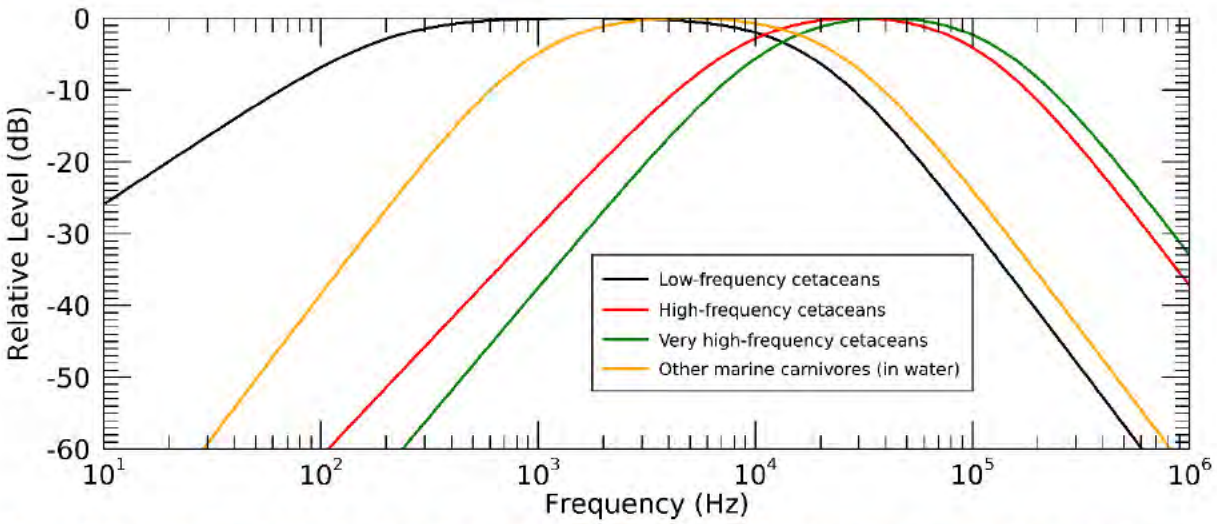


Figure A-3. Auditory weighting functions for functional marine mammal hearing groups used in this project as recommended by Southall et al. (2019).

Appendix B. Acoustic Source Model

B.1. Airgun Array Source Model

The source levels and directivity of the seismic source were predicted with JASCO's Airgun Array Source Model (AASM). AASM includes low- and high-frequency modules for predicting different components of the seismic source spectrum. The low-frequency module is based on the physics of oscillation and radiation of airgun bubbles, as originally described by Ziolkowski (1970), that solves the set of parallel differential equations that govern bubble oscillations. Physical effects accounted for in the simulation include pressure interactions between airguns, port throttling, bubble damping, and generator-injector (GI) gun behaviour discussed Dragoset (1984), Laws et al. (1990), and Landro (1992). A global optimisation algorithm tunes free parameters in the model to a large library of airgun source signatures.

While airgun signatures are highly repeatable at the low frequencies, which are used for seismic imaging, their sound emissions have a large random component at higher frequencies that cannot be predicted using a deterministic model. Therefore, AASM uses a stochastic simulation to predict the high-frequency (800−25,000 Hz) sound emissions of individual airguns, using a data-driven multiple-regression model. The multiple-regression model is based on a statistical analysis of a large collection of high quality seismic source signature data recently obtained from the Joint Industry Program (JIP) on Sound and Marine Life (Mattsson and Jenkerson 2008). The stochastic model uses a Monte-Carlo simulation to simulate the random component of the high-frequency spectrum of each airgun in an array. The mean high-frequency spectra from the stochastic model augment the low-frequency signatures from the physical model, allowing AASM to predict airgun source levels at frequencies up to 25,000 Hz.

AASM produces a set of "notional" signatures for each array element based on:

- Array layout
- Volume, tow depth, and firing pressure of each airgun
- Interactions between different airguns in the array

These notional signatures are the pressure waveforms of the individual airguns at a standard reference distance of 1 m; they account for the interactions with the other airguns in the array. The signatures are summed with the appropriate phase delays to obtain the far-field source signature of the entire array in all directions. This far-field array signature is filtered into decidecade-bands to compute the source levels of the array as a function of frequency band and azimuthal angle in the horizontal plane (at the source depth), after which it is considered a directional point source in the far field.

A seismic array consists of many sources and the point source assumption is invalid in the near field where the array elements add incoherently. The maximum extent of the near field of an array (R_{nf}) is:

$$R_{\mathrm{nf}} < \frac{l^2}{4\lambda} \tag{B-1}$$

where λ is the sound wavelength and l is the longest dimension of the array (Lurton 2002, §5.2.4). For example, a seismic source length of l = 21 m yields a near-field range of 147 m at 2 kHz and 7 m at 100 Hz. Beyond this R_{nf} range, the array is assumed to radiate like a directional point source and is treated as such for propagation modelling.

The interactions between individual elements of the array create directionality in the overall acoustic emission. Generally, this directionality is prominent mainly at frequencies in the mid-range between

tens of hertz to several hundred hertz. At lower frequencies, with acoustic wavelengths much larger than the inter-airgun separation distances, the directionality is small. At higher frequencies, the pattern of lobes is too finely spaced to be resolved and the effective directivity is less.

B.2. Seismic Source

The layout of the seismic source used for modelling in this study is provided in Figure B-1 and details of the airgun parameters are provided in Table B-1.

For the modelled array, the layout is presented in a nominal cartesian coordinate system. In this coordinate system the direction of vessel travel determines the relative position of the array elements as plotted and tabulated. The layout used for acoustic modelling was produced by transforming the coordinates of client supplied layouts such that the resultant layouts correspond to a vessel travel direction along the positive X-axis and the array is centred on the X-Y origin. When used with an acoustic model the positive X-axis in this nominal coordinate system aligns with the vessel tow direction or survey line azimuth.

Table B-1. Layout of the modelled 2495 in^3 array. Tow depth is 6 m. Firing pressure for all guns is 2000 psi. Also see Figure B-1.

Gun	*x* (m)	*y* (m)	*z* (m)	Volume (in^3)	Gun	*x* (m)	*y* (m)	*z* (m)	Volume (in^3)
1	7.5	-4.4	6.0	90	13	7.5	3.6	6.0	60
2	7.5	-3.6	6.0	90	14	7.5	4.4	6.0	60
3	4.5	-4.5	6.0	250	15	4.5	3.5	6.0	250
4	4.5	-3.5	6.0	250	17	1.5	3.5	6.0	250
6	1.5	-3.5	6.0	250	18	1.5	4.5	6.0	250
8	-1.5	-3.6	6.0	100	19	-1.5	3.6	6.0	120
9	-4.5	-4.4	6.0	70	20	-1.5	4.4	6.0	120
10	-4.5	-3.6	6.0	70	21	-4.5	3.6	6.0	100
11	-7.5	-4.4	6.0	150	23	-7.5	3.6	6.0	70
12	-7.5	-3.6	6.0	150	24	-7.5	4.4	6.0	70

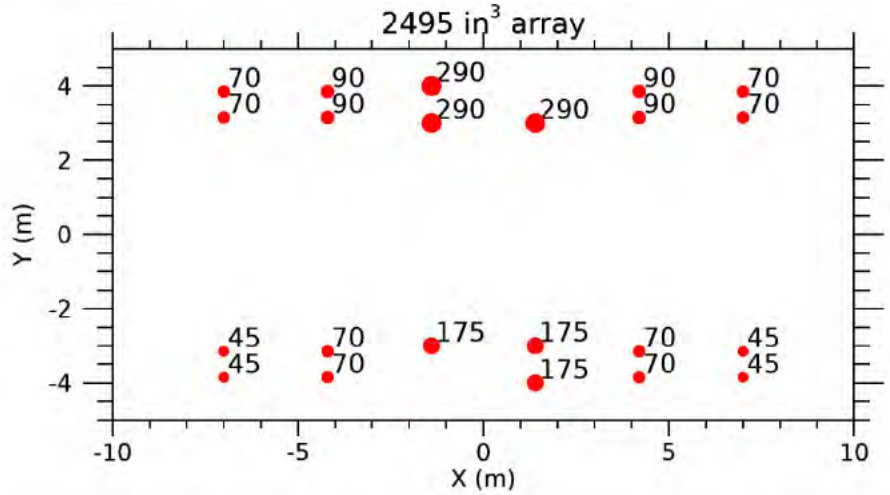


Figure B-1. Layout of the modelled 2495 in^3 array. Tow depth is 6 m. The labels indicate the firing volume (in cubic inches) for each airgun. Also see Table B-1.

B.3. Array Source Levels and Directivity

Figure B-2 shows the broadside (perpendicular to the tow direction), endfire (parallel to the tow direction) and vertical overpressure signature and corresponding power spectrum levels for the seismic source (Appendix B.2). Horizontal decidecade-band source levels are shown as a function of band centre frequency and azimuth in Figure B-3.

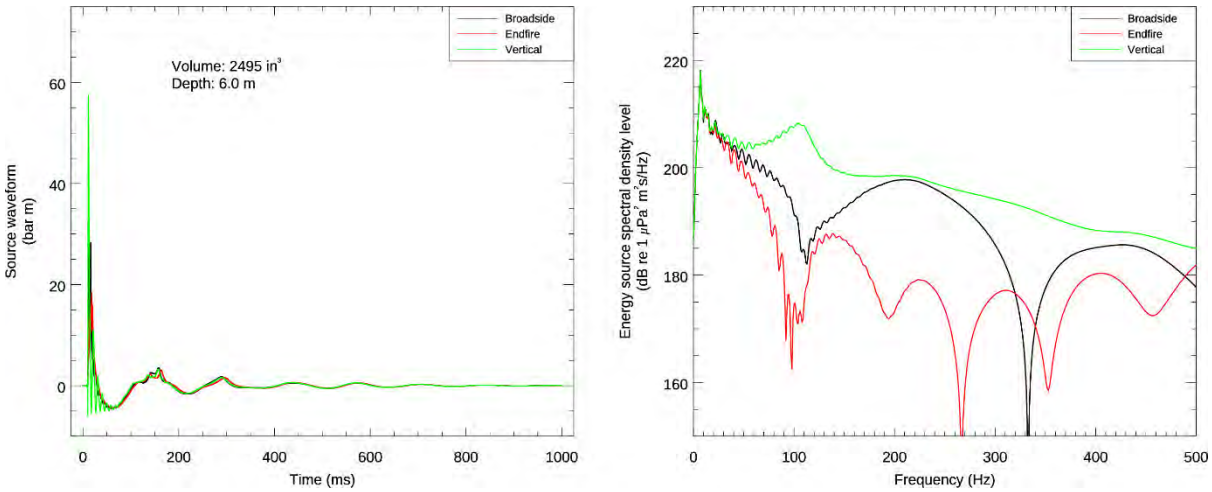


Figure B-2. Predicted source level details for the 2495 in^3 seismic source with a 6 m towed depth. (Left) the overpressure signature and (right) the power spectrum for in-plane horizontal (broadside), perpendicular (endfire), and vertical directions (no surface ghost).

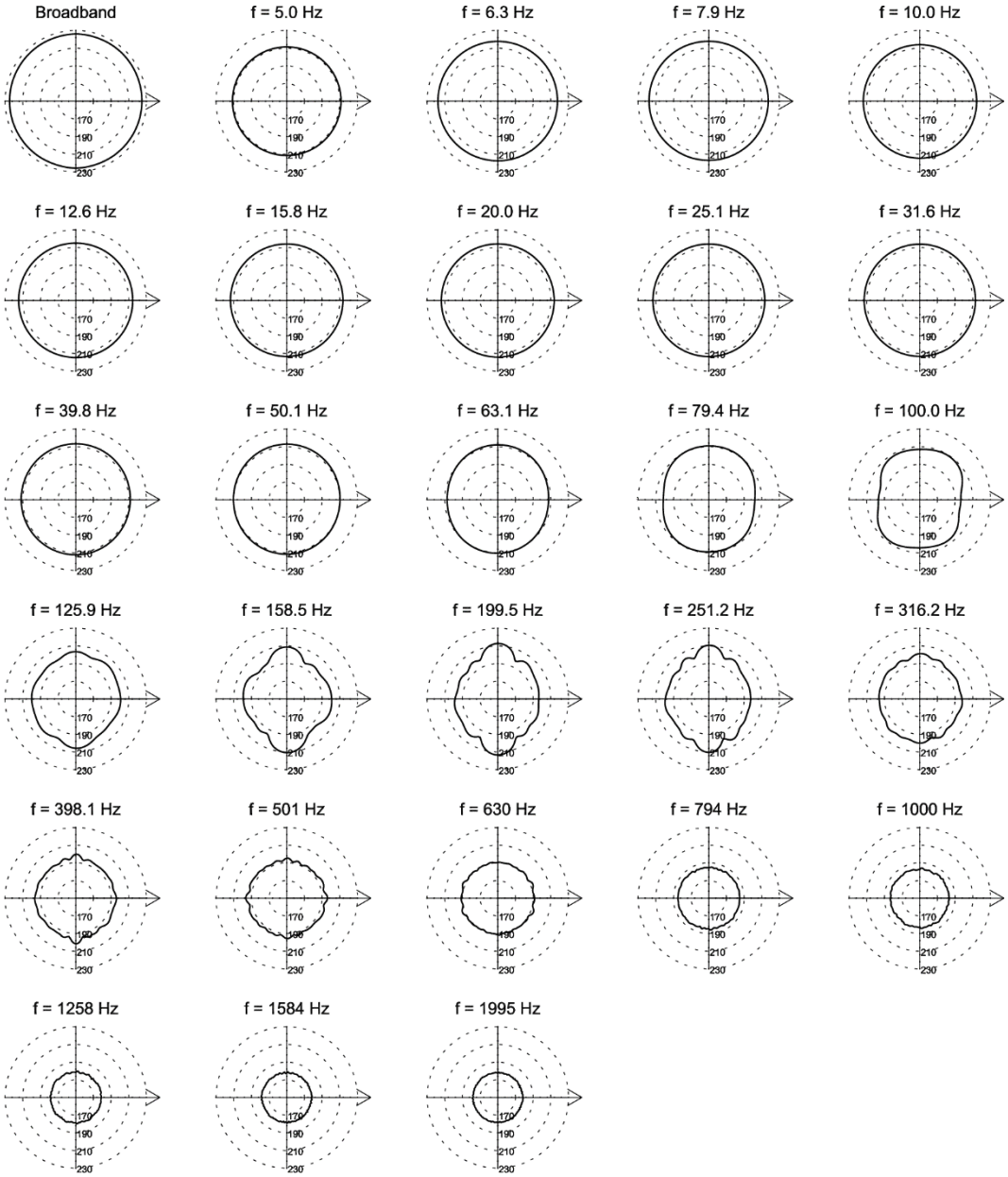


Figure B-3. Directionality of the predicted horizontal source levels for the 2495 in^3 seismic source, 5 Hz to 2 kHz. Source levels (in dB re 1 $\mu Pa^2 \cdot s\ m^2$) are shown as a function of azimuth for the centre frequencies of the decidecade bands modelled; frequencies are shown above the plots. The perpendicular direction to the frame is to the right. Tow depth is 6 m.

Appendix C. Sound Propagation Models

C.1. MONM-BELLHOP

Long-range sound fields were computed using JASCO's Marine Operations Noise Model (MONM). Compared to VSTACK, MONM less accurately predicts steep-angle propagation for environments with higher shear speed but is well suited for effective longer-range estimation. This model computes sound propagation at frequencies of 5 Hz to 1 kHz via a wide-angle parabolic equation solution to the acoustic wave equation (Collins 1993) based on a version of the US Naval Research Laboratory's Range-dependent Acoustic Model (RAM), which has been modified to account for a solid seabed (Zhang and Tindle 1995). MONM computes sound propagation at frequencies >1 kHz via the BELLHOP Gaussian beam acoustic ray-trace model (Porter and Liu 1994).

The parabolic equation method has been extensively benchmarked and is widely employed in the underwater acoustics community (Collins et al. 1996). MONM accounts for the additional reflection loss at the seabed, which results from partial conversion of incident compressional waves to shear waves at the seabed and sub-bottom interfaces, and it includes wave attenuations in all layers. MONM incorporates the following site-specific environmental properties: a bathymetric grid of the modelled area, underwater sound speed as a function of depth, and a geoacoustic profile based on the overall stratified composition of the seafloor.

This version of MONM accounts for sound attenuation due to energy absorption through ion relaxation and viscosity of water in addition to acoustic attenuation due to reflection at the medium boundaries and internal layers (Fisher and Simmons 1977). The former type of sound attenuation is significant for frequencies higher than 5 kHz and cannot be neglected without noticeably affecting the model results.

MONM computes acoustic fields in three dimensions by modelling transmission loss within two-dimensional (2-D) vertical planes aligned along radials covering a 360° swath from the source, an approach commonly referred to as N×2-D. These vertical radial planes are separated by an angular step size of $\Delta\theta$, yielding N = 360°/$\Delta\theta$ number of planes (Figure C-1).

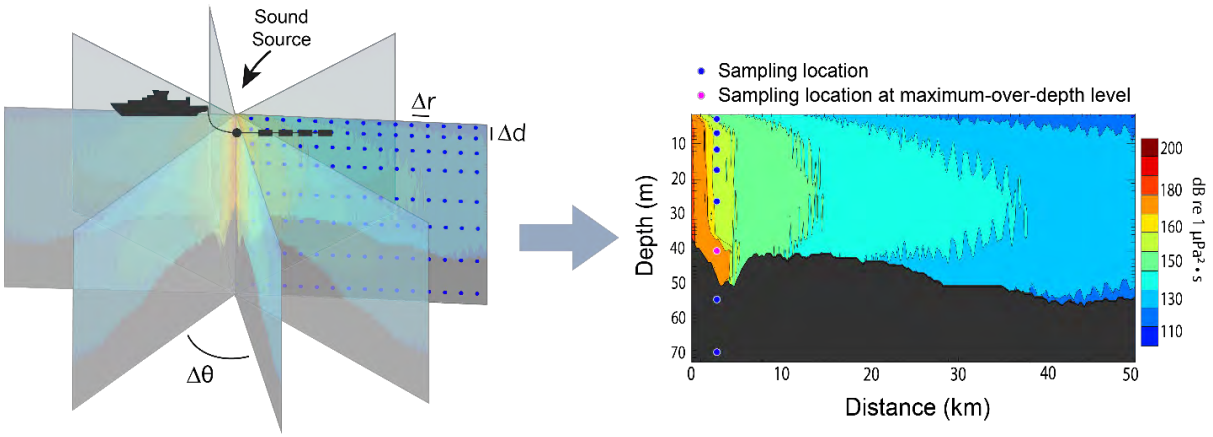


Figure C-1. The N×2-D and maximum-over-depth modelling approach used by MONM.

MONM treats frequency dependence by computing acoustic transmission loss at the centre frequencies of decidecade bands. Sufficiently many decidecade bands, starting at 5 Hz, are modelled to include most of the acoustic energy emitted by the source. At each centre frequency, the transmission loss is modelled within each of the N vertical planes as a function of depth and range from the source. The decidecade band received per-pulse SEL are computed by subtracting the band transmission loss values from the directional source level in that frequency band. Composite

broadband received per-pulse SEL are then computed by summing the received decidecade band levels.

The received per-pulse SEL sound field within each vertical radial plane is sampled at various ranges from the source, generally with a fixed radial step size. At each sampling range along the surface, the sound field is sampled at various depths, with the step size between samples increasing with depth below the surface. The step sizes are chosen to provide increased coverage near the depth of the source and at depths of interest in terms of the sound speed profile. The maximum received per-pulse SEL at many sampling depths are taken over all samples within the water column, i.e., the maximum-over-depth received per-pulse SEL. These maximum-over-depth per-pulse SEL are presented as contours around the source.

C.2. Full Waveform Range-dependent Acoustic Model: FWRAM

For impulsive sounds from the seismic source, time-domain representations of the pressure waves generated in the water are required to calculate SPL and PK. Furthermore, the seismic source must be represented as a distributed source to accurately characterise vertical directivity effects in the near-field zone. For this study, synthetic pressure waveforms were computed using FWRAM, which is a time-domain acoustic model based on the same wide-angle parabolic equation (PE) algorithm as MONM. FWRAM computes synthetic pressure waveforms versus range and depth for range-varying marine acoustic environments, and it takes the same environmental inputs as MONM (bathymetry, water sound speed profile, and seafloor geoacoustic profile). Unlike MONM, FWRAM computes pressure waveforms via Fourier synthesis of the modelled acoustic transfer function in closely spaced frequency bands. FWRAM employs the array starter method to accurately model sound propagation from a spatially distributed source (MacGillivray and Chapman 2012).

Besides providing direct calculations of the PK and SPL, the synthetic waveforms from FWRAM can also be used to convert the SEL values from MONM to SPL.

C.3. Wavenumber Integration Model

Sound pressure levels near the seismic source were modelled using JASCO's VSTACK wavenumber integration model. VSTACK computes synthetic pressure waveforms versus depth and range for arbitrarily layered, range-independent acoustic environments using the wavenumber integration approach to solve the exact (range-independent) acoustic wave equation. This model is valid over the full angular range of the wave equation and can fully account for the elasto-acoustic properties of the sub-bottom. Wavenumber integration methods are extensively used in the field of underwater acoustics and seismology where they are often referred to as reflectivity methods or discrete wavenumber methods. VSTACK computes sound propagation in arbitrarily stratified water and seabed layers by decomposing the outgoing field into a continuum of outward-propagating plane cylindrical waves. Seabed reflectivity in the model is dependent on the seabed layer properties: compressional and shear wave speeds, attenuation coefficients, and layer densities. The output of the model can be post-processed to yield estimates of the SEL, SPL, and PK.

VSTACK accurately predicts steep-angle propagation in the proximity of the source, but it is computationally slow at predicting sound pressures at large distances due to the need for smaller wavenumber steps with increasing distance. Additionally, VSTACK assumes range-invariant bathymetry with a horizontally stratified medium (i.e., a range-independent environment) which is azimuthally symmetric about the source. VSTACK is thus best suited to modelling the sound field near the source.

C.3.1. Particle Motion

VSTACK was also used to compute estimates of particle acceleration and velocity for two sites (100 and 200 m water depth) for both airgun arrays. Particle motion waveforms were modelled, and pulse metrics were computed from the time-domain traces. VSTACK uses the wavenumber integration approach to solve the exact acoustic wave equation for arbitrarily layered range-independent acoustic environments.

The VSTACK model setup for the particle velocity scenarios was identical to that for the peak pressure scenarios in terms of source treatment, frequency range and environmental model. The particle acceleration and velocity waveforms were computed to a maximum distance of 1000 m in the broadside and endfire directions from the centre of the airgun array for a receiver 5 cm above the seafloor.

As discussed above in Appendix A.2, particle velocity (v) is the physical speed of a particle in a material. It can be derived from the pressure gradient and Euler's linearised momentum equation where ρ_0 is the density of the medium. Since the wavenumber integration kernel is a product of analytic expressions in terms of range and depth, VSTACK computes particle velocity by computing the spatial gradient of the pressure field analytically in the frequency domain. Fourier synthesis is applied to compute time series synthetic pressure and/or velocity waveforms at depth and range receivers by convolving the source waveforms with the impulse response of the waveguide. Particle velocity metrics at each receiver location were calculated from the modelled particle motion along three perpendicular axes (horizontal and along the source-receiver path, horizontal and perpendicular to the source-receiver path, and vertical).

The particle velocity results were converted to acceleration by time differentiation. The peak particle acceleration and velocity were calculated from the maximum of the predicted acceleration and velocity magnitude, defined as "peak magnitude" and are presented as plots of peak value versus range.

C.3.2. Limestone Seabed Propagation Loss

For all modelled sites, an additional broadband correction was applied to the propagation loss results from MONM to better account for the additional propagation loss associated with a calcarenite/limestone seabed. The differences between the broadband per-pulse SEL from MONM and VSTACK were extracted at the same modelled ranges and depths for corresponded range independent environments. The 90th percentile of the resultant dB differences in range bins were selected to generate a correction function for representative sites to be modelled. The conversion functions were applied after to the summed decidecade band levels from MONM, but before gridding, and radii calculations for each modelled site in each modelled scenario considered.

Appendix D. Methods and Parameters

This section the environmental parameters used in the propagation models.

D.1. Estimating Range to Thresholds Levels

Sound level contours were calculated based on the underwater sound fields predicted by the propagation models, sampled by taking the maximum value over all modelled depths above the sea floor for each location in the modelled region. The predicted distances to specific levels were computed from these contours. Two distances relative to the source are reported for each sound level: 1) R_{max}, the maximum range to the given sound level over all azimuths, and 2) $R_{95\%}$, the range to the given sound level after the 5% farthest points were excluded (see examples in Figure D-1).

The $R_{95\%}$ is used because sound field footprints are often irregular in shape. In some cases, a sound level contour might have small protrusions or anomalous isolated fringes. This is demonstrated in the image in Figure D-1(a). In cases such as this, where relatively few points are excluded in any given direction, R_{max} can misrepresent the area of the region exposed to such effects, and $R_{95\%}$ is considered more representative. In strongly asymmetric cases such as shown in Figure D-1(b), on the other hand, $R_{95\%}$ neglects to account for significant protrusions in the footprint. In such cases R_{max} might better represent the region of effect in specific directions. Cases such as this are usually associated with bathymetric features affecting propagation. The difference between R_{max} and $R_{95\%}$ depends on the source directivity and the non-uniformity of the acoustic environment.

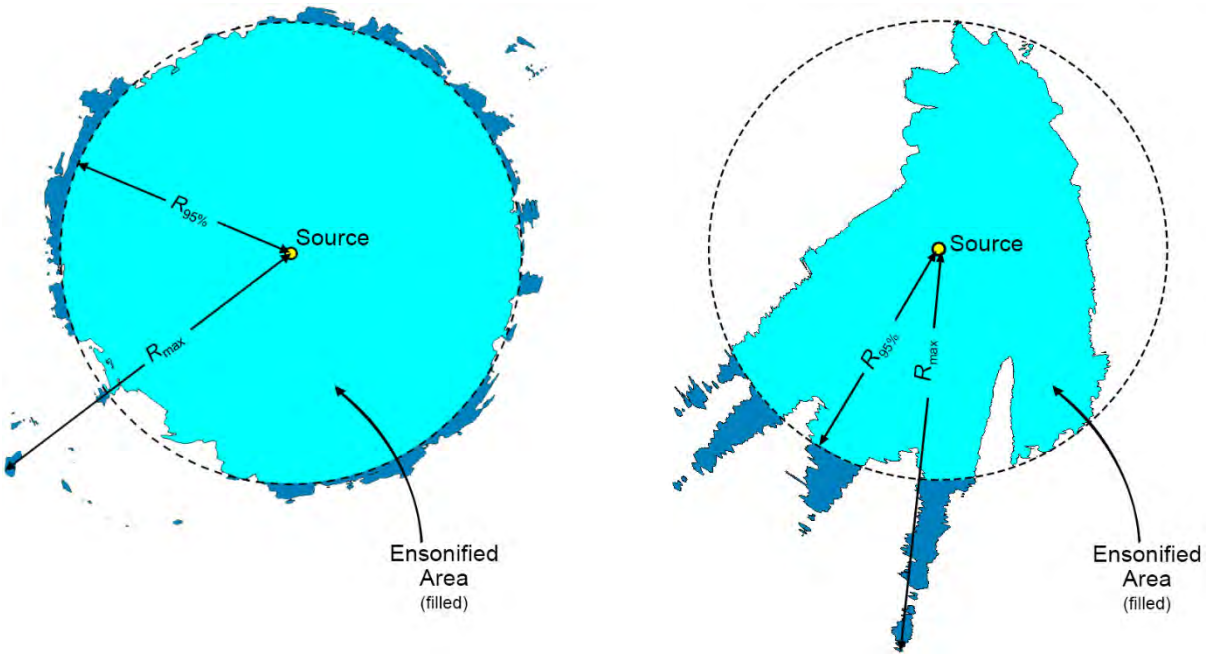


Figure D-1. Sample areas ensonified to an arbitrary sound level with R_{max} and $R_{95\%}$ ranges shown for two scenarios. (a) Largely symmetric sound level contour with small protrusions. (b) Strongly asymmetric sound level contour with long protrusions. Light blue indicates the ensonified areas bounded by $R_{95\%}$; darker blue indicates the areas outside this boundary which determine R_{max}.

D.2. Estimating SPL from Modelled SEL Results

The per-pulse SEL of sound pulses is an energy-like metric related to the dose of sound received over a pulse's entire duration. The pulse SPL on the other hand, is related to its intensity over a specified time interval. Seismic pulses typically lengthen in duration as they propagate away from their source, due to seafloor and surface reflections, and other waveguide dispersion effects. The changes in pulse length, and therefore the time window considered, affect the numeric relationship between SPL and SEL. This study has applied a fixed window duration to calculate SPL (T_{fix} = 125 ms; see Appendix A.1), as implemented in Martin et al. (2017b). Full-waveform modelling was used to estimate SPL, but this type of modelling is computationally intensive and can be prohibitively time consuming when run at high spatial resolution over large areas.

For the current study, FWRAM (Appendix C.2) was used to model synthetic seismic pulses over the frequency range 10–1024 Hz. This was performed along all broadside and endfire radials at three sites. FWRAM uses Fourier synthesis to recreate the signal in the time domain so that both the SEL and SPL from the source can be calculated. The differences between the SEL and SPL were extracted for all ranges and depths that corresponded to those generated from the high spatial-resolution results from MONM. A 125 ms fixed time window positioned to maximize the SPL over the pulse duration was applied. The resulting SEL-to-SPL offsets were averaged in 0.02 km range bins along each modelled radial and depth, and the 90th percentile was selected at each range to generate a generalised range-dependent conversion function for each site. The range-dependent conversion function was applied to predicted per-pulse SEL results from MONM to model SPL values. Figures D-2 and D-3 show the conversion offsets for Sites 3 and 5 for the 2495 in^3 array; the spatial variation is caused by changes in the received airgun pulse as it propagates from the source.

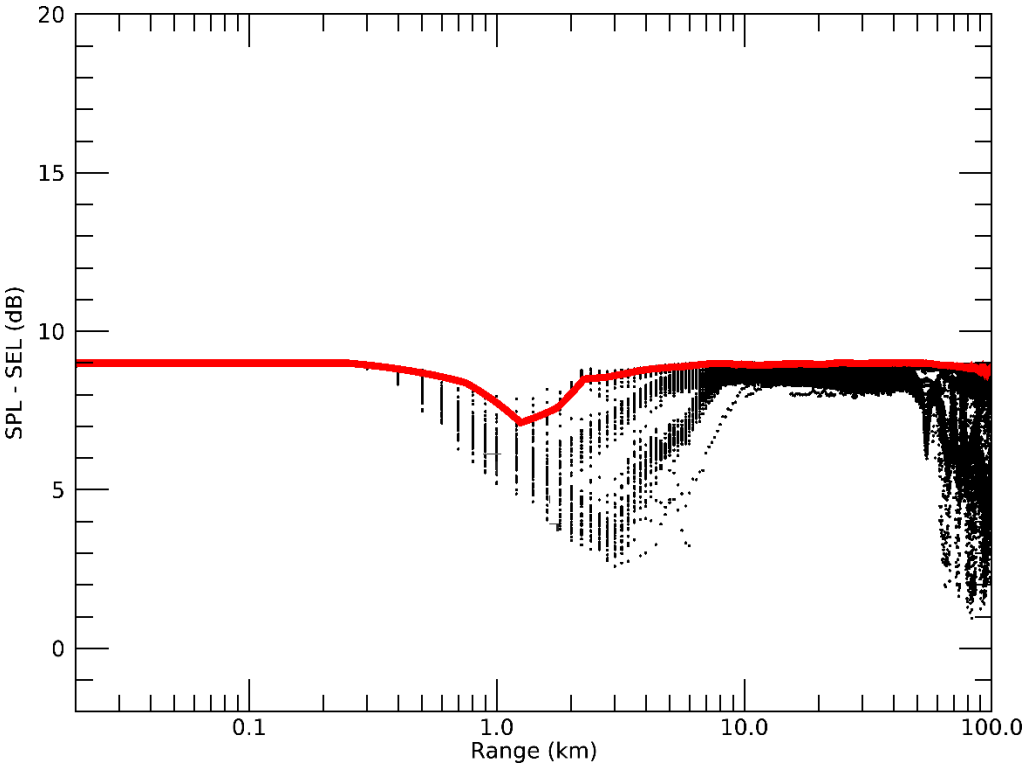


Figure D-2. *Site 3*: Range-and-depth-dependent conversion offsets for converting sound exposure level (SEL) to sound pressure level (SPL) for seismic pulses. Black lines are the modelled differences between SEL and SPL across different radials and receiver depths; the solid red line is the 90th percentile of the modelled differences at each range.

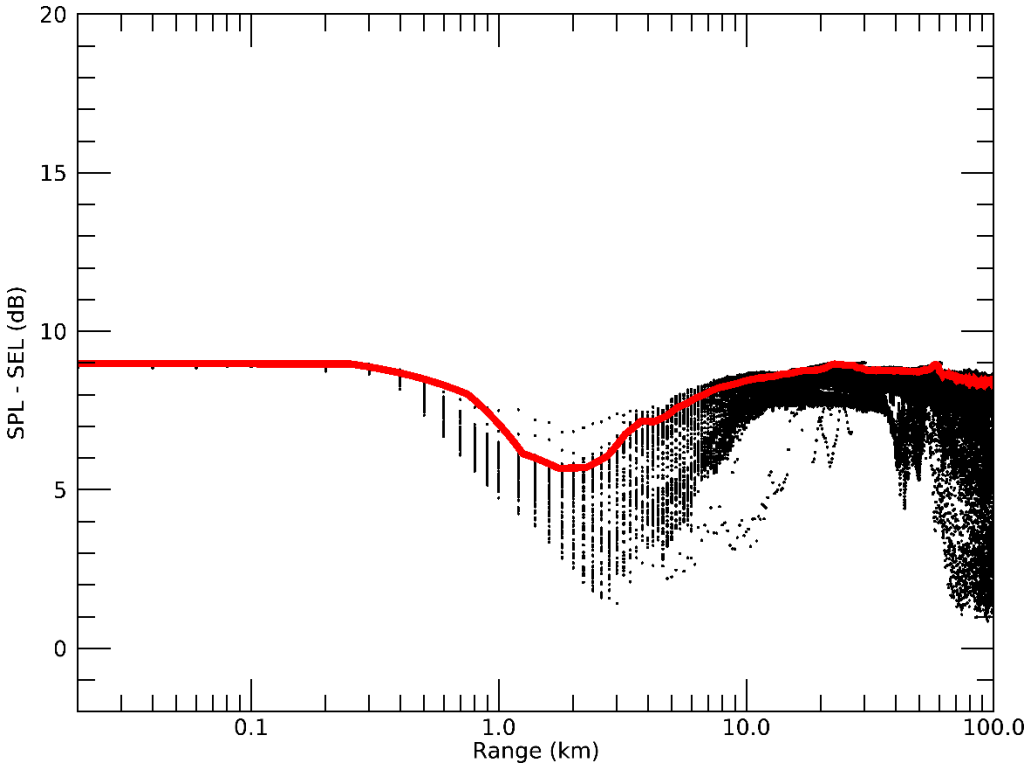


Figure D-3. *Site 5*: Range-and-depth-dependent conversion offsets for converting sound exposure level (SEL) to sound pressure level (SPL) for seismic pulses. Black lines are the modelled differences between SEL and SPL across different radials and receiver depths; the solid red line is the 90th percentile of the modelled differences at each range.

D.3. Environmental Parameters

D.3.1. Bathymetry

Water depths throughout the modelled area were extracted from high resolution bathymetry data supplied by the client and. The Australian Bathymetry and Topography Grid is a 9 arc-second grid rendered for Australian waters (Whiteway 2009). Re-rendering and merging of these two data sets was conducted by re-gridding and averaging the fine resolution bathymetry with the larger scale Australian Bathymetry and Topography Grid. The final dataset was grid onto a Map Grid of Australia (MGA) coordinate projection (Zone 50) with a regular grid spacing of 200 × 200 m to generate the bathymetry in Figure D-4. This process may result in some water depth mismatch between higher resolution data and the Australian Bathymetry and Topography Grid; however, care was taken to reduce the potential for edge artefacts in merged data corrupting numerical predictions.

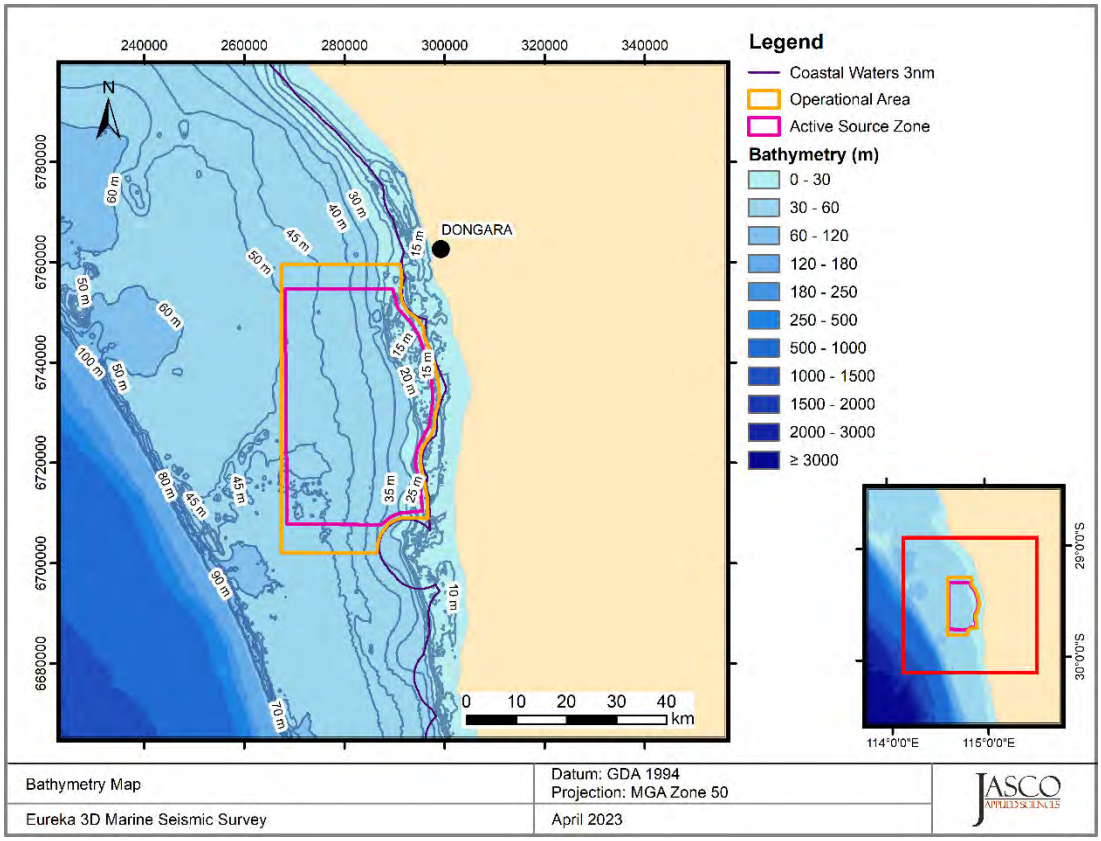


Figure D-4. Bathymetry map of the modelling area for the Eureka Marine Seismic Survey.

D.3.2. Sound Speed Profile

The sound speed profiles for the modelled sites were derived from temperature and salinity profiles from the US Naval Oceanographic Office's Generalized Digital Environmental Model V 3.0 (GDEM; Teague et al. 1990, Carnes 2009). GDEM provides an ocean climatology of temperature and salinity for the world's oceans on a latitude-longitude grid with 0.25° resolution, with a temporal resolution of one month, based on global historical observations from the US Navy's Master Oceanographic Observational Data Set (MOODS). The climatology profiles include 78 fixed depth points to a

maximum depth of 6800 m (where the ocean is that deep). The GDEM temperature-salinity profiles were converted to sound speed profiles according to Coppens (1981).

Mean monthly sound speed profiles were derived from the GDEM profiles within a 100 km box radius encompassing all modelled sites. The August sound speed profile is expected to be most favourable to longer-range sound propagation during the proposed survey time frame. As such, August was selected for sound propagation modelling to ensure precautionary estimates of distances to received sound level thresholds. Figure D-5 shows the resulting profile used as input to the sound propagation modelling.

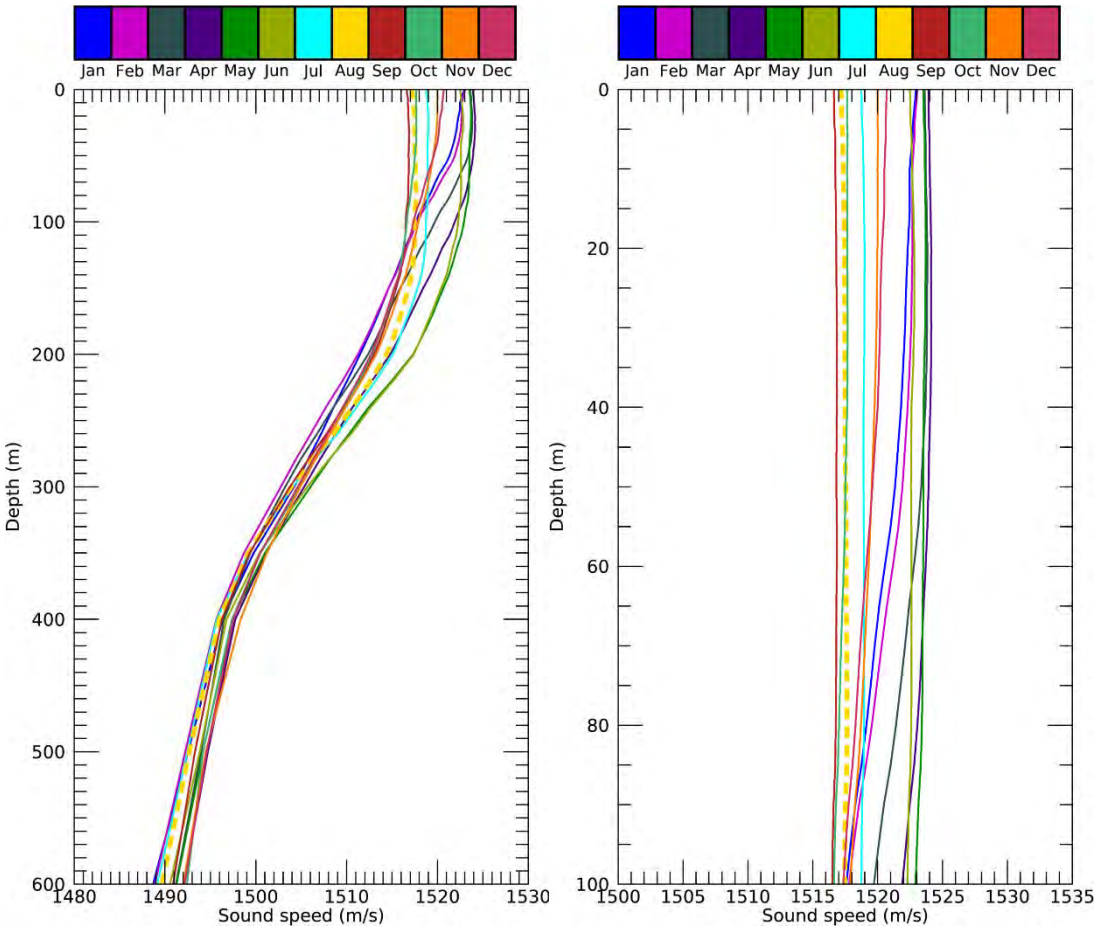


Figure D-5. The sound speed profile used for sound propagation modelling at all sites (August).

D.3.3. Geoacoustics

The propagation models used in this study consider a single geoacoustic profile. Several papers describe a potential geoacoustic models estimated via acoustic inversion (Duncan et al. 2008, Fan et al. 2009). These models consist of a thin sand layer underlain by a semi-cemented limestone/calcarenite bottom. A nominal three-layer representation of the seabed has been proposed based on this information; however, the studies all give slightly different geoacoustic values and layer thicknesses. The seabed model consists of sand/calcarenite/limestone basement where the geoacoustic parameters were averaged and adjusted slightly to obtain representative geoacoustic values. The selected seabed profile is indicative of benthic an environment located on the continental shelf and are consistent with larger scale geological data and interpretations of the Australian continental shelf environment (James and Bone 2010).

Acoustic propagation over calcarenite seabeds generally results in higher rates of loss at distance away from the source as compared to seabeds that contain thick packages of unconsolidated sediments (Duncan et al. 2009), as such additional modelling was conducted to account for the propagation loss associated with a limestone seabed (See Appendix C.3.2). The geoacoustic parameters considered for modelling are provided in Table D-1.

Table D-1. Geoacoustic profile for modelled sites.

Depth below seafloor (m)	Material	Density (g/cm^3)	P-wave speed (m/s)	P-wave attenuation (dB/λ)	S-wave speed (m/s)	S-wave attenuation (dB/λ)
0–1	Sand	1.73	1848	0.43	400	0.5
1–451	Semi-cemented Calcarenite	2.37	2672	0.21		
>451	Limestone Basement	2.40	3550	0.2		

Appendix E. Model Validation Information

Predictions from JASCO's Airgun Array Source Model (AASM) and propagation models (MONM, FWRAM and VSTACK) have been validated against experimental data from a number of underwater acoustic measurement programs conducted by JASCO globally, including the United States and Canadian Artic, Canadian and southern United States waters, Greenland, Russia and Australia (Hannay and Racca 2005, Aerts et al. 2008, Funk et al. 2008, Ireland et al. 2009, O'Neill et al. 2010, Warner et al. 2010, Racca et al. 2012a, Racca et al. 2012b, Matthews and MacGillivray 2013, Martin et al. 2015, Racca et al. 2015, Martin et al. 2017a, Martin et al. 2017b, Warner et al. 2017, MacGillivray 2018, McPherson et al. 2018, McPherson and Martin 2018).

In addition, JASCO has conducted measurement programs associated with a significant number of anthropogenic activities which have included internal validation of the modelling (including McCrodan et al. 2011, Austin and Warner 2012, McPherson and Warner 2012, Austin and Bailey 2013, Austin et al. 2013, Zykov and MacDonnell 2013, Austin 2014, Austin et al. 2015, Austin and Li 2016, Martin and Popper 2016).

JASCO APPLIED SCIENCES

Unit 1, 14 Hook Street
Capalaba, Queensland, 4157

Tel: +61 7 3823 2620
www.jasco.com

Technical Memo

DATE: 20 December 2023

FROM: (JASCO Applied Sciences (Australia) Pty Ltd)

TO: RPS

DOCUMENT 03171

VERSION 1.0

Subject: Animal Movement Modelling for the Eureka 3D MSS

JASCO Applied Sciences (JASCO) previously conducted modelling for the Eureka 3D Marine Seismic Survey (MSS) and considered a seismic source array with a volume of 2495 in^3. A change has been requested to include animal movement and exposure modelling for the 2495 in^3 scenario with a shot point interval (12.5 m). Foraging and northbound migrating pygmy blue whales *(Balaenoptera musculus brevicauda)* have been considered. The acoustic and animal movement modelling has been conducted with particular focus on the amount of ensonification of biologically important areas (BIAs) for pygmy blue whales. The migration and known foraging areas for pygmy blue whales are considered herein.

1. Modelling Scenarios

One acquisition scenario was considered using animal movement and exposure modelling. The previous acoustic modelling consisted of both source and propagation modelling, which was conducted at three individual single-impulse sites (Koessler and McPherson 2023). The single impulse sites and the accumulated SEL scenarios were determined based on proposed survey line plans. This study considered a 2495 in^3 seismic source towed in a double array configuration at an assumed speed of ~4.5 knots with an impulse interval (inter-pulse interval) of 12.5 m and a crossline array separation of 50 m.

Table 1 presents the particulars of the scenario and Table 2 presents the sites used in the modelling. Figure 1 presents a map of the spatial extent of the modelled survey lines, sites, and BIAs.

Table 1. Parameters for modelled scenario

Scenario	Source volume (in^3)	Tow depth (m)	Tow direction (°)	Source configuration	Impulse interval (m)	Discharged impulses
2†	2495	6	0 & 180	Double	12.5	8558

† As presented in Koessler and McPherson (2023).

Table 2. Location details for the single impulse modelled sites

Site	Latitude (°S)	Longitude (°E)	MGA[1] Zone 50		Water depth (m)
			X (m)	Y (m)	
4	29° 23' 08.13"	114° 40' 10.60"	273835	6747035	45.0
5	29° 30' 13.53"	114° 40' 17.24"	274276	6733941	47.0
6	29° 22' 53.53"	114° 38' 08.87"	270544	6747419	48.0

[1] Map Grid of Australia (MGA)

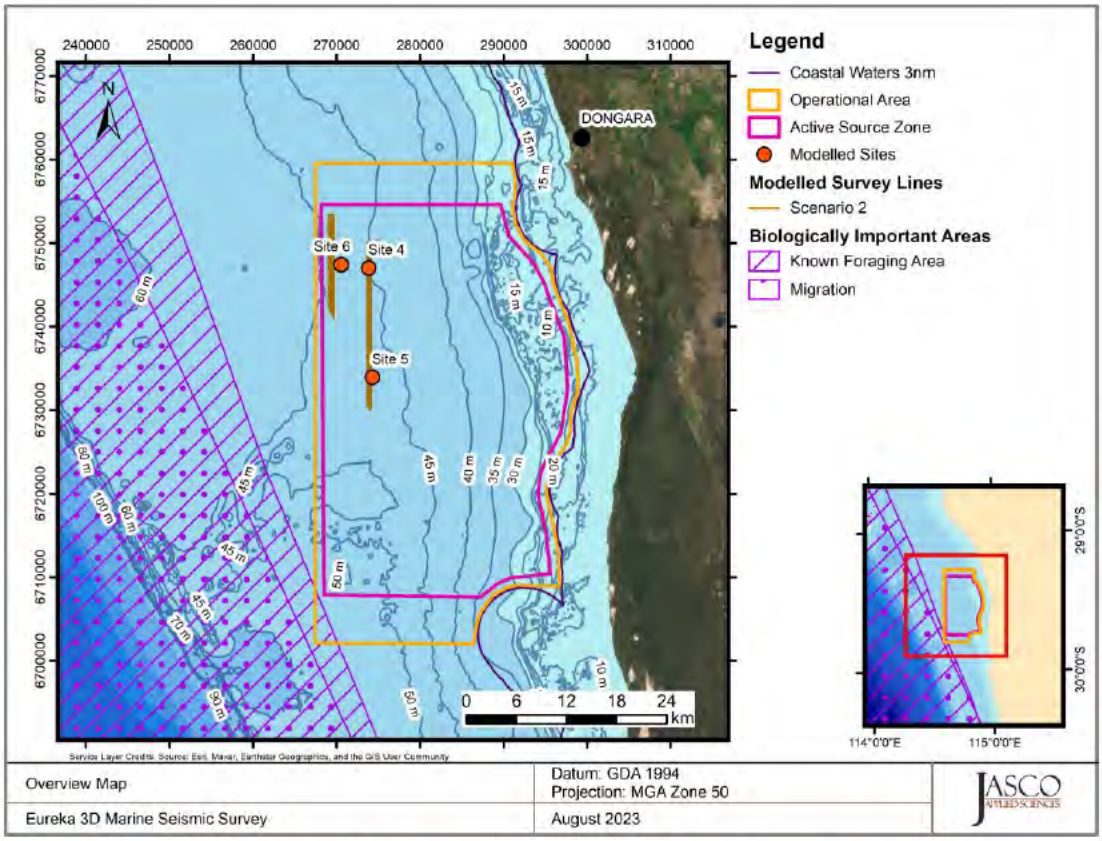


Figure 1. Overview of key survey features, modelled locations, and the survey scenario.

2. Noise Effect Criteria

The perceived loudness of sound, especially impulsive noise such as that from seismic airguns, is not generally proportional to the instantaneous acoustic pressure. Rather, perceived loudness depends on the pulse rise-time and duration, and the frequency content. The acoustic metrics in this report reflect the updated ISO standard for acoustic terminology, ISO/DIS 18405:2017 (2017).

Whether acoustic exposure levels might injure or disturb marine mammals is an active research topic. Since 2007, several expert groups have developed SEL-based assessment approaches for evaluating auditory injury, with key works including Southall et al. (2007), Finneran and Jenkins (2012), Popper et al. (2014), United States National Marine Fisheries Service (NMFS 2018) and Southall et al. (2019). The number of studies that have investigated the level of behavioural disturbance to marine fauna by anthropogenic sound has also increased substantially.

The following noise criteria were chosen because they include standard thresholds, thresholds suggested by the best available science:

1. Frequency-weighted accumulated sound exposure levels (SEL; $L_{E,24h}$) from Southall et al. (2019) for the onset of Permanent Threshold Shift (PTS) and Temporary Threshold Shift (TTS) in marine mammals as applied to pygmy blue whales (low-frequency cetaceans, baleen whales).

Further detail on noise effect criteria is provided in Koessler and McPherson (2023).

3. Methods

The methods for acoustic modelling applied herein are the same as presented in Koessler and McPherson (2023). For completeness, the methods employed for animal movement modelling are presented below in Section 3.1.

3.1. Animal Movement and Exposure Modelling

3.1.1. Methodology

The JASCO Animal Simulation Model Including Noise Exposure (JASMINE) was used to predict the exposure of animats to sound arising from the seismic activity. JASMINE integrates the predicted sound field with biologically meaningful movement rules for each marine mammal species (pygmy blue whales for the current analysis) that results in an exposure history for each animat in the model. An overview of the exposure modelling process using JASMINE is shown in Figure 2.

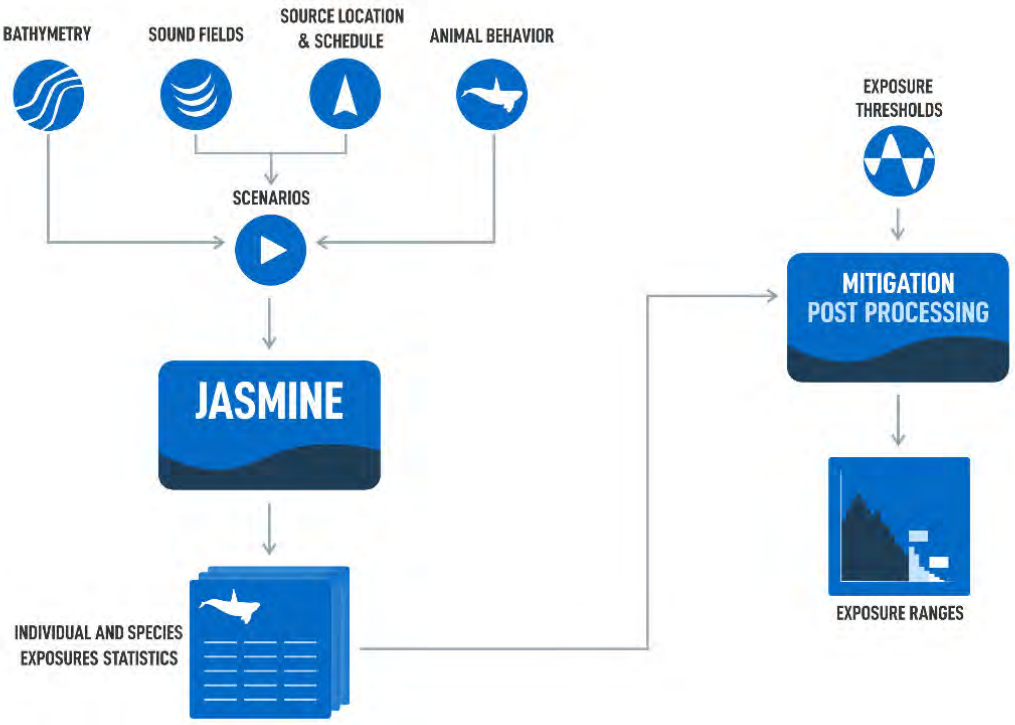


Figure 2. Exposure modelling process overview.

In JASMINE, the sound received by the animats is determined by the proposed seismic operations. As illustrated in Figure 3, animats are programmed to behave like the marine animals that may be present in an area. The parameters used for forecasting realistic behaviours (e.g., diving and foraging depth, swim speed, surface times) are determined and interpreted from marine mammal studies (e.g., tagging studies) where available, or reasonably extrapolated from related or comparable species. For cumulative metrics, an individual animats sound exposure levels are summed over a 24 h duration to determine its total received energy, and then compared to the relevant threshold criteria. For single-exposure metrics, the maximum exposure is evaluated against threshold criteria for each 24 h period. For additional information on JASMINE, see Appendix A.

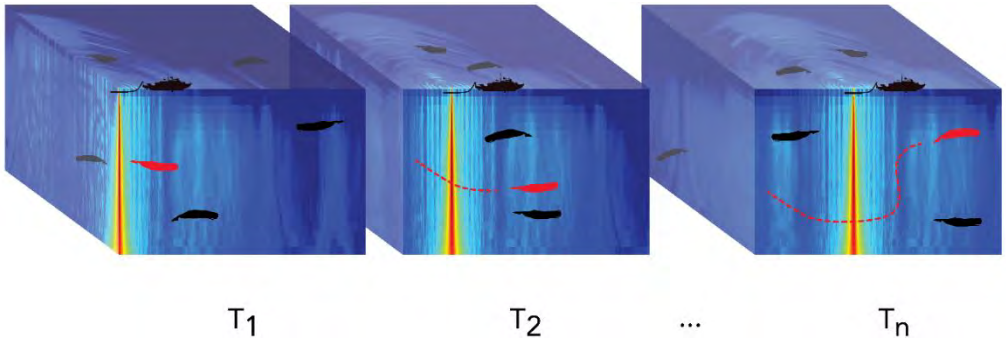


Figure 3. Depiction of animats in a moving sound field. Example animat (red) shown moving with each time step (T_n). The acoustic exposure of each animat is determined by where it is in the sound field, and its exposure history is accumulated as the simulation steps through time.

The exposure criteria for impulsive sounds (described in Koessler and McPherson (2023)) were used to determine the number of animats that exceeded thresholds. To generate statistically reliable probability density functions, model simulations were run with animat sampling densities of 4 animats/km^2. The modelling results are not related to real-world density estimates for pygmy blue whales within BIAs or known core range area, as the density of animals is not known. To evaluate PTS and TTS, exposure results were obtained using detailed behavioural information for pygmy blue whales (Section 3.1.3.1).

The seismic source was modelled as a vessel towing an airgun array at a speed of 4.5 knots, with an impulse interval of 12.5 m. The simulated source tracks followed a racetrack configuration with no acquisition occurring during turns. At the time and location of each seismic pulse, the modelled source location with the closest distance was selected for exposure modelling. The track lines, along with the acoustic modelling locations, are shown in Figure 1.

Figure 4 shows an example animat track (generated for information purposes only and not related to the results presented in this report) with associated received levels from a stationary point source. The top panel displays the animat track relative to the point source, and the bottom panel displays the accumulation of SEL_{24h} for TTS and PTS criteria. At approximately 50 seconds, the animat is exposed so that the TTS threshold is exceeded, and at approximately 700 seconds the animat is exposed so that the PTS threshold is exceeded.

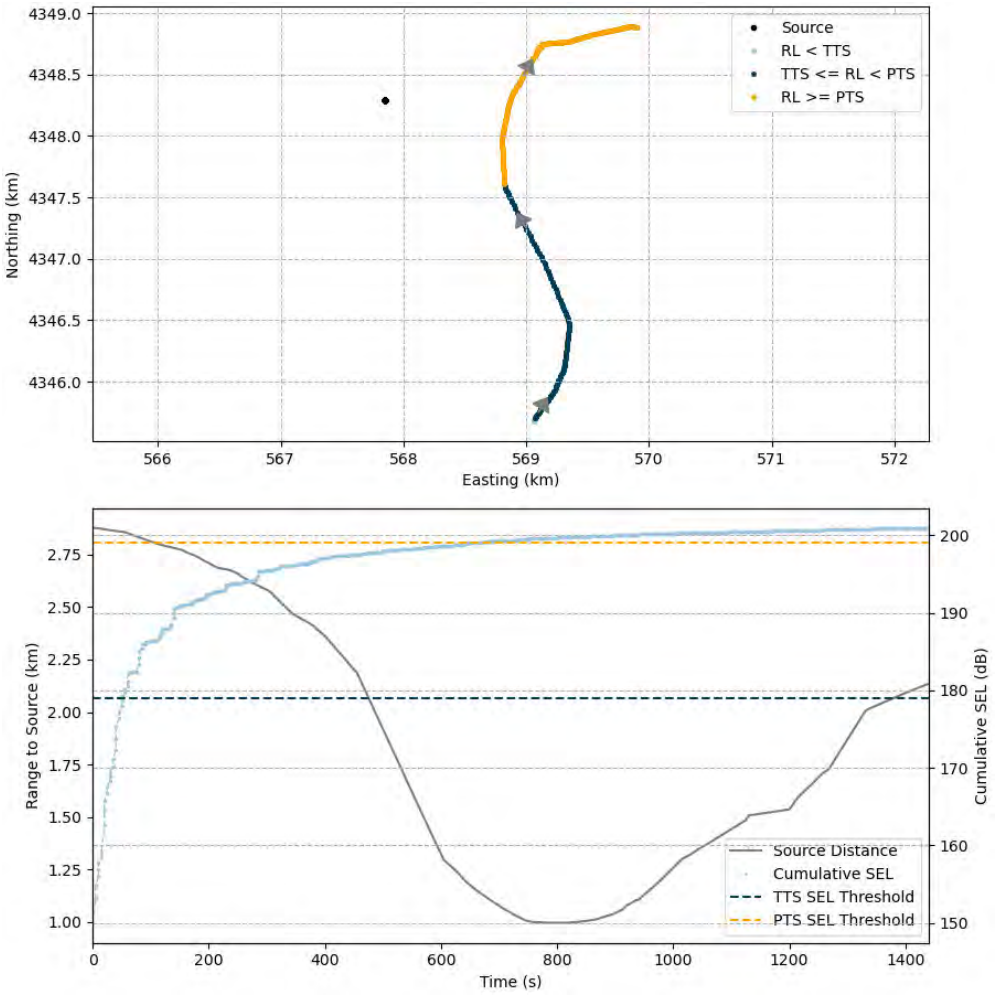


Figure 4. Animat track from an example simulation showing northward movement over a 1400 s duration. The upper panel shows a plan view of both a stationary point source and a foraging animat. Animat steps are coloured to indicate whether the accumulated sound energy at that point has exceeded either TTS or PTS threshold criteria. The lower panel shows horizontal distance in kilometres to the source (grey line; left y-axis) and cumulative 24-h SEL ($L_{E,24h}$, dB re 1 µPa²·s; right y-axis) as a function of time. Note that this example does not use data from the current study.

3.1.2. Exposure–based Radial Distance Estimation

The results from the animal movement and exposure modelling provided a way to estimate radial distances to effect thresholds. The distance to the closest point of approach (CPA) for each of the animats was recorded. The $ER_{95\%}$ (95% Exposure Range) is the horizontal distance that includes 95% of the animat CPAs that exceeded a given effect threshold. Within the $ER_{95\%}$, there is generally some proportion of animats that do not exceed threshold criteria. This occurs for several reasons, including the spatial and temporal characteristics of the sound field and the way in which animats sample the sound field over time, both vertically and horizontally. The sound field varies as a function of range, depth, and azimuth based on a variety of factors such as bathymetry, sound speed profile, and geoacoustic parameters. The way the animats sample the sound field depends upon species-typical swimming and diving characteristics (e.g., swim speed, dive depth, surface intervals, and reversals). Furthermore, even within a particular species definition, these characteristics vary with behavioural state (e.g., feeding, migrating). As this results in some animats not exceeding threshold criteria even within the $ER_{95\%}$, the probability that an animat within that distance was exposed above threshold within the $ER_{95\%}$ was also computed (P_{exp}) to provide additional context.

Acoustic ranges are reported for both $R_{95\%}$ and R_{max} (see Appendix D, Koessler and McPherson (2023)), however, exposure ranges are reported for $ER_{95\%}$ only since, statistically, ER_{max} is not defined. JASMINE is a Monte Carlo simulation, and the results are probabilistic in nature. This is in contrast with acoustic modelling, where there is a specific maximum isopleth range for a given source/environment setup.

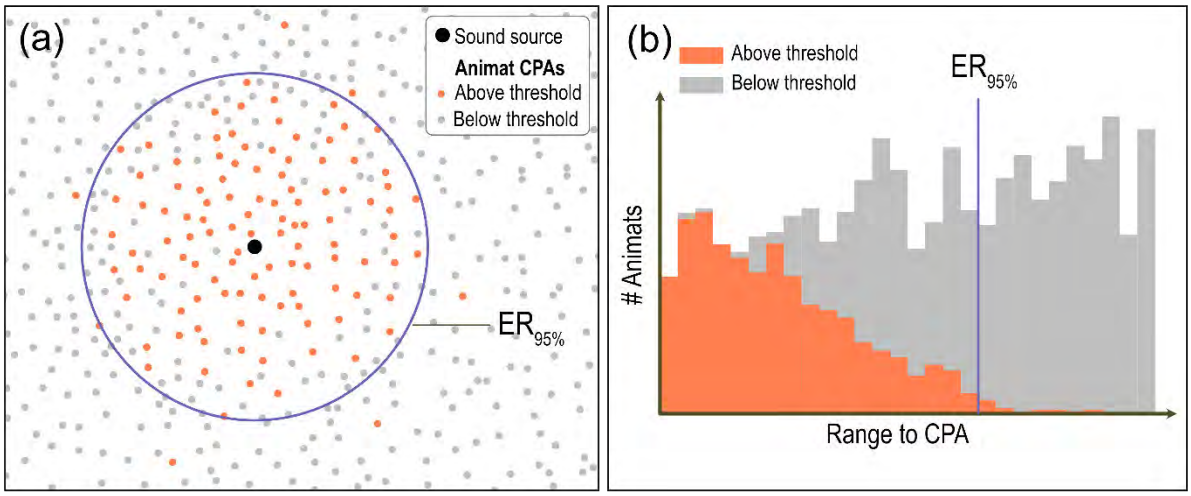


Figure 5. Example distribution of animat closest points of approach (CPAs). Panel (a) shows the horizontal distribution of animats near a sound source. Panel (b) shows the distribution of distances to animat CPAs. The 95% exposure range ($ER_{95\%}$) is indicated in both panels.

3.1.3. Species Specific Behaviour Profile Parameterisation

3.1.3.1. Pygmy Blue Whale Behaviour Profile

The project area is adjacent to the known foraging BIA for pygmy blue whales (DoE (AU) 2015-2025), as well as to the pygmy blue whale migratory BIA (Figure 1). Therefore, animat modelling was undertaken for both foraging and migrating behaviours.

Fine-scale data on foraging behaviour are not currently available for pygmy blue whales. Therefore, data from multi-sensor tags deployed on blue whales (B. musculus) in the North Pacific were used to inform the feeding behaviours. Using intermediate-duration archival tags (SPLASH MK10) attached to

eight blue whales off the coast of California, Irvine et al. (2019) determined two primary feeding behaviours: shallow and deep feeding. These two feeding behaviours differed between male and female blue whales, with females generally diving deeper than males during both shallow and deep feeding. In order to account for these differences, foraging female and male pygmy blue whales were modelled separately, with values derived from Irvine et al. (2019). The remaining parameters for feeding behaviour were primarily sourced from Goldbogen et al. (2011b), who deployed 25 multi-sensor suction cup tags (DTAGs) on blue whales off the coast of California. The exceptions were the values for travel speed, which was derived from satellite tags deployed on pygmy blue whales off southern Australia (Möller et al. 2020), and surface interval, which was derived from a satellite tag deployed on a pygmy blue whale off western Australia (Davenport et al. 2022).

The migratory pygmy blue whale behaviour profile was not split by gender as there is no evidence for sex-related differences in migratory behaviour. The migratory profile included both migratory and exploratory dives (i.e., shallow dives with no indication of feeding) based on detailed information from Owen et al. (2016), who equipped a sub-adult pygmy blue whale with a multi-sensor tag off Western Australia. Migrating pygmy blue whales were not modelled undertaking feeding behaviour, as per the findings of Owen et al. (2016). In the migratory profile, the two dive types were modelled together such that the animats were migrating 95% of the time and engaged in exploratory dives 5% of the time (Owen et al. 2016). Using data from Owen et al. (2016), the approximate length of a bout of exploratory dives could be determined, as well as the average (± SD) depth of this dive type. The analysis of the dive data showed that the depth of migratory dives was highly consistent over time and unrelated to local bathymetry. The mean depth of migratory dives was 14 ± 4 m while the mean maximum depth of exploratory dives was 107 ± 81 m. Additional parameters regarding pygmy blue whale behaviour were derived from sources that used multi-sensor tags to record fine-scale dive and movement data (Owen et al. 2016, Möller et al. 2020). Where information was unavailable for pygmy blue whales, parameters were derived from blue whale tagging data (Goldbogen et al. 2011a), as per the foraging profile.

The behaviour of migrating pygmy blue whales was modelled to reflect animats transiting through the modelling area on a 334° track during the northbound migration. This represents the animals migrating along the west coast of Australia to Indonesia (Double et al. 2014, DoE (AU) 2015-2025). The speed of travel for migratory behaviour (1.17 ± 0.60 m/s) and exploratory dives (0.88 ± 0.14 m/s) were calculated from data presented in Möller et al. (2020).

4. Results

Details of the acoustic modelling results can be found in Koessler and McPherson (2023).

4.1. Animal Movement Exposure Ranges

A summary of radial distances to exposure thresholds for pygmy blue whales, along with probability of exposure for each modelled scenario (Section 1) are included below. Table 3 shows results for scenarios for foraging and migrating pygmy blue whale animats. Results include $ER_{95\%}$ exposure ranges calculated for the SEL_{24h} thresholds for both TTS and PTS, and the probability of an animat being exposed above the threshold within the $ER_{95\%}$.

Section 4.1.1 includes histograms of CPA ranges to SEL_{24h} PTS and TTS with results in Table 3.

Table 3. Summary of animat simulation results for pygmy blue whales. The 95th percentile exposures ranges ($ER_{95\%}$) in km and probability of animats being exposed above threshold within the $ER_{95\%}$ (P_{exp} (%)) are provided. The modelled array volume and inter-pulse interval are also provided in brackets below.

Noise Effect Criteria Description	Scenario 2 (2495 in^3, 12.5 m)					
	Foraging				Migrating	
	Female		Male			
	$ER_{95\%}$ (km)	P_{exp} (%)	$ER_{95\%}$ (km)	P_{exp} (%)	$ER_{95\%}$ (km)	P_{exp} (%)
PTS (SEL_{24h})[1]	0.89	63	0.82	66	0.63	54
TTS (SEL_{24h})[2]	14.5	57	13.7	59	8.47	70

[1] LF-weighted SEL_{24h} (183 dB re 1 $\mu Pa^2 \cdot s$) (Southall et al. (2019))
[2] LF-weighted SEL_{24h} (168 dB re 1 $\mu Pa^2 \cdot s$) (Southall et al. (2019))

4.1.1. Exposure Range Histograms: Pygmy Blue Whales

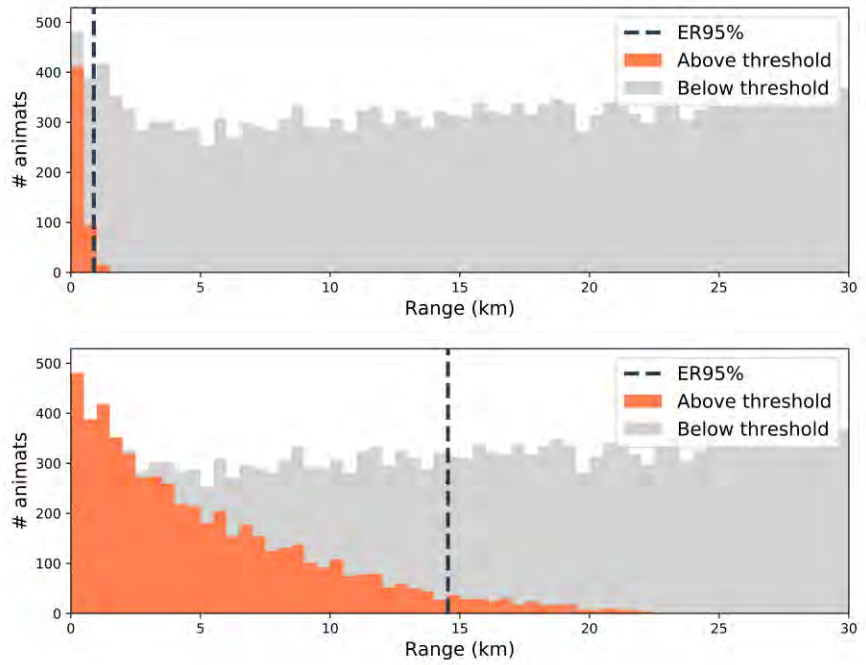


Figure 6. *Scenario 2*, *foraging female pygmy blue whale animats*: CPA range histogram for animats, SEL_{24h} PTS threshold (top panel) and SEL_{24h} TTS threshold (bottom panel).Bar colours indicate whether the animats exceeded the threshold.

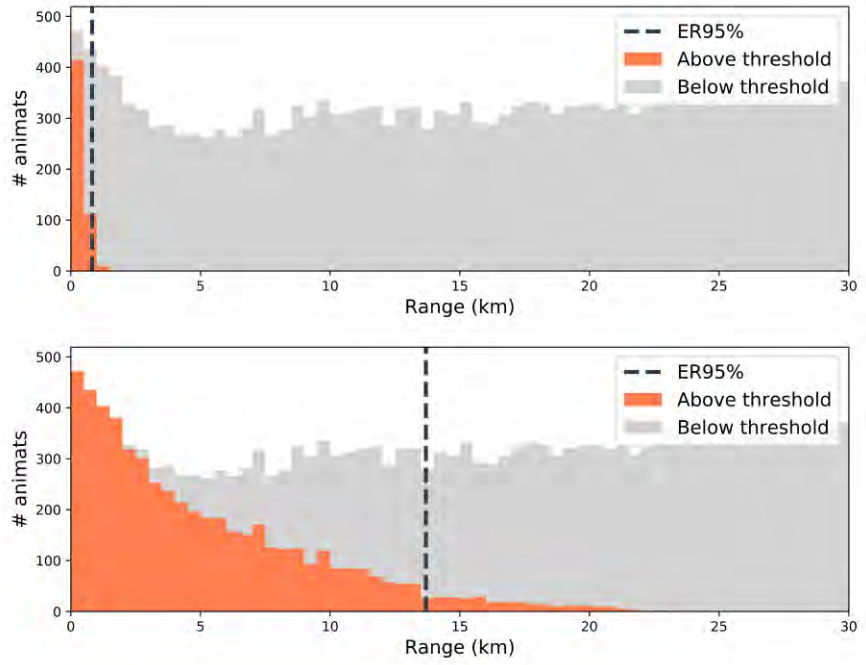


Figure 7. *Scenario 2, foraging male pygmy blue whale animats*: CPA range histogram for animats, SEL_{24h} PTS threshold (top panel) and SEL_{24h} TTS threshold (bottom panel).Bar colours indicate whether the animats exceeded the threshold.

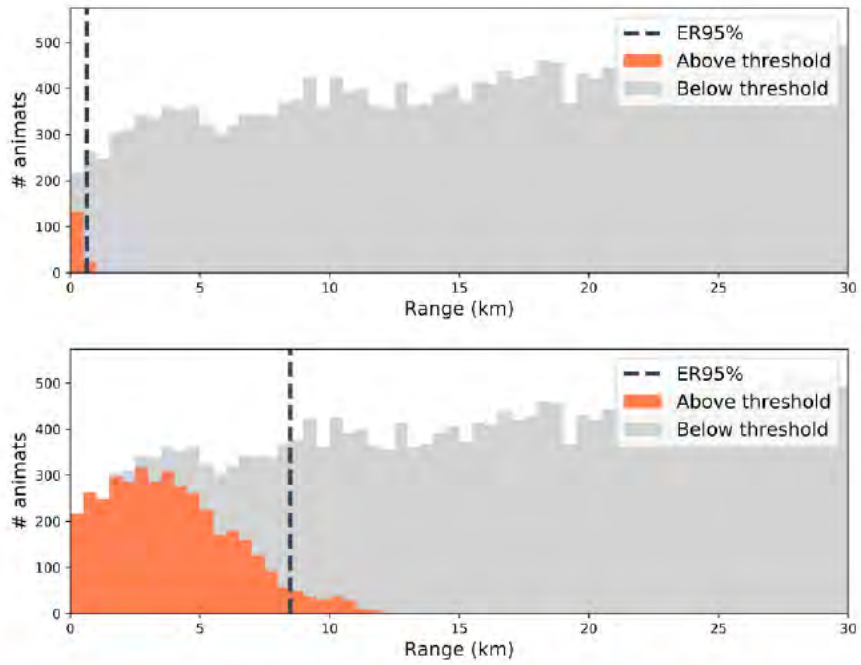


Figure 8. *Scenario 2, migrating pygmy blue whale animats*: CPA range histogram for animats, SEL_{24h} PTS threshold (top panel) and SEL_{24h} TTS threshold (bottom panel).Bar colours indicate whether the animats exceeded the threshold.

5. Discussion

5.1. Animal Movement Modelling

The estimated sound fields produced by source and propagation models for the planned Eureka MSS were incorporated into an animat sound exposure model for pygmy blue whales to estimate the radial distance within which 95% of exposure exceedances occur ($ER_{95\%}$), along with the probability that an animat with its closest point of approach within that distance would be exposed above the relevant threshold (P_{exp}).

For this exposure analysis, one nominal acquisition scenario with an impulse interval of 12.5 m was run for foraging and northbound migrating pygmy blue whales. The nominal acquisition scenario is located approximately 13.5 and 18.5 km outside of the known core range area and the migrating BIA, respectively. Animats were not restricted to the known core range area or BIA.

Section 5.1.1 summarises the PTS and TTS exposure range results, with the summarised results presented in Table 4.

Table 4. Summary of animat simulation results for PTS and TTS criteria for pygmy blue whales. Maximum exposure ranges show $ER_{95\%}$ (km) first and probability of exposure of animats travelling within the $ER_{95\%}$ (P_{exp} (%)) in parentheses.

Species	Scenario	TTS (SEL_{24h})[2]	PTS (SEL_{24h})[2]
		168[1]	183[1]
Pygmy blue whale	2 (2495 in^3,12.5 m)	14.5	0.89

[1] LF-weighted SEL_{24h} ($L_{E,24h}$; dB re 1 $\mu Pa^2 \cdot s$)
[2] Southall et al. (2019) criteria for marine fauna.

5.1.1. PTS and TTS

Exposure ranges from animal movement modelling for PTS and TTS criteria are typically shorter than those predicted using acoustic propagation modelling because moving animats generally accumulate sound energy over a shorter time (‘dwell time’). In this study, PTS and TTS exposure ranges were substantially shorter than acoustic ranges to threshold.

All considered scenarios with unrestricted animat seeding resulted in exposures above the PTS and TTS thresholds. The maximum $ER_{95\%}$ for PTS and TTS were 0.89 and 14.5 km, respectively, with corresponding exposure probabilities for animats travelling within that range of 63% and 57%, indicating that 37% and 43% of animats that travelled within the 95th percentile range were not exposed above threshold. This is because the modelled animats move in and out of the ensonified area and change their vertical position in the water column, thereby influencing the length of time they are within the exposure radius. For example, an animat might approach within the predicted exposure range but if they are traveling more quickly on average than other animats, they may not accumulate as much sound exposure, or they may spend more time at depths where sound levels are lower.

The animal movement and exposure modelling presented herein is a more realistic estimate of the dosimetric impact potential for accumulated sound exposure compared to static receiver accumulated sound exposure modelling scenarios presented in Koessler and McPherson (2023) .

Literature Cited

[ISO] International Organization for Standardization. 2017. *ISO 18405:2017. Underwater acoustics – Terminology*. Geneva. https://www.iso.org/standard/62406.html.

[NMFS] National Marine Fisheries Service (US). 2018. *2018 Revision to: Technical Guidance for Assessing the Effects of Anthropogenic Sound on Marine Mammal Hearing (Version 2.0): Underwater Thresholds for Onset of Permanent and Temporary Threshold Shifts*. US Department of Commerce, NOAA. NOAA Technical Memorandum NMFS-OPR-59. 167 p. https://media.fisheries.noaa.gov/dam-migration/tech_memo_acoustic_guidance_(20)_(pdf)_508.pdf.

Australian Government - Department of the Environment. 2015-2025. *Conservation Management Plan for the Blue Whale: A Recovery Plan under the Environment Protection and Biodiversity Conservation Act 1999*. Department of the Environment, 2015. 57 p. http://www.environment.gov.au/system/files/resources/9c058c02-afd1-4e5d-abff-11cac2ebc486/files/blue-whale-conservation-management-plan.pdf.

Davenport, A.M., C. Erbe, M.-N.M. Jenner, K.C.S. Jenner, B.J. Saunders, and R.D. McCauley. 2022. Pygmy Blue Whale Diving Behaviour Reflects Song Structure. *Journal of Marine Science and Engineering* 10(9): 1227.

Department of the Environment (Australian Government). 2015-2025. *Conservation Management Plan for the Blue Whale: A Recovery Plan under the Environment Protection and Biodiversity Conservation Act 1999*. Department of the Environment, 2015. 57 p. http://www.environment.gov.au/system/files/resources/9c058c02-afd1-4e5d-abff-11cac2ebc486/files/blue-whale-conservation-management-plan.pdf.

Double, M.C., V. Andrews-Goff, K.C.S. Jenner, M.-N. Jenner, S.M. Laverick, T.A. Branch, and N.J. Gales. 2014. Migratory Movements of Pygmy Blue Whales (*Balaenoptera musculus brevicauda*) between Australia and Indonesia as Revealed by Satellite Telemetry. *PLOS One* 9(4). https://doi.org/10.1371/journal.pone.0093578.

Ellison, W.T., C.W. Clark, and G.C. Bishop. 1987. *Potential use of surface reverberation by bowhead whales, Balaena mysticetus, in under-ice navigation: Preliminary considerations*. Report of the International Whaling Commission. Volume 37. 329-332 p.

Finneran, J.J. and A.K. Jenkins. 2012. *Criteria and thresholds for U.S. Navy acoustic and explosive effects analysis*. SPAWAR Systems Center Pacific, San Diego, CA, USA. 64 p.

Frankel, A.S., W.T. Ellison, and J. Buchanan. 2002. Application of the acoustic integration model (AIM) to predict and minimize environmental impacts. *OCEANS 2002*. 29-31 Oct 2002. IEEE, Biloxi, MI, USA. pp. 1438-1443. https://doi.org/10.1109/OCEANS.2002.1191849.

Goldbogen, J.A., J. Calambokidis, E. Oleson, J. Potvin, N.D. Pyenson, G. Schorr, and R.E. Shadwick. 2011a. Mechanics, hydrodynamics and energetics of blue whale lunge feeding: Efficiency dependence on krill density. *Journal of Experimental Biology* 214: 131-146. https://doi.org/10.1242/jeb.054726.

Goldbogen, J.A., J. Calambokidis, E.M. Oleson, J. Potvin, N.D. Pyenson, G. Schorr, and R.E. Shadwick. 2011b. Mechanics, hydrodynamics and energetics of blue whale lunge feeding: Efficiency dependence on krill density. *Journal of Experimental Biology* 214: 131-146. https://doi.org/10.1242/jeb.054726.

Houser, D.S. and M.J. Cross. 1999. *Marine Mammal Movement and Behavior (3MB): A Component of the Effects of Sound on the Marine Environment (ESME) Distributed Model*. Version 8.08, by BIOMIMETICA.

Houser, D.S. 2006. A method for modeling marine mammal movement and behavior for environmental impact assessment. *IEEE Journal of Oceanic Engineering* 31(1): 76-81. https://doi.org/10.1109/JOE.2006.872204.

Irvine, L.M., D.M. Palacios, B.A. Lagerquist, and B.R. Mate. 2019. Scales of Blue and Fin Whale Feeding Behavior off California, USA, With Implications for Prey Patchiness. *Frontiers in Ecology and Evolution* 7(338). https://doi.org/10.3389/fevo.2019.00338.

Koessler, M.W. and C.R. McPherson. 2023. *Eureka 3D Marine Seismic Survey: Acoustic Modelling for Assessing Marine Fauna Sound Exposures*. Document Number 03034, Version 1.0. Technical report by JASCO Applied Sciences for RPS Australia.

Möller, L.M., C.R.M. Attard, K. Bilgmann, V. Andrews-Goff, I. Jonsen, D. Paton, and M.C. Double. 2020. Movements and behaviour of blue whales satellite tagged in an Australian upwelling system. *Scientific Reports* 10(1): 21165. https://doi.org/10.1038/s41598-020-78143-2.

Owen, K., C.S. Jenner, M.-N.M. Jenner, and R.D. Andrews. 2016. A week in the life of a pygmy blue whale: Migratory dive depth overlaps with large vessel drafts. *Animal Biotelemetry* 4: 17. https://doi.org/10.1186/s40317-016-0109-4.

Popper, A.N., A.D. Hawkins, R.R. Fay, D.A. Mann, S. Bartol, T.J. Carlson, S. Coombs, W.T. Ellison, R.L. Gentry, et al. 2014. *Sound Exposure Guidelines for Fishes and Sea Turtles: A Technical Report prepared by ANSI-Accredited Standards Committee S3/SC1 and registered with ANSI*. ASA S3/SC1.4 TR-2014. SpringerBriefs in Oceanography. ASA Press and Springer. https://doi.org/10.1007/978-3-319-06659-2.

Southall, B.L., A.E. Bowles, W.T. Ellison, J.J. Finneran, R.L. Gentry, C.R. Greene, Jr., D. Kastak, D.R. Ketten, J.H. Miller, et al. 2007. Marine Mammal Noise Exposure Criteria: Initial Scientific Recommendations. *Aquatic Mammals* 33(4): 411-521. https://doi.org/10.1080/09524622.2008.9753846.

Southall, B.L., J.J. Finneran, C. Reichmuth, P.E. Nachtigall, D.R. Ketten, A.E. Bowles, W.T. Ellison, D.P. Nowacek, and P.L. Tyack. 2019. Marine Mammal Noise Exposure Criteria: Updated Scientific Recommendations for Residual Hearing Effects. *Aquatic Mammals* 45(2): 125-232. https://doi.org/10.1578/AM.45.2.2019.125.

Appendix A. Animal Movement and Exposure Modelling

Animal movement and exposure modelling considers the movement of both sound sources and animals over time. Acoustic source and propagation modelling are used to generate 3-D sound fields that vary as a function of distance to source, depth, and azimuth. Sound sources are modelled at representative sites and the resulting sound fields are assigned to source locations using the minimum Euclidean distance. The sound received by an animal at any given time depends on its location relative to the source. Because the true locations of the animals within the sound fields are unknown, realistic animal movements are simulated using repeated random sampling of various behavioural parameters. The Monte Carlo method of simulating many animals within the operations area is used to estimate the sound exposure history of the population of simulated animals (animats).

Monte Carlo methods provide a heuristic approach for determining the probability distribution function (PDF) of complex situations, such as animals moving in a sound field. The probability of an events occurrence is determined by the frequency with which it occurs in the simulation. The greater the number of random samples, in this case the more simulated animats, the better the approximation of the PDF. Animats are randomly placed, or seeded, within the simulation boundary at a specified density (animats/km^2). Higher densities provide a finer PDF estimate resolution but require more computational resources. To ensure good representation of the PDF, the animat density is set as high as practical allowing for computation time. The animat density is typically much higher than real-world animal density to ensure good representation of the PDF. The resulting PDF can be scaled using real-world density when such data are available.

Several models for marine mammal movement have been developed (Ellison et al. 1987, Frankel et al. 2002, Houser 2006). These models use an underlying Markov chain to transition from one state to another based on probabilities determined from measured swimming behaviour. The parameters may represent simple states, such as the speed or heading of the animal, or complex states, such as likelihood of participating in foraging, play, rest, or travel. Attractions and aversions to variables like anthropogenic sounds and different depth ranges can be included in the models.

The JASCO Animal Simulation Model Including Noise Exposure (JASMINE) was based on the open-source marine mammal movement and behaviour model (3MB, Houser 2006) and used to predict the exposure of animats to sound arising from the anthropogenic activities. Animats are programmed to behave like the species likely to be present in the survey area. The parameters used for forecasting realistic behaviours (e.g., diving, foraging, aversion, surface times, etc.) are determined and interpreted from marine species studies (e.g., tagging studies) where available, or reasonably extrapolated from related species. An individual animats modelled sound exposure levels are summed over the total simulation duration to determine its total received energy, and then compared to the assumed threshold criteria.

JASMINE uses the same animal movement algorithms as 3MB (Houser, 2006), but has been extended to be directly compatible with JASCO's Marine Operations Noise Model (MONM) and Full Waveform Range-dependent Acoustic Model (FRAWM) acoustic field predictions, for inclusion of source tracks, and importantly for animats to change behavioural states based on time and space dependent modelled variables such as received levels for aversion behaviour, although aversion was not considered in this study.

A.1.1. Animal Movement Parameters

JASMINE uses previously measured behaviour to forecast behaviour in new situations and locations. The parameters used for forecasting realistic behaviour are determined (and interpreted) from marine species studies (e.g., tagging studies). Each parameter in the model is described as a probability

distribution. When limited or no information is available for a species parameter, a Gaussian or uniform distribution may be chosen for that parameter. For the Gaussian distribution, the user determines the mean and standard deviation of the distribution from which parameter values are drawn. For the uniform distribution, the user determines the maximum and minimum distribution from which parameter values are drawn. When detailed information about the movement and behaviour of a species are available, a user-created distribution vector, including cumulative transition probabilities, may be used (referred to here as a vector model; Houser 2006). Different sets of parameters can be defined for different behaviour states. The probability of an animat starting out in or transitioning into a given behaviour state can in turn be defined in terms of the animats current behavioural state, depth, and the time of day. In addition, each travel parameter and behavioural state has a termination function that governs how long the parameter value or overall behavioural state persists in simulation.

The parameters used in JASMINE describe animal movement in both the vertical and horizontal planes. The parameters relating to travel in these two planes are briefly described below.

Travel sub-models

- **Direction**– determines an animats choice of direction in the horizontal plane. Sub-models are available for determining the heading of animats, allowing for movement to range from strongly biased to undirected. A random walk model can be used for behaviours with no directional preference, such as feeding and playing. In a random walk, all bearings are equally likely at each parameter transition time step. A correlated random walk can be used to smooth the changes in bearing by using the current heading as the mean of the distribution from which to draw the next heading. An additional variant of the correlated random walk is available that includes a directional bias for use in situations where animals have a preferred absolute direction, such as migration. A user-defined vector of directional probabilities can also be input to control animat heading. For more detailed discussion of these parameters, see Houser (2006) and Houser and Cross (1999).
- **Travel rate**–defines an animats rate of travel in the horizontal plane. When combined with vertical speed and dive depth, the dive profile of the animat is produced.

Dive sub-models

- **Ascent rate**–defines an animats rate of travel in the vertical plane during the ascent portion of a dive.
- **Descent rate**–defines an animats rate of travel in the vertical plane during the descent portion of a dive.
- **Depth**–defines an animats maximum dive depth.
- **Reversals**–determines whether multiple vertical excursions occur once an animat reaches the maximum dive depth. This behaviour is used to emulate the foraging behaviour of some marine mammal species at depth. Reversal-specific ascent and descent rates may be specified.
- **Surface interval**–determines the duration an animat spends at, or near, the surface before diving again.

A.1.2. Exposure Integration Time

The interval over which acoustic exposure (LE) should be integrated and maximal exposure (Lp) determined is not well defined. Both Southall et al. (2007) and the NMFS (2018) recommend a 24 h baseline accumulation period, but state that there may be situations where this is not appropriate (e.g., a high-level source and confined population). Resetting the integration after 24 h can lead to overestimating the number of individual animals exposed because individuals can be counted multiple times during an operation. The type of animal movement engine used in this study simulates realistic movement using swimming behaviour collected over relatively short periods (hours to days) and does

not include large-scale movement such as migratory circulation patterns. For this study, a representative 24-hour period was simulated.

Ideally, a simulation area is large enough to encompass the entire range of a population so that any animal that could approach the source during an operation is included. However, there are limits to the simulation area, and computational overhead increases with area. For practical reasons, the simulation area is limited. In the simulation, every animat that reaches a border is replaced by another animat entering at the opposing border—e.g., an animat crossing the northern border of the simulation is replaced by one entering the southern border at the same longitude. When this action places the animat in an inappropriate water depth, the animat is randomly placed on the map at a depth suited to its species definition. The exposures of all animats (including those leaving the simulation and those entering) are kept for analysis. This approach maintains a consistent animat density and allows for longer integration periods with finite simulation areas.

A.1.3. Seeding Density and Scaling

Seeding density refers to the spatial sample rate, in units of animats/km^2, used in the simulation. It is not related to the real-world animal density, but rather is a model parameter that controls how samples are drawn from the model space. The minimum required seeding density for any given project depends on several factors such as bathymetry, source characteristics, and the behavioural profile of the animats, with the main constraint being computation time and resources. Seeding density is adjusted as needed based on model conditions specific to a project or project area.

In the present study, the exposure criteria for impulsive sounds were used to determine the number of animats exceeding exposure thresholds. To generate statistically reliable probability density functions, all simulations were seeded with an animat density of 4 animat/km^2 over the entire simulation area. The modelling results are not related to real-world animal densities as this data is not available, and the number of real-world animals potentially exposed could not be calculated.

Technical Memo

DATE: 9 May 2025

FROM: Matthew Koessler (JASCO Applied Sciences (Australia) Pty Ltd)

TO: Pennie Ginn, Matt Fraser (Klarite)

DOCUMENT 03816

VERSION 1.0

Subject: Acoustic Modelling for the Eureka 3D MSS with seabed nodes

JASCO Applied Sciences (JASCO) previously conducted modelling for the Eureka 3D Marine Seismic Survey (MSS). A change has been requested to investigate the underwater noise emissions considering a 1440 in^3 source with a shot point interval of 50 m. The use of this source will be used with seabed seismometer nodes. The acoustic modelling has been conducted with particular focus when the survey is in operations over shallow coastal waters.

1. Modelling Scenarios

A single acquisition scenario was considered using acoustic modelling. Acoustic modelling consisted of both source and propagation modelling, which was conducted at two individual single-impulse sites. The single impulse sites and the accumulated SEL scenarios were determined based on proposed survey line plans. This study considered a 1440 in^3 seismic source towed in a double array configuration at an assumed speed of ~5 knots with an impulse interval (inter-pulse interval) of either 50 m and a crossline array separation of 50 m. For comparison purposes refer the other scenarios, parameters, and results from Koessler and McPherson (2023), which consider a 12.5 m inter-pulse interval and a 2495 in^3 array.

Table 1 presents the particulars of the scenarios and Table 2 presents the sites used in the modelling. Figure 1 presents a map of the spatial extent of the modelled survey lines, sites, and BIAs.

Table 1. Parameters for modelled scenarios

Scenario	Source volume (in^3)	Tow depth (m)	Tow direction (°)	Source configuration	Impulse interval (m)	Discharged impulses
1-A	1440	5	0 & 180	Double	50	3455

Table 2. Location details for the single impulse modelled sites.

Site	Latitude (°S)	Longitude (°E)	MGA[1] Zone 50		Water depth (m)
			X (m)	Y (m)	
1-A	29° 24' 10.17"	114° 51' 16.44"	291825	6745469	14.7
2-A	29° 29' 31.85"	114° 51' 24.52"	292225	6735569	26.9

[1] Map Grid of Australia (MGA)

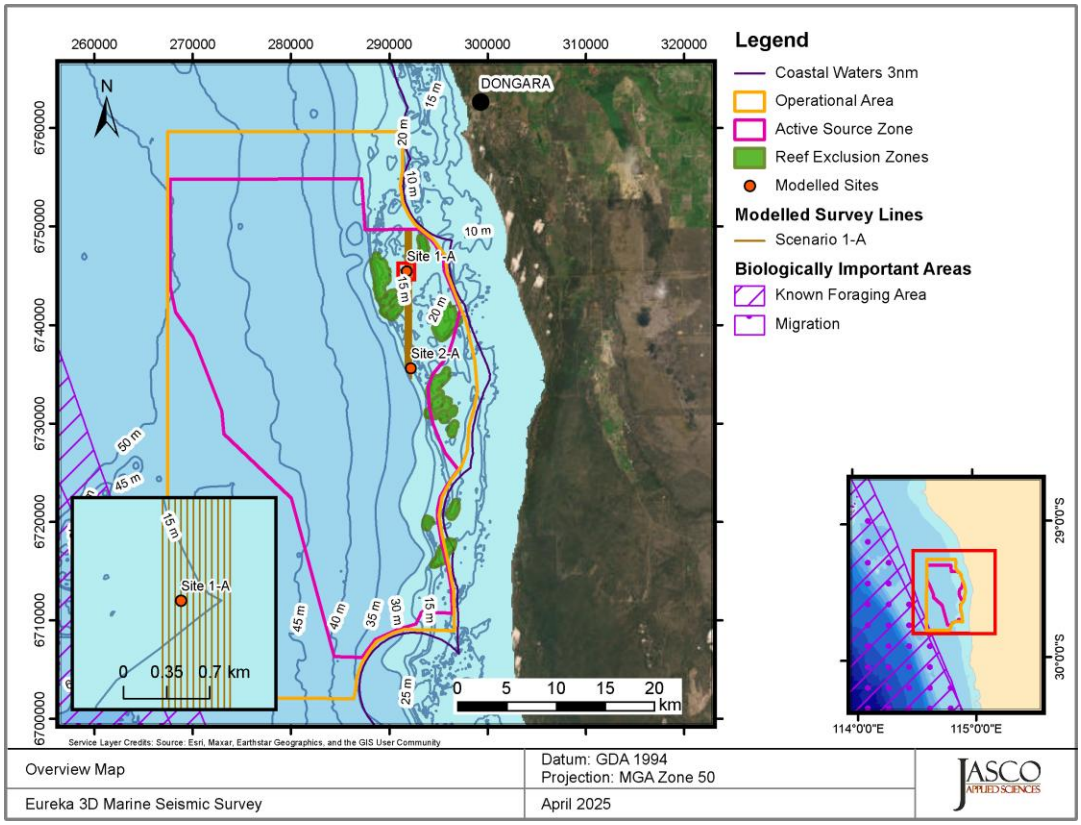


Figure 1. Overview of key survey features, modelled locations, and the survey scenario.

2. Noise Effect Criteria

The perceived loudness of sound, especially impulsive noise such as that from seismic airguns, is not generally proportional to the instantaneous acoustic pressure. Rather, perceived loudness depends on the pulse rise-time and duration, and the frequency content. The acoustic metrics in this report reflect the updated ISO standard for acoustic terminology, ISO/DIS 18405:2017 (2017).

Whether acoustic exposure levels might injure or disturb marine mammals is an active research topic. Since 2007, several expert groups have developed SEL-based assessment approaches for evaluating

auditory injury, with key works including Southall et al. (2007), Finneran and Jenkins (2012), Popper et al. (2014), United States National Marine Fisheries Service (NMFS 2018) and Southall et al. (2019). The number of studies that have investigated the level of behavioural disturbance to marine fauna by anthropogenic sound has also increased substantially.

The following noise criteria were chosen because they include standard thresholds, thresholds suggested by the best available science:

- Peak pressure levels (PK; L_{pk}) and frequency-weighted accumulated sound exposure levels (SEL; $L_{E,24h}$) from Southall et al. (2019) for the onset of Permanent Threshold Shift (PTS) and Temporary Threshold Shift (TTS) in marine mammals.
- Marine mammal behavioural threshold based on the current US National Oceanic and Atmospheric Administration (NOAA 2019) criterion for marine mammals of 160 dB re 1 µPa (SPL; L_p) for impulsive sound sources.
- Sound exposure guidelines for fish, fish eggs and larvae (including plankton) (Popper et al. 2014).
- Peak pressure levels (PK; L_{pk}) and frequency-weighted accumulated sound exposure levels (SEL; $L_{E,24h}$) from Finneran et al. (2017) for the onset of permanent threshold shift (PTS) and temporary threshold shift (TTS) in turtles.
- Sea turtle behavioural response threshold of 166 dB re 1 µPa (SPL; L_p) for impulsive noise, along with a sound level associated with behavioural disturbance 175 dB re 1 µPa (SPL; L_p) (McCauley et al. 2000).
- Peak-peak pressure levels (PK-PK; $L_{pk\text{-}pk}$) and peak particle acceleration magnitude (ms^{-2}) at the seafloor to help assess effects of noise on crustaceans through comparing to results in Day et al. (2016a), Day et al. (2019), Day et al. (2016b), Day et al. (2017) and Payne et al. (2008).
- A sound level of 226 dB re 1 µPa (PK; L_{pk}) reported for comparing to Heyward et al. (2018) for sponges and corals.
- A startle (inking) response sound level of 162 dB re 1 μPa^2s per–pulse SEL (L_E) for squid from Fewtrell and McCauley (2012).
- An SPL human health assessment threshold of 145 dB re 1 µPa (SPL; L_p) for sound exposure to people swimming and diving derived from Parvin (2005), and considering Ainslie (2008).

Further detail on noise effect criteria is provided in Koessler and McPherson (2023).

3. Methods

The methods for acoustic modelling applied herein are the same as presented in Koessler and McPherson (2023).

4. Results

4.1. Acoustic source levels and directivity

Table 3 shows the PK and per-pulse SEL source levels in the horizontal-plane broadside (perpendicular to the tow direction), endfire (along the tow direction), and vertical directions for the seismic array considered (1440 in^3 array with 5 m tow depth). The broadside, endfire, and vertical overpressure signature and corresponding power spectrum levels for the array are provided in Appendix A.

Table 3. Far-field source level specifications for the 1440 in^3 array with a 5 m tow depth. Source levels are for a point-like acoustic source with equivalent far-field acoustic output in the specified direction. Sound level metrics are per-pulse and unweighted.

Total Volume (in^3)	Direction	Peak source pressure level ($L_{S,pk}$; dB re 1 µPa m)	Per-pulse source SEL ($L_{S,E}$; dB 1 μPa^2m^2s)	
			10-2000 Hz	2000-25000 Hz
1440	Broadside	247.1	222.6	181.9
1440	Endfire	245.0	221.7	180.1
1440	Vertical	253.2	225.4	187.1

4.2. Per-pulse Sound Fields

This section presents the per-pulse sound fields in terms of maximum-over-depth SPL, SEL, PK, and seafloor PK and PK-PK. The different metrics are presented for the following reasons:

- SPL sound fields were used to determine the distances to marine mammal and turtle behavioural thresholds.
- Per-pulse SEL sound fields are used as inputs into the 24 h SEL scenario and to provide context for the range to 160 dB re 1 µPa2·s, relevant for the EPBC Act Policy Statement 2.1 (DEWHA 2008).
- Per-pulse SEL sound fields to determine the distances to the level associated with squid startle (inking) response (Fewtrell and McCauley 2012).
- PK metrics within the water column are relevant to thresholds and guidelines for marine mammals, sea turtles, fish, fish eggs and larvae (as well as plankton)
- PK metrics at the seafloor are relevant to guidelines for fish, fish eggs and larvae and the sound level for no effect on corals and sponges.
- PK-PK metrics at the seafloor are relevant to sound levels used in the assessment of effect on benthic invertebrates.

Seafloor sound levels were assessed at eight different representative depths and Tables 7– 8 present the PK and PK-PK results. At these same water depths particle motion was also calculated and presented in Table 9

4.2.1.1. Entire Water Column

Table 4. Maximum (R_{max}) and 95% ($R_{95\%}$) horizontal distances (in km) from the seismic source to modelled maximum-over-depth (also maximised over tow modelled tow direction) unweighted per-pulse sound exposure level (SEL) isopleths from the modelled single impulse sites, with water depth indicated.

Per-pulse SEL (L_E; dB re 1 µPa²·s)	Site 1-A (14.7 m)		Site 2-A (26.9 m)	
	R_{max}	$R_{95\%}$	R_{max}	$R_{95\%}$
190	0.08	0.06	0.06	0.05
180	0.30	0.26	0.26	0.22
170	0.84	0.70	0.86	0.72
162[1]	2.30	1.90	2.56	2.10
160[2]	1.94	1.59	2.14	1.74
150	5.05	4.21	5.87	4.99
140	7.61	6.40	12.1	10.2
130	21.2	15.4	34.3	29.6

[1] Startle response level for squid (Fewtrell and McCauley 2012).
[2] Low power zone assessment criteria DEWHA (2008).

Table 5. Maximum (R_{max}) and 95% ($R_{95\%}$) horizontal distances (in km) from the seismic source to modelled maximum-over-depth (also maximised over tow modelled tow direction) per-pulse sound pressure level (SPL) isopleths from the modelled single impulse sites, with water depth indicated.

SPL (L_p; dB re 1 µPa)	Site 1-A (14.7 m)		Site 2-A (26.9 m)	
	R_{max}	$R_{95\%}$	R_{max}	$R_{95\%}$
200	0.08	0.06	0.06	0.05
190	0.28	0.22	0.24	0.18
180	0.74	0.62	0.72	0.62
175[1]	1.28	1.04	1.28	1.06
170	2.06	1.67	2.22	1.80
166[2]	2.96	2.37	3.37	2.80
160[3]	4.94	4.06	5.53	4.75
150	7.26	5.99	11.1	9.48
145[4]	10.2	7.91	19.8	15.9
140	18.9	12.5	30.9	26.5
130	46.6	39.1	66.3	53.8

[1] Threshold for turtle behavioural disturbance from impulsive noise.
[2] Threshold for turtle behavioural response to impulsive noise (NSF 2011).
[3] Marine mammal behavioural threshold for impulsive sound sources (NOAA 2019).
[4] Human health assessment threshold derived from (Parvin 2005).

Table 6. Maximum (R_{max}) horizontal distances (in km) from the seismic source to modelled maximum-over-depth (also maximised over tow modelled tow direction) peak pressure level (PK) thresholds based on Southall et al. (2019) for marine mammals, and Popper et al. (2014) for fish and Finneran et al. (2017) for sea turtles, Sites 3 and 5), with water depth indicated.

Hearing group	PK threshold (L_{pk}; dB re 1 µPa)	Distance R_{max} (km)	
		Site 1-A (14.7 m)	Site 2-A (26.9 m)
Low-frequency cetaceans (PTS)	219	0.06	0.03
Low-frequency cetaceans (TTS)	213	0.11	0.09
High-frequency cetaceans (PTS)	230	–	–
High-frequency cetaceans (TTS)	224	–	–
Very-high-frequency cetaceans (PTS)	202	0.45	0.34
Very-high-frequency cetaceans (TTS)	196	0.82	0.85
Other Carnivores in Water (PTS)	232	–	–
Other Carnivores in Water (TTS)	226	–	–
Sea Turtles (PTS)	232	–	–
Sea Turtles (TTS)	226	–	–
Fish: No swim bladder (also applied to sharks)	213	0.11	0.09
Fish: Swim bladder not involved in hearing, Swim bladder involved in hearing Fish eggs, and larvae	207	0.28	0.20

A dash indicates the threshold is not reached within the limits of the modelling resolution (20 m).

4.2.1.2. Seafloor

Ranges presented at the seafloor (50 and 5 cm above the interface) provided in Tables 7 and 8 are different to those for the maximum-over-depth modelling results presented in Table 6. This is because the model used for the water column results, calculated using FWRAM do not represent the maximum sound levels at the seafloor close to the array. This is because FWRAM is based on a wide-angle parabolic equation (PE) algorithm which is valid to only approximately 70° down angle from the horizontal, and while it provides accurate predictions in the horizontal direction, it cannot predict sound levels directly under the array. The VSTACK model is used to determine the levels at the seafloor directly under the array, and due to seafloor interactions, these can be greater than those elsewhere in the water column.

Table 7. Maximum (R_{max}) horizontal distances (in m) from the seismic source to modelled seafloor (receiver located 50 cm above seafloor) peak pressure level thresholds (PK) at two water depths within the Active Source Area.

Hearing group/animal type	PK threshold (L_{pk}; dB re 1 µPa)	Water Depth	
		10 m	15 m
		Distance R_{max} (m)	
Sound levels for sponges and corals[1]	226	2	4
Fish: No swim bladder (also applied to sharks)	213	45	44
Fish: Swim bladder not involved in hearing, Swim bladder involved in hearing Fish eggs, and larvae	207	94	72

[1] Heyward et al. (2018)
An asterisk indicates that the sound level was not reached.

Table 8. Maximum (R_{max}) horizontal distances (in m) from the seismic source to modelled seafloor (receiver located 5 cm above seafloor) peak-peak pressure levels (PK-PK) at two water depths within the Active Source Area. Results included in relation to benthic invertebrates.

PK-PK ($L_{pk\text{-}pk}$; dB re 1 µPa)	Water Depth	
	10 m	15 m
	Distance R_{max} (m)	
213[1,2,3]	70	66
212[2,3]	75	69
210[1,2]	93	85
209[1,2]	103	91
202[4]	183	212

[1] Day et al. (2019), lobster
[2] Day et al. (2016a), lobster and scallops
[3] Day et al. (2017), scallops.
[4] Payne et al. (2008), lobster

4.2.1.2.1. Particle Motion Metrics

Table 9. Maximum (R_{max}) horizontal distances (in m) from the seismic source to particle motion threshold: Peak acceleration magnitude level (m/s^2) threshold for benthic invertebrates 5 cm above the seafloor, with water depth indicated.

Hearing group/animal type	Peak Acceleration Magnitude (m/s^2)	Water Depth	
		10 m	15 m
		Distance R_{max} (m)	
Benthic invertebrates	37.57	42	35

4.2.2. Sound Level Contour Maps

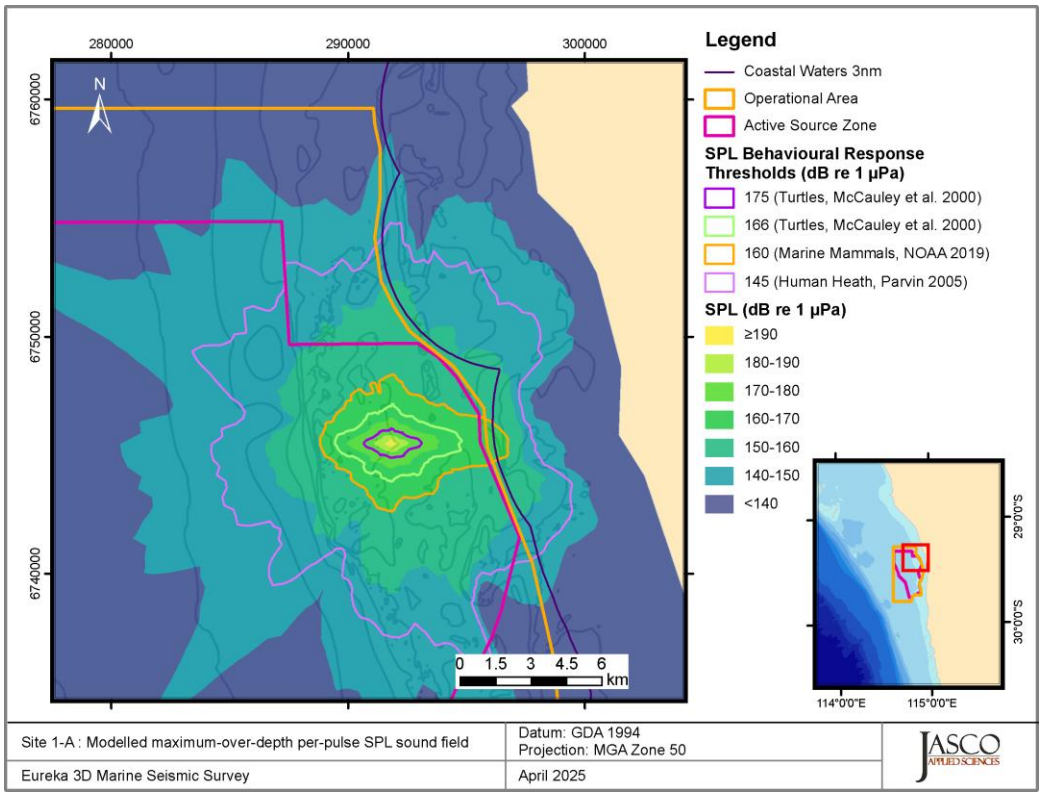


Figure 2. *Site 1-A, SPL, 1440 in³ source, tow azimuth 0°*: Sound level contour map of unweighted maximum-over-depth sound field in 10 dB steps, and the isopleths for behavioural response thresholds for marine mammals and turtles.

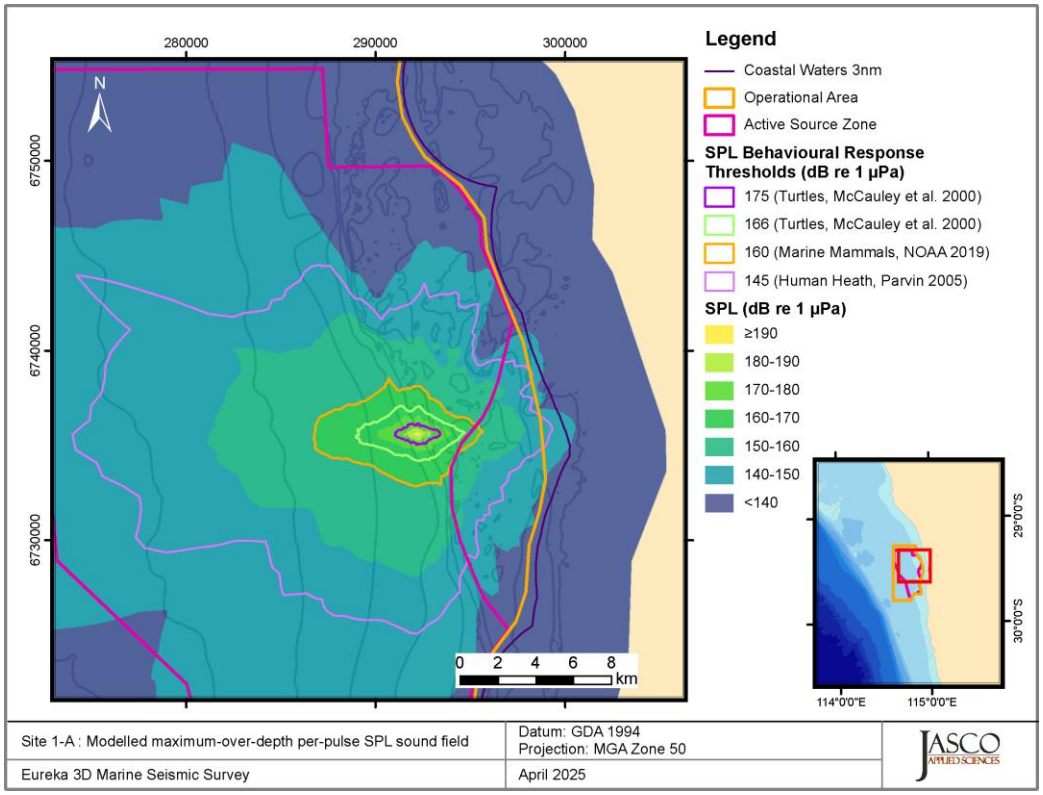


Figure 3. *Site 2-A, SPL, 1440 in³ source, tow azimuth 0°*: Sound level contour map of unweighted maximum-over-depth sound field in 10 dB steps, and the isopleths for behavioural response thresholds for marine mammals and turtles.

4.3. Multiple Source Fields

This section presents the sound fields in terms of SEL accumulated over 24 hours of survey, for the modelled scenarios. Frequency-weighted SEL_{24h} sound fields were used to estimate the maximum horizontal distances (R_{max}) to low frequency cetacean PTS and TTS thresholds.

The SEL_{24h} sound fields are presented as contour maps in Figure 4, it present's the unweighted SEL_{24h} in 10 dB steps, as well as the isopleths corresponding to thresholds for which R_{max} is greater than 20 m.

4.3.1. Tabulated Results

Table 10. Marine mammal criteria as applied to pygmy blue whales: Maximum (R_{max}) horizontal distances (in km) and ensonified area (km^2) from the survey lines to permanent threshold shift (PTS) and temporary threshold shift (TTS) thresholds considering 24 hours of survey activity (maximum-over-depth). The modelled array volume and inter-pulse intervals are also provided in brackets below each scenario number.

Hearing group	Weighted SEL thresholds ($L_{E,24h}$; dB re 1 µPa^2·s)	Scenario 1-A	
		R_{max} (km)	Area (km^2)
PTS			
Low-frequency cetaceans	183	1.72	50.3
High-frequency cetaceans	185	–	–
Very-high-frequency cetaceans	155	0.07	2.78
Pinnipeds	203	–	–
Sea Turtles	204	0.07	2.78
TTS			
Low-frequency cetaceans	168	11.9	351.2
Low-frequency cetaceans	168	0.05	0.44
High-frequency cetaceans	170	0.10	10.3
Very-high-frequency cetaceans	140	0.07	2.53
Pinnipeds	188	0.98	31.9
Sea turtles	189	1.72	50.3

A dash indicates the threshold was not reached within the limits of the modelling resolution (20 m).

Table 11. *Fish criteria*: Maximum horizontal distances (R_{max}, in km) from the survey lines and area (km²) to injury and temporary threshold shift (TTS) thresholds considering 24 h of survey activity.

Marine fauna group	Threshold for SEL_{24h} ($L_{E,24h}$; dB re 1 µPa²·s)	Scenario 1-A	
		R_{max} (km)	Area (km²)
Mortality and potential mortal injury			
I	219	0.06	1.33
II, fish eggs and larvae	210	0.07	2.78
III	207	0.07	2.78
Fish recoverable injury			
I	216	0.07	2.78
II, III	203	0.07	5.33
Fish TTS			
I, II, III	186	2.46	65.0

Fish I–No swim bladder; Fish II–Swim bladder not involved with hearing; Fish III–Swim bladder involved with hearing. An asterisk indicates that the sound level was not reached.

4.3.2. Sound Level Contour Maps

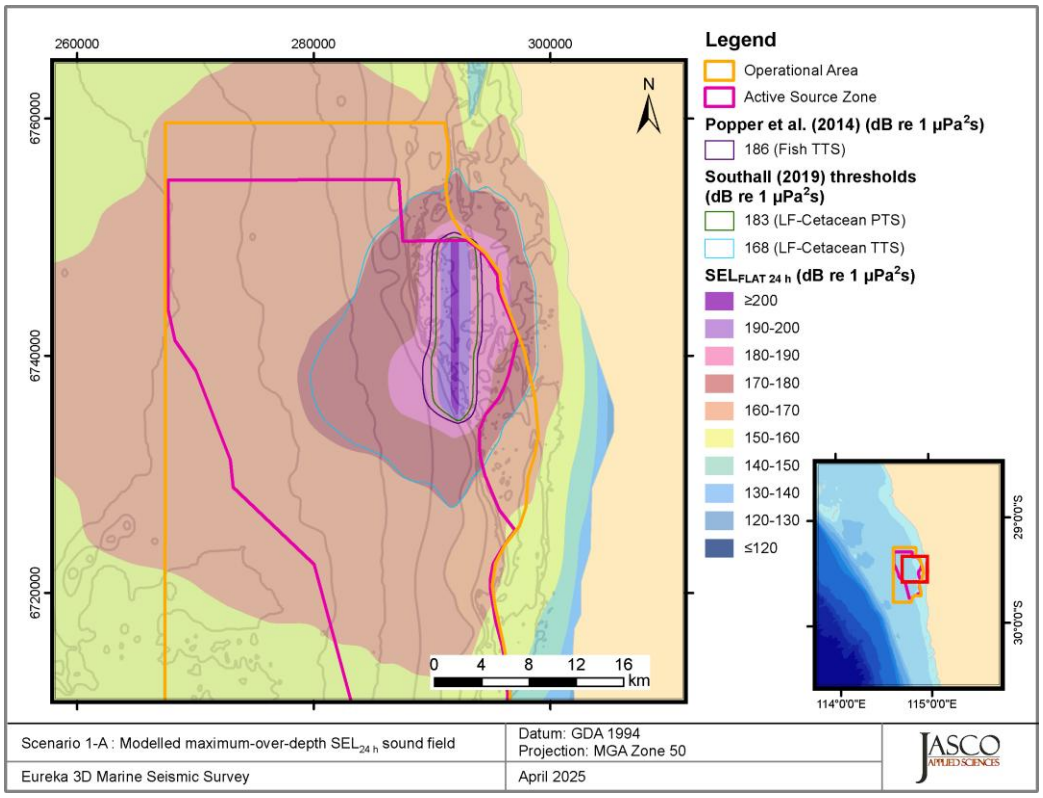


Figure 4. *Scenario .1-A, 1440 in³ with 50 m inter-pulse interval*: Sound level contour map showing unweighted maximum-over-depth SEL_{24h}, along with thresholds for LF-cetaceans. Thresholds omitted here were not reached or not large enough to display graphically. Refer to Table 10 for tabulated radii.

5. Discussion

5.1. Multiple Pulse Sound Fields

The accumulated SEL over 24 hours of seismic source operation was modelled considering representative scenarios with realistic acquisition patterns for shallow sections of the Eureka 3D MSS. The footprints and range maxima for SEL_{24h} criteria are substantially influenced by the number of impulses discharged. Compared to the original acoustic modelling, a smaller array volume and larger inter-pulse intervals reduced the maximum ranges to all relevant SEL_{24h} thresholds.

For the accumulated sound exposure scenarios, the SEL_{24h} is a cumulative metric that reflects the dosimetric effect of noise levels within 24 hours. It assumes a receiver (e.g., an animal) is consistently exposed to the noise at a fixed position. More realistically, marine animals would not stay in the same location for 24 hours. Therefore, a radius for the SEL_{24h} criteria does not mean that marine fauna within this radius will be impaired, but rather that the animal could be exposed to the sound level associated with impairment, either Permanent Threshold Shift (PTS) or Temporary Threshold Shift (TTS), if it remained at that location for 24 hours. The animal movement and exposure modelling discussed below presents a more realistic estimate of the dosimetric impact potential for accumulated sound exposure.

6. Literature Cited

[DEWHA] Department of the Environment, Water, Heritage, and the Arts (Australia). 2008. *EPBC Act Policy Statement 2.1 - Interaction Between Offshore Seismic Exploration and Whales*. 14 p. http://www.environment.gov.au/resource/epbc-act-policy-statement-21-interaction-between-offshore-seismic-exploration-and-whales.

[ISO] International Organization for Standardization. 2017. *ISO 18405:2017. Underwater acoustics – Terminology*. Geneva. https://www.iso.org/standard/62406.html.

[NMFS] National Marine Fisheries Service (US). 2018. *2018 Revision to: Technical Guidance for Assessing the Effects of Anthropogenic Sound on Marine Mammal Hearing (Version 2.0): Underwater Thresholds for Onset of Permanent and Temporary Threshold Shifts*. US Department of Commerce, NOAA. NOAA Technical Memorandum NMFS-OPR-59. 167 p. https://www.fisheries.noaa.gov/webdam/download/75962998.

[NOAA] National Oceanic and Atmospheric Administration (US). 2019. *ESA Section 7 Consultation Tools for Marine Mammals on the West Coast* (webpage), 27 Sep 2019. https://www.fisheries.noaa.gov/west-coast/endangered-species-conservation/esa-section-7-consultation-tools-marine-mammals-west.

[NSF] National Science Foundation (US). 2011. *Final Programmatic Environmental Impact Statement/Overseas. Environmental Impact Statement for Marine Seismic Research Funded by the National Science Foundation or Conducted by the US Geological Survey*. National Science Foundation, Arlington, VA, USA. https://www.nsf.gov/geo/oce/envcomp/usgs-nsf-marine-seismic-research/nsf-usgs-final-eis-oeis_3june2011.pdf.

Ainslie, M.A. 2008. *Review of Published Safety Thresholds for Human Divers Exposed to Underwater Sound (Veilige maximale geluidsniveaus voor duikers-beoordeling van publicaties)*. Report Number TNO-DV-2007-A598. DTIC Document, TNO Defence Security and Safety, The Hague (Netherlands). 17 p. http://www.dtic.mil/dtic/tr/fulltext/u2/a485758.pdf

Day, R.D., R.D. McCauley, Q.P. Fitzgibbon, K. Hartmann, J.M. Semmens, and Institute for Marine and Antarctic Studies. 2016a. *Assessing the Impact of Marine Seismic Surveys on Southeast Australian Scallop and Lobster Fisheries*. Impacts of Marine Seismic Surveys on Scallop and Lobster Fisheries. Fisheries Ressearch & Development Corporation. FRDC Project No 2012/008, University of Tasmania, Hobart. 159 p.

Day, R.D., R.D. McCauley, Q.P. Fitzgibbon, and J.M. Semmens. 2016b. Seismic air gun exposure during early-stage embryonic development does not negatively affect spiny lobster *Jasus edwardsii larvae* (Decapoda:Palinuridae). *Scientific Reports* 6: 1-9. https://doi.org/10.1038/srep22723.

Day, R.D., R.D. McCauley, Q.P. Fitzgibbon, K. Hartmann, and J.M. Semmens. 2017. Exposure to seismic air gun signals causes physiological harm and alters behavior in the scallop *Pecten fumatus*. *Proceedings of the National Academy of Sciences* 114(40): E8537-E8546. https://doi.org/10.1073/pnas.1700564114.

Day, R.D., R.D. McCauley, Q.P. Fitzgibbon, K. Hartmann, and J.M. Semmens. 2019. Seismic air guns damage rock lobster mechanosensory organs and impair righting reflex. *Proceedings of the Royal Society B* 286(1907). https://doi.org/10.1098/rspb.2019.1424.

Fewtrell, J.L. and R.D. McCauley. 2012. Impact of air gun noise on the behaviour of marine fish and squid. *Marine Pollution Bulletin* 64(5): 984-993. https://doi.org/10.1016/j.marpolbul.2012.02.009.

Finneran, J.J. and A.K. Jenkins. 2012. *Criteria and thresholds for U.S. Navy acoustic and explosive effects analysis*. SPAWAR Systems Center Pacific, San Diego, CA, USA. 64 p.

Finneran, J.J., E. Henderson, D.S. Houser, K. Jenkins, S. Kotecki, and J. Mulsow. 2017. *Criteria and Thresholds for U.S. Navy Acoustic and Explosive Effects Analysis (Phase III)*. Technical report by Space and Naval Warfare Systems Center Pacific (SSC Pacific). 183 p.

Heyward, A., J. Colquhoun, E. Cripps, D. McCorry, M. Stowar, B. Radford, K. Miller, I. Miller, and C. Battershill. 2018. No evidence of damage to the soft tissue or skeletal integrity of mesophotic corals exposed to a 3D marine seismic survey. *Marine Pollution Bulletin* 129(1): 8-13. https://doi.org/10.1016/j.marpolbul.2018.01.057.

Koessler, M.W. and C.R. McPherson. 2023. *Eureka 3D Marine Seismic Survey: Acoustic Modelling for Assessing Marine Fauna Sound Exposures*. Document Number 03034, Version 1.0. Technical report by JASCO Applied Sciences for RPS Australia.

McCauley, R.D., J. Fewtrell, A.J. Duncan, C. Jenner, M.-N. Jenner, J.D. Penrose, R.I.T. Prince, A. Adhitya, J. Murdoch, et al. 2000. *Marine seismic surveys: Analysis and propagation of air-gun signals; and effects of air-gun exposure on humpback whales, sea turtles, fishes and squid*. Report Number R99-15. Prepared for Australian Petroleum Production Exploration Association by Centre for Maine Science and Technology, Western Australia. 198 p. https://cmst.curtin.edu.au/wp-content/uploads/sites/4/2016/05/McCauley-et-al-Seismic-effects-2000.pdf.

Parvin, S. 2005. *Limits for underwater noise exposure of human divers and swimmers*. Subacoustech. Presented at the National Physics Laboratory Seminar on Underwater Acoustics, Teddington, UK. http://www.subacoustech.com/wp-content/uploads/NPLDiverNoisePresentation.pdf.

Payne, J.F., C. Andrews, L. Fancey, D. White, and J. Christian. 2008. *Potential Effects of Seismic Energy on Fish and Shellfish: An Update since 2003*. Report Number 2008/060. Canadian Science Advisory Secretariat. 22 p.

Popper, A.N., A.D. Hawkins, R.R. Fay, D.A. Mann, S. Bartol, T.J. Carlson, S. Coombs, W.T. Ellison, R.L. Gentry, et al. 2014. *Sound Exposure Guidelines for Fishes and Sea Turtles: A Technical Report prepared by ANSI-Accredited Standards Committee S3/SC1 and registered with ANSI*. ASA S3/SC1.4 TR-2014. SpringerBriefs in Oceanography. ASA Press and Springer. https://doi.org/10.1007/978-3-319-06659-2.

Southall, B.L., A.E. Bowles, W.T. Ellison, J.J. Finneran, R.L. Gentry, C.R. Greene, Jr., D. Kastak, D.R. Ketten, J.H. Miller, et al. 2007. Marine Mammal Noise Exposure Criteria: Initial Scientific Recommendations. *Aquatic Mammals* 33(4): 411-521. https://doi.org/10.1080/09524622.2008.9753846.

Southall, B.L., J.J. Finneran, C. Reichmuth, P.E. Nachtigall, D.R. Ketten, A.E. Bowles, W.T. Ellison, D.P. Nowacek, and P.L. Tyack. 2019. Marine Mammal Noise Exposure Criteria: Updated Scientific Recommendations for Residual Hearing Effects. *Aquatic Mammals* 45(2): 125-232. https://doi.org/10.1578/AM.45.2.2019.125.

Appendix A. Seismic Source

The layout of the seismic source used for modelling in this study is provided in Figure A-1 and details of the airgun parameters are provided in Table A-1.

For the modelled array, the layout is presented in a nominal cartesian coordinate system. In this coordinate system the direction of vessel travel determines the relative position of the array elements as plotted and tabulated. The layout used for acoustic modelling was produced by transforming the coordinates of client supplied layouts such that the resultant layouts correspond to a vessel travel direction along the positive X-axis and the array is centred on the X-Y origin. When used with an acoustic model the positive X-axis in this nominal coordinate system aligns with the vessel tow direction or survey line azimuth.

Table A-1. Layout of the modelled 1440 in^3 array. Tow depth is 5 m. Firing pressure for all guns is 2000 psi. Also see Figure A-1.

String	Gun	*x* (m)	*y* (m)	*z* (m)	Vol (in^3)	String	Gun	*x* (m)	*y* (m)	*z* (m)	Vol (in^3)
1	1	6.25	-5.35	6.0	60	2	13	6.25	4.65	6.0	60
	2	6.25	-4.65	6.0	60		14	6.25	5.35	6.0	60
	5	1.25	-5.35	6.0	150		17	1.25	4.65	6.0	150
	6	1.25	-4.65	6.0	150		18	1.25	5.35	6.0	150
	7	-1.25	-5.35	6.0	60		19	-1.25	4.65	6.0	60
	8	-1.25	-4.65	6.0	60		20	-1.25	5.35	6.0	60
	9	-3.75	-5.35	6.0	60		21	-3.75	4.65	6.0	60
	10	-3.75	-4.65	6.0	60		22	-3.75	5.35	6.0	60
	11	-6.25	-5.35	6.0	60		23	-6.25	4.65	6.0	60

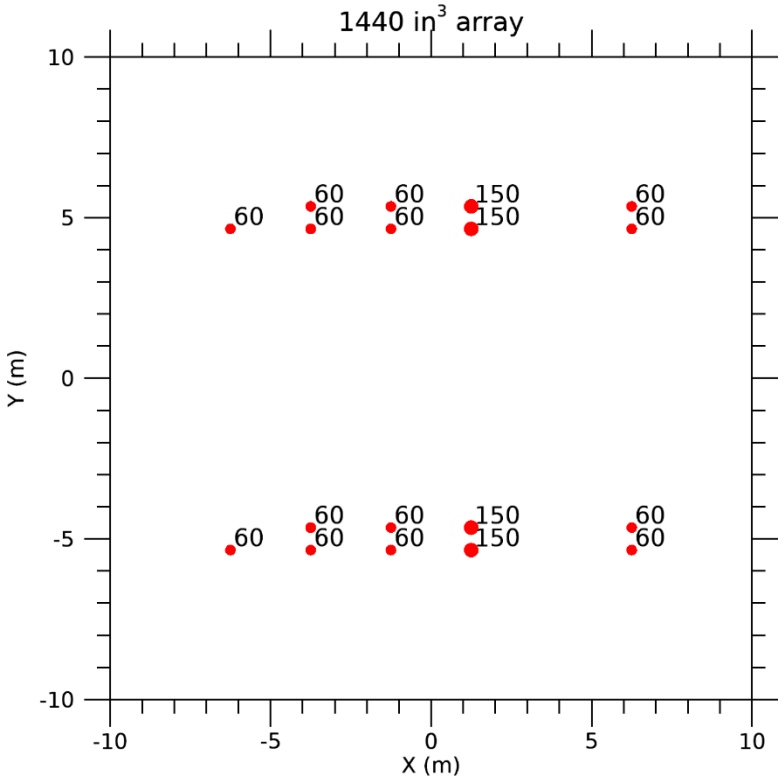


Figure A-1. Layout of the modelled 1440 in^3 seismic array where the plotted layout is such that the array is centred on the origin and vessel travel direction is in the positive x-direction. Tow depth is 5 m. The labels indicate the firing volume (in cubic inches) for each airgun. Also see Table A-1.

A.1. Array Source Levels and Directivity

Figure A-2 shows the broadside (perpendicular to the tow direction), endfire (parallel to the tow direction) and vertical overpressure signature and corresponding power spectrum levels for the seismic source. Horizontal decidecade-band source levels are shown as a function of band centre frequency and azimuth in Figure A-3.

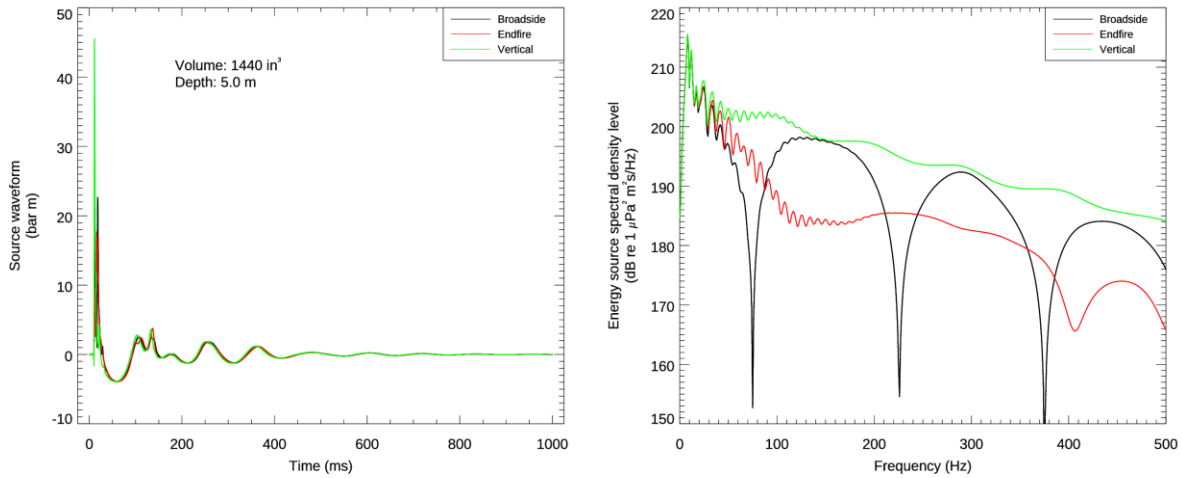


Figure A-2. Predicated source level details for the 1440 in^3 array at 5 m tow depth. (Left) overpressure signature and (right) the power spectrum for in-plane horizontal (broadside), perpendicular (endfire), and vertical directions (no surface ghost).

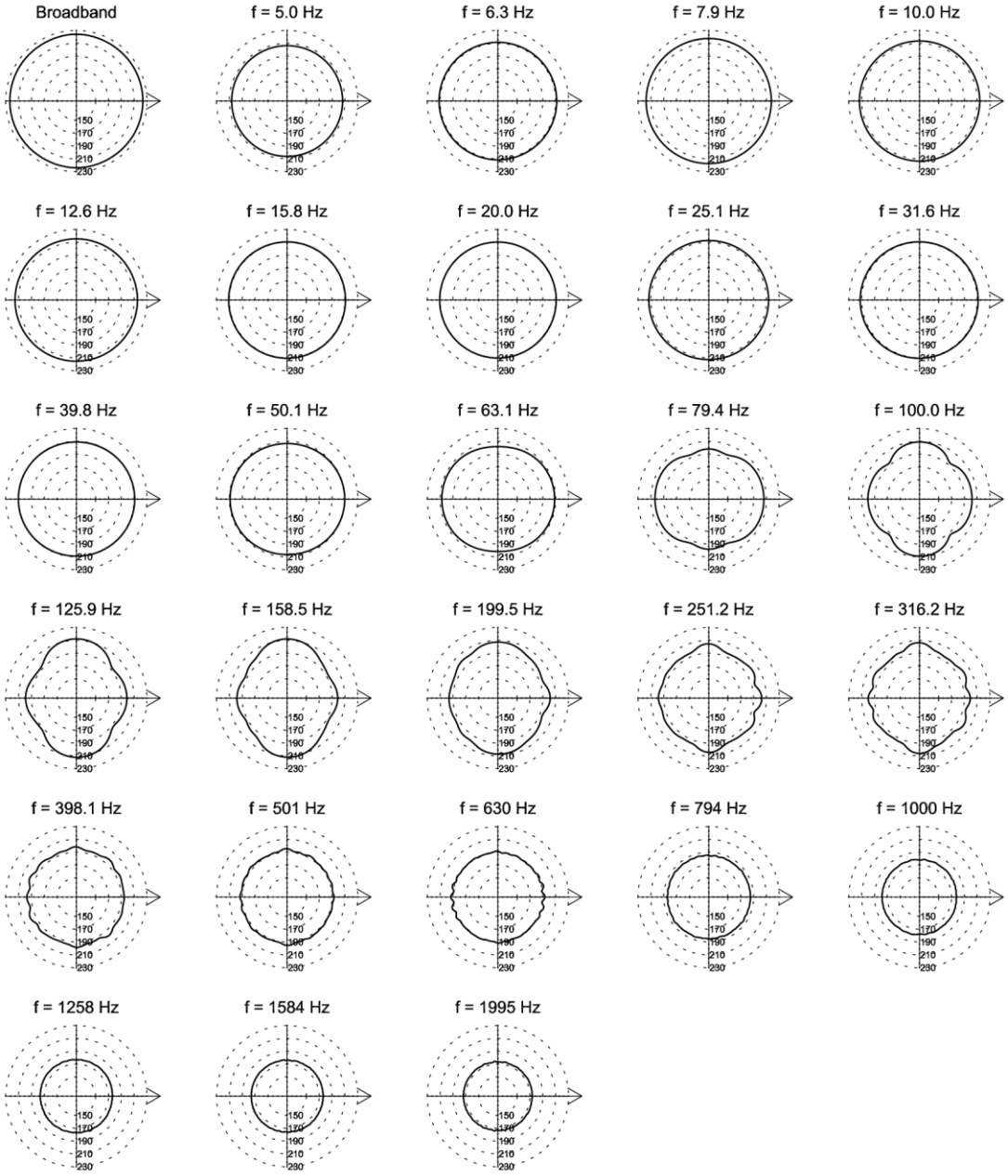


Figure A-3. Directionality of the predicted horizontal source levels for the 1440 in^3 seismic source, 5 Hz to 2 kHz. Source levels (in dB re 1 $\mu Pa^2 \cdot s\ m^2$) are shown as a function of azimuth for the centre frequencies of the decidecade bands modelled; frequencies are shown above the plots. The vessel travel direction is to the right of frame. Tow depth is 5 m.

Appendix B. Estimating Range to Thresholds Levels

Sound level contours were calculated based on the underwater sound fields predicted by the propagation models, sampled by taking the maximum value over all modelled depths above the sea floor for each location in the modelled region. The predicted distances to specific levels were computed from these contours. Two distances relative to the source are reported for each sound level: 1) R_{max}, the maximum range to the given sound level over all azimuths, and 2) $R_{95\%}$, the range to the given sound level after the 5% farthest points were excluded (see examples in Figure B-1).

The $R_{95\%}$ is used because sound field footprints are often irregular in shape. In some cases, a sound level contour might have small protrusions or anomalous isolated fringes. This is demonstrated in the image in Figure B-1(a). In cases such as this, where relatively few points are excluded in any given direction, R_{max} can misrepresent the area of the region exposed to such effects, and $R_{95\%}$ is considered more representative. In strongly asymmetric cases such as shown in Figure B-1(b), on the other hand, $R_{95\%}$ neglects to account for significant protrusions in the footprint. In such cases R_{max} might better represent the region of effect in specific directions. Cases such as this are usually associated with bathymetric features affecting propagation. The difference between R_{max} and $R_{95\%}$ depends on the source directivity and the non-uniformity of the acoustic environment.

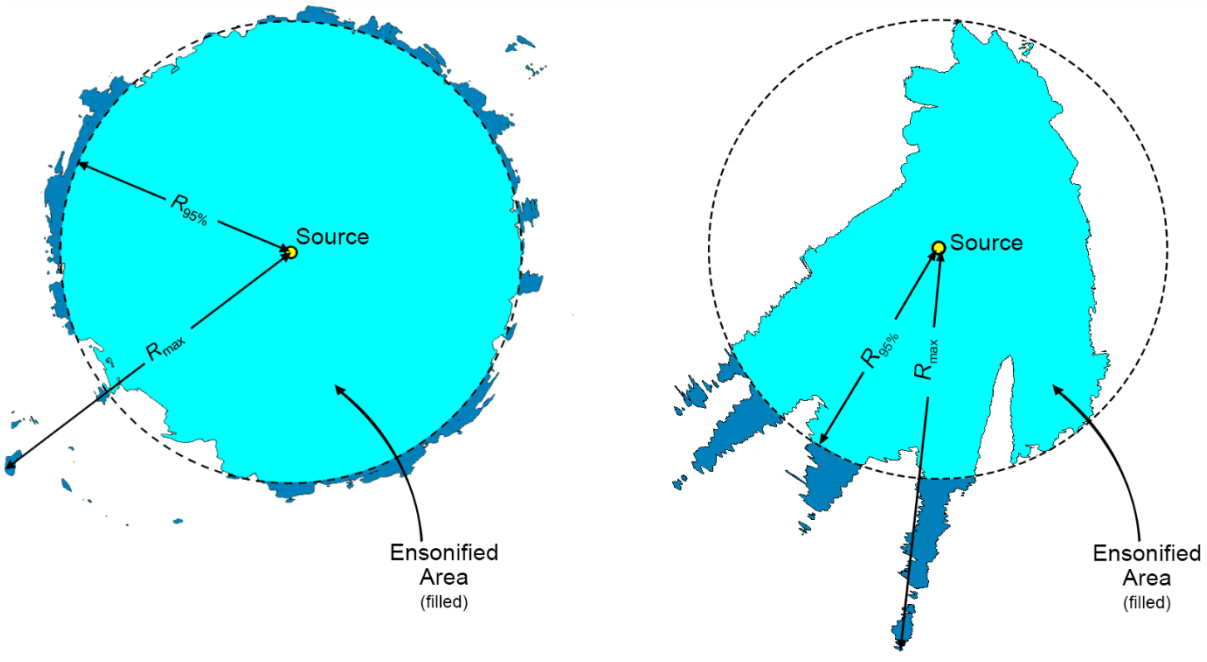


Figure B-1. Sample areas ensonified to an arbitrary sound level with R_{max} and $R_{95\%}$ ranges shown for two scenarios. (a) Largely symmetric sound level contour with small protrusions. (b) Strongly asymmetric sound level contour with long protrusions. Light blue indicates the ensonified areas bounded by $R_{95\%}$; darker blue indicates the areas outside this boundary which determine R_{max}.